Crystallography and Crystal Chemistry
IX International School-Conference of Young Scientists 2024

How can modeling help in materials synthesis?

Dr. Anton Boev

Skoltech Energy
Center for Energy Science and Technology

November, 2024

Three Pillars of Science and Engineering

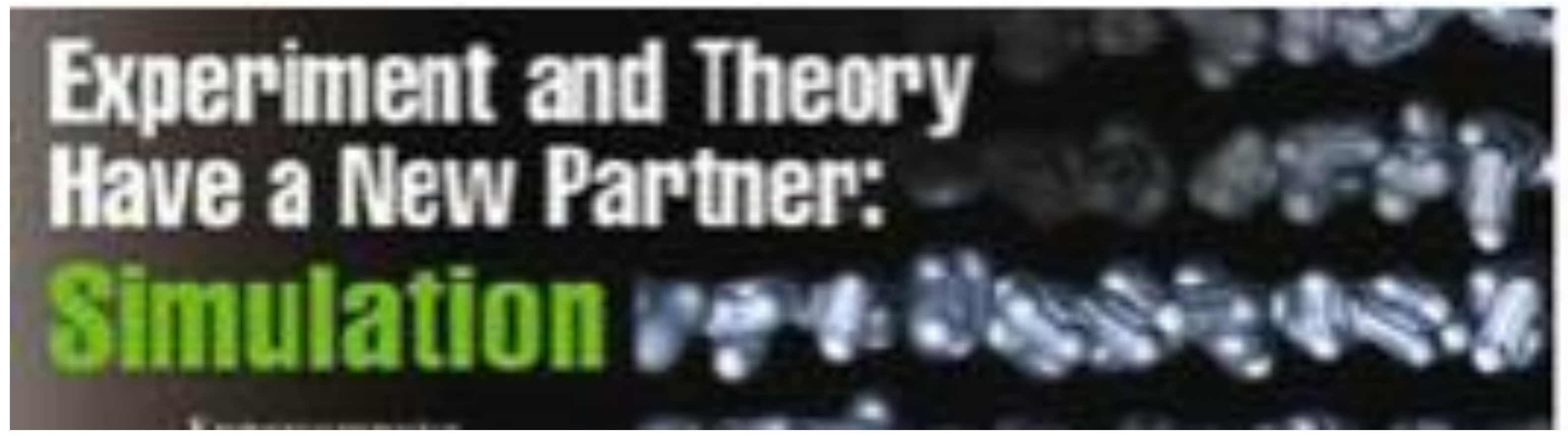

HELLER, A.; PARKER, A. Experiment and theory have a new partner: simulation. Science Technology Review. 4–13, 2005.

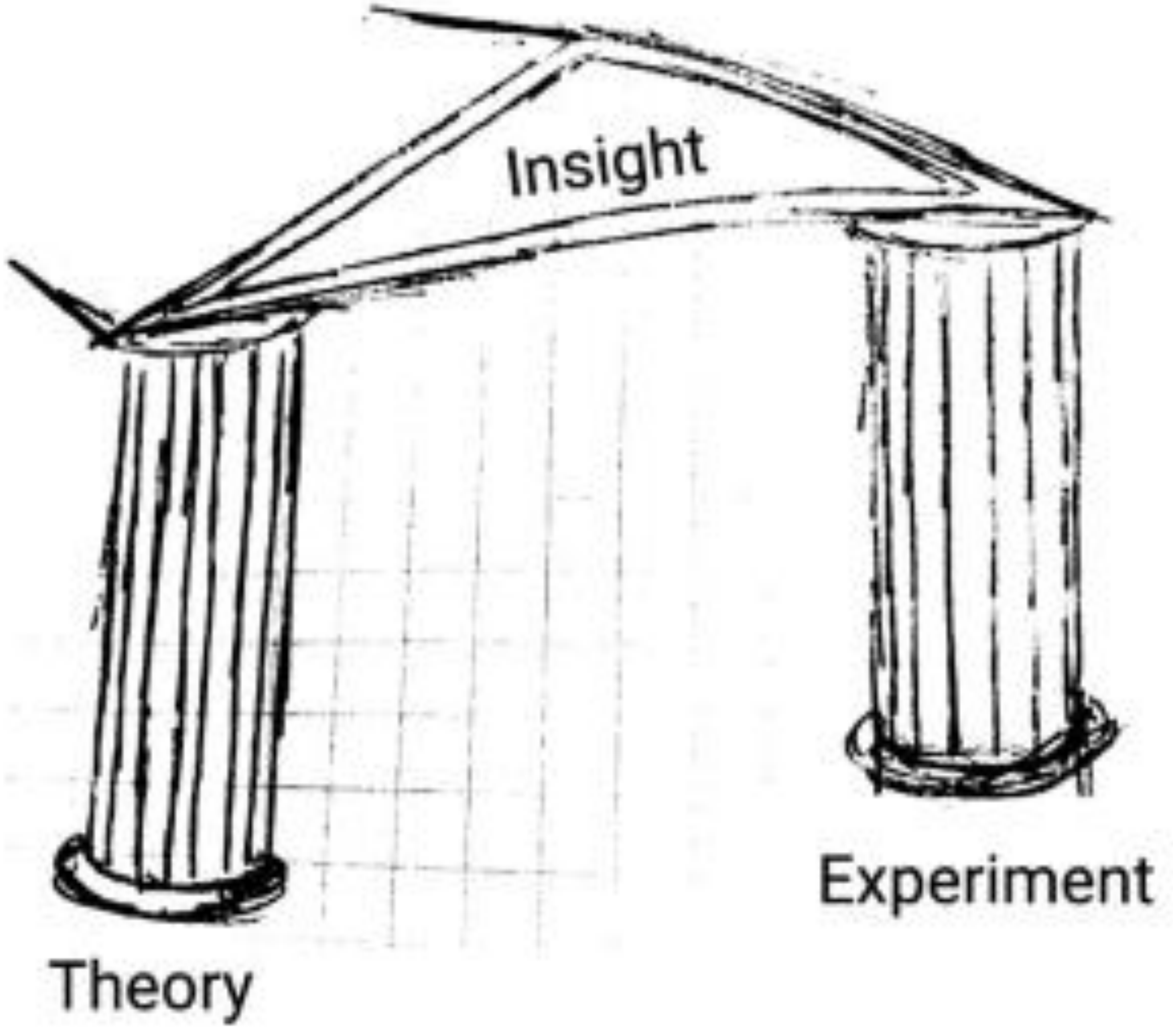

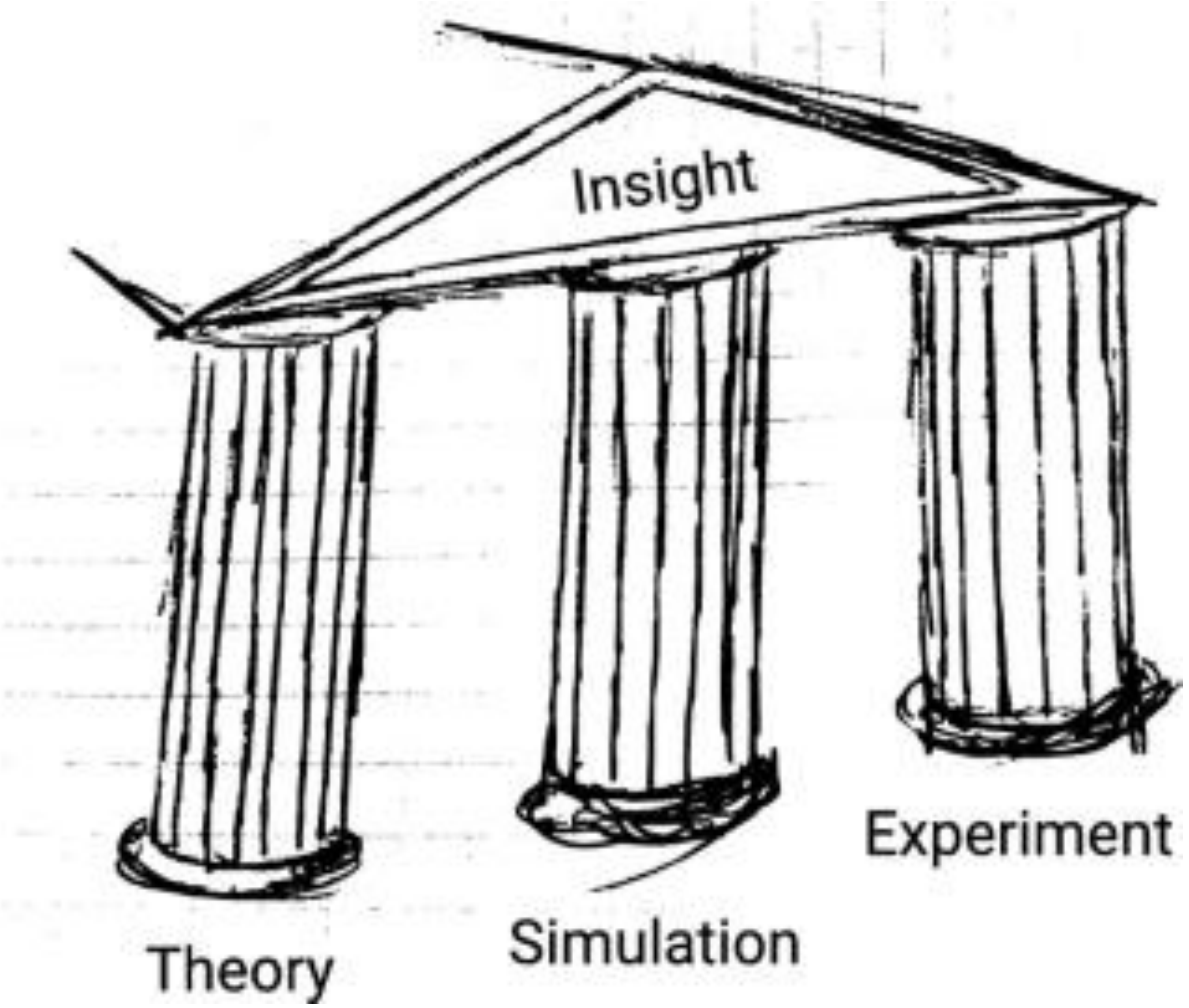

Weinzierl, T. (2021). The Pillars of Science. In: Principles of Parallel Scientific Computing. Undergraduate Topics in Computer Science. Springer, Cham.

ВВЕДЕНИЕ

Актуальность темы. Компьютерный эксперимент на атомном уровне, начиная с первого молекулярно-динамического моделирования в 1959 году, привлекает внимание материаловедов возможностью получать информацию о структуре надмолекулярных образований, их термодинамических характеристиках и механизмах процессов в материалах на уровне детальности, не доступном современным экспериментальным методам исследований. С развитием в конце XX – го и начале XXI – го веков нанотехнологий и увеличением мощности вычислительной техники эта

Введение

Разработка новых материалов требует детальных сведений о их структуре и физических механизмах на атомном уровне. Сегодня можно считать устоявшимся подход к разработке новых материалов, в котором помимо проведения экспериментальных исследований, для расширения спектра доступной информации о веществе, прогнозирования его свойств и сокращения затрачиваемых временных и материальных ресурсов используются методы компьютерного моделирования. В частности, большое распространение получили методы моделирования «из первых принципов», которые, базируясь на квантово-механических расчётах, обеспечивают хорошее согласие с экспериментальными данными [1]. При этом, становится актуальной разработка новых идей, принципов, моделей и подходов, повышающих эффективность использования данных компьютерного моделирования и предоставляющих возможности их сравнения с экспериментальными данными.

Введение

Методы компьютерного моделирования на атомном уровне позволяют значительно сократить стоимость разработки новых материалов и исследования уже существующих. Кроме этого они позволяют исследовать процессы в материалах на уровне, недоступном для существующих экспериментальных методов. Самыми точными на данный момент являются расчеты «из первых принципов», которые учитывают вклады квантовых эффектов в межатомные взаимодействия. Одним из наиболее широко используемых вариантов данного метода являются расчеты «из первых принципов» в рамках теории функционала плотности.

Diploma A. Boev (2015)

Введение

Сплавы на основе титана и ванадия имеют множество приложений в аэрокосмической индустрии, например диски газотурбинных компрессоров, лопатки и связанные с ними компоненты, также эти сплавы, легированные хромом являются хорошими кандидатами для применения в термоядерных реакторах в качестве первой стенки и внешней оболочки [1]. Для разработки таких материалов с заданными свойствами недостаточно только экспериментальных исследований, так как последние не могут в достаточной степени давать все данные, необходимые для изучения свойств и понимания процессов, протекающих в сплавах на атомном уровне. Поэтому для более подробного

Введение

Ключевой характеристикой
ся стойкость к радиационному р
процессу увеличения объема ма
ционного происхождения после
цами.

Одним из основных подходо
лов является выбор компонентно
торой происходит значительное
дефектов: вакансий и межузель
шать вероятность рекомбинации
препятствовать накоплению изб
ми дефектами, в структуре мате
распухания.

Предпоследний абзац введения

Атомистическое моделирование позволяет получать информацию о процессах в материалах на уровне детальности, недоступном экспериментальным подходам. В связи с этим методы моделирования широко используются для изучения процессов радиационного повреждения в части исследования каскадов атомных смещений и эволюции системы точечных дефектов радиационного происхождения.

Установление влияния титана на структуру и подвижность собственных точечных дефектов радиационного происхождения в ванадии будет полезно при разработке новых радиационно-стойких материалов на основе ОЦК металлов для прогнозирования их устойчивости к распуханию в условиях высокоэнергетичного облучения.

1. INTRODUCTION

Lithium-ion batteries (LIBs) have proven to be an efficient energy storage system for various applications, starting from portable electronics and ending with stationary storage. Compared to other battery technologies, LIBs posses highest energy density, power rate, and cycle life characteristics. Yet, booming development of portable electronics and electric transportation calls for even higher energy densities, while the existing LIBs are approaching their energy density limit [1–3].

The modern LIBs have volumetric and gravimetric energy densities of 770 Wh l^{-1} and 260 Wh kg^{-1}, respectively [4]. These values are limited by the capacity and redox potentials of intercalation materials used in anode and cathode. The commercially used anode materials are graphite and lithium-titanate with 372 and 180 mAh/g theoretical capacities, respectively. By replacing them with metallic lithium, the specific capacity of anode can be increased up to 3860

Main scientific journal for modeling in materials science

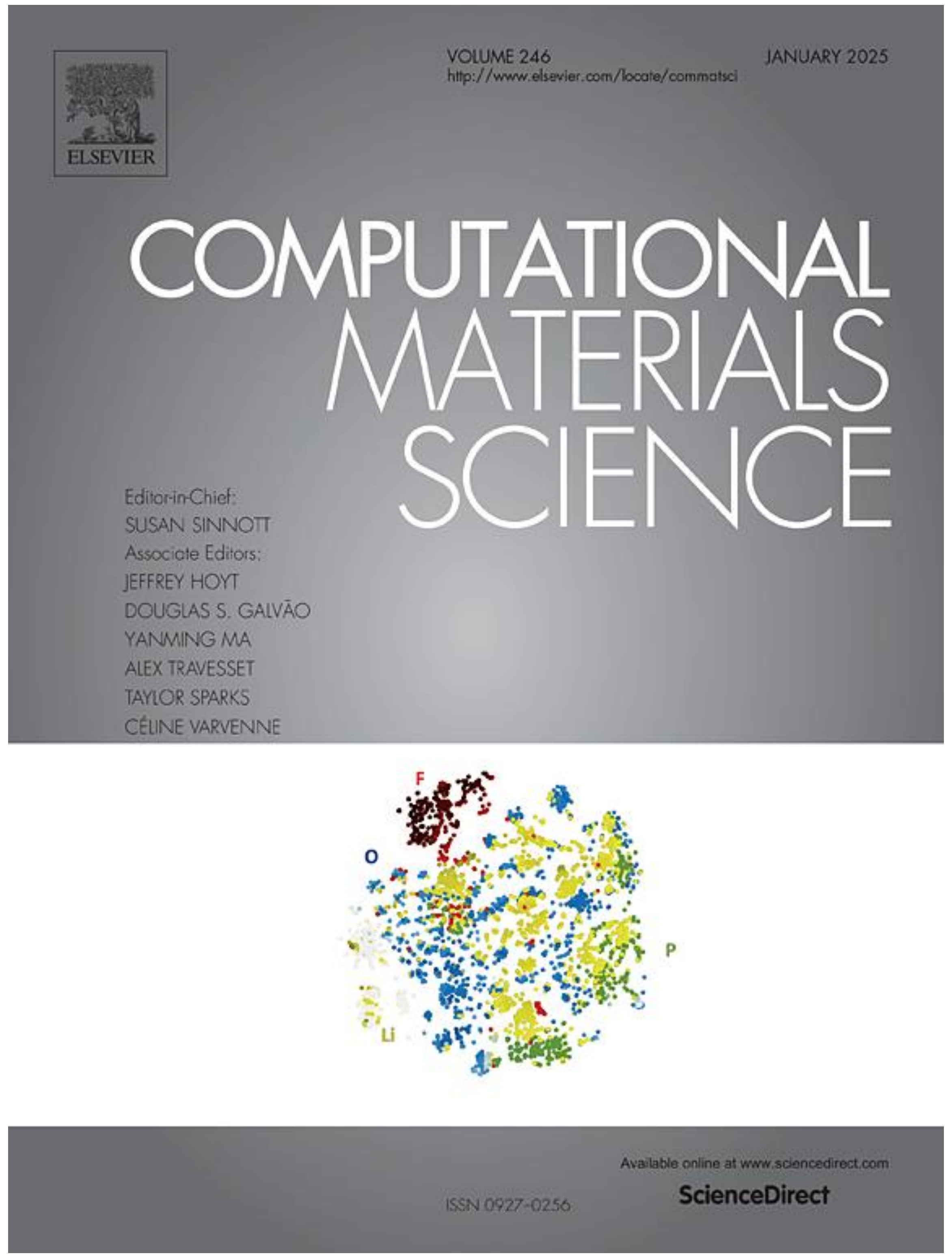

Computational Materials Science is a monthly peer-reviewed scientific journal published by Elsevier. It was established in October 1992. The editor-in-chief is Susan Sinnott. The journal covers computational modeling and practical research for advanced materials and their applications.[1]

Main scientific journal for modeling in materials science

Computational Materials Science is a monthly peer-reviewed scientific journal published by Elsevier. It was established in October 1992. The editor-in-chief is Susan Sinnott. The journal covers computational modeling and practical research for advanced materials and their applications.[1]

Reviewers' comments:

Computational materials Science no longer accepts papers whose sole contribution is the ground state properties of a compound. These computations are considered routine.

Apr 29, 2020	Reject

Let’s move on to synthesis

How to synthesize the material?

How to synthesize the material?

1. Determine the desired composition and crystal structure

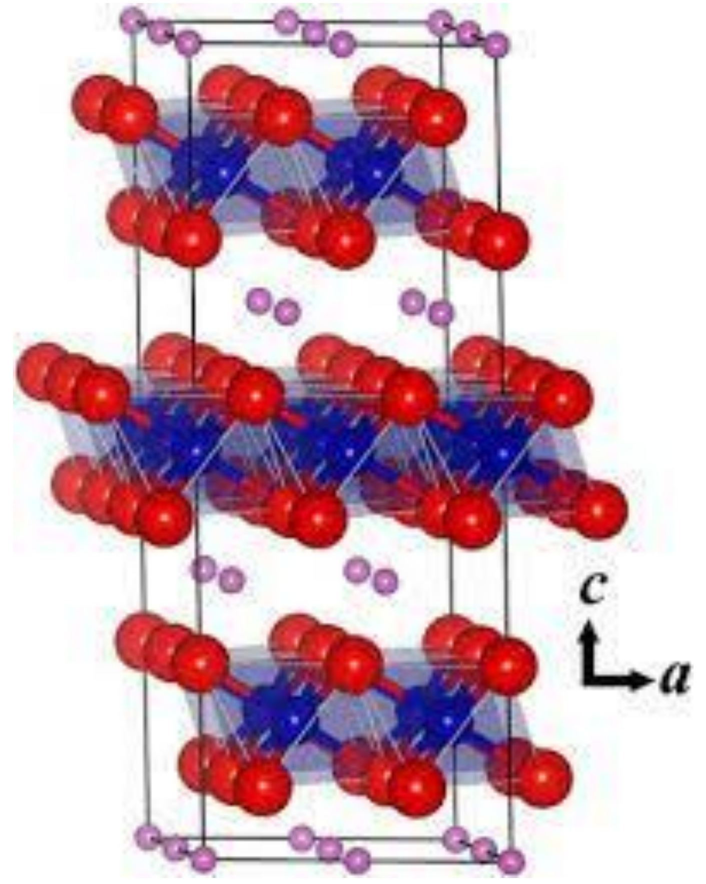

How to synthesize the material?

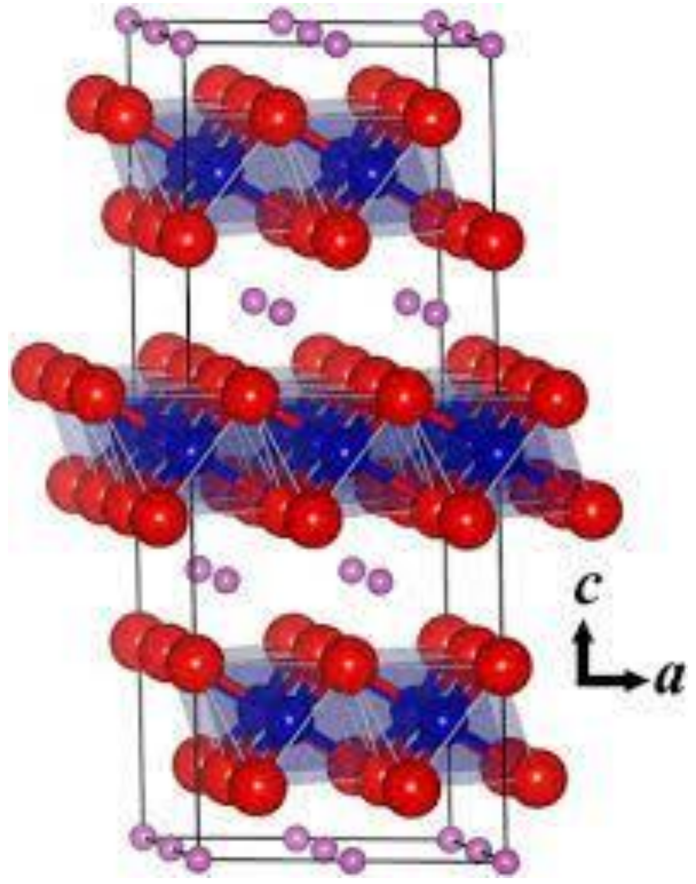

1. Determine the desired composition and crystal structure

2. Determine the recipe

How to synthesize the material?

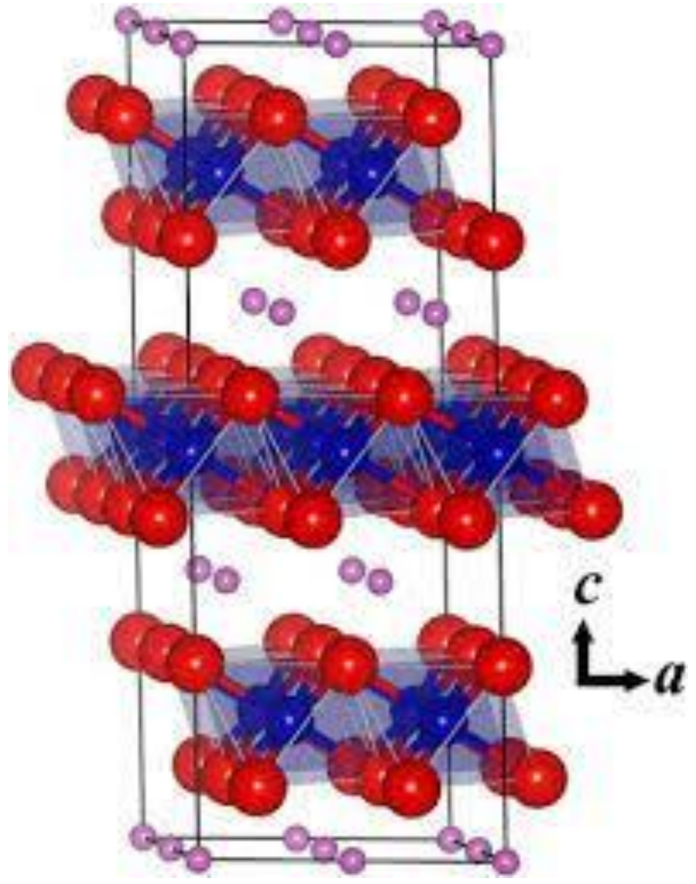

1. Determine the desired composition and crystal structure

2. Determine the recipe

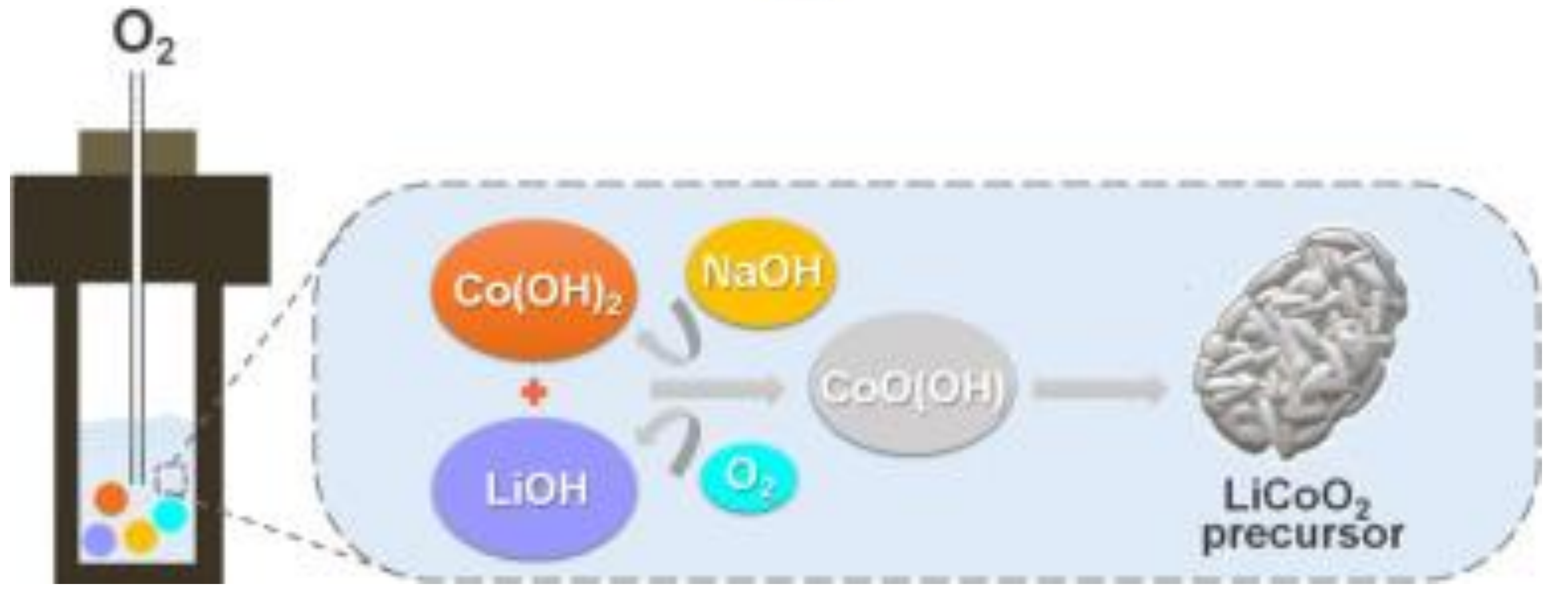

3. Follow the receipt

How to synthesize the material?

1. Determine the desired composition and crystal structure

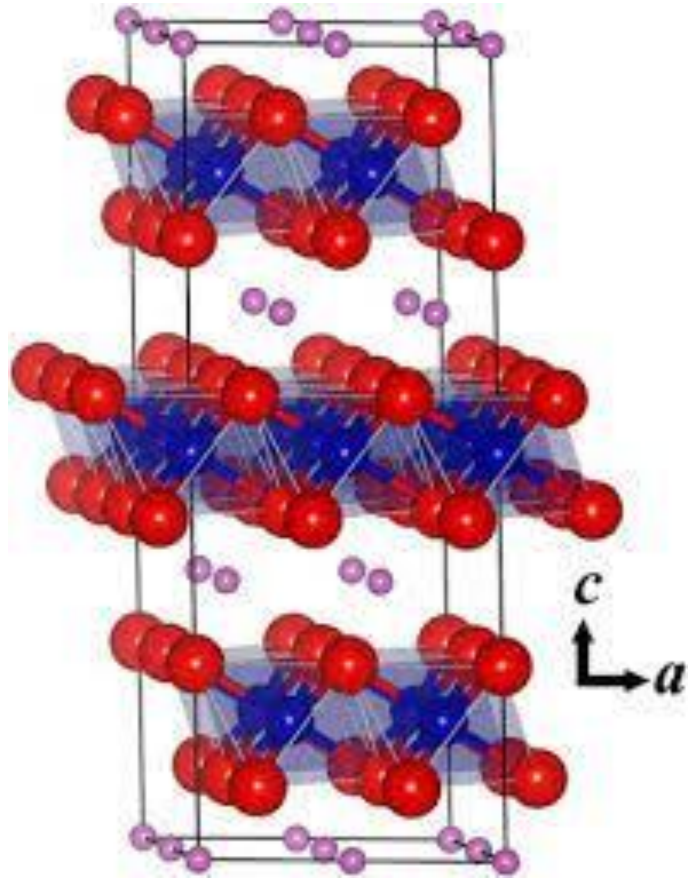

2. Determine the recipe

3. Follow the receipt

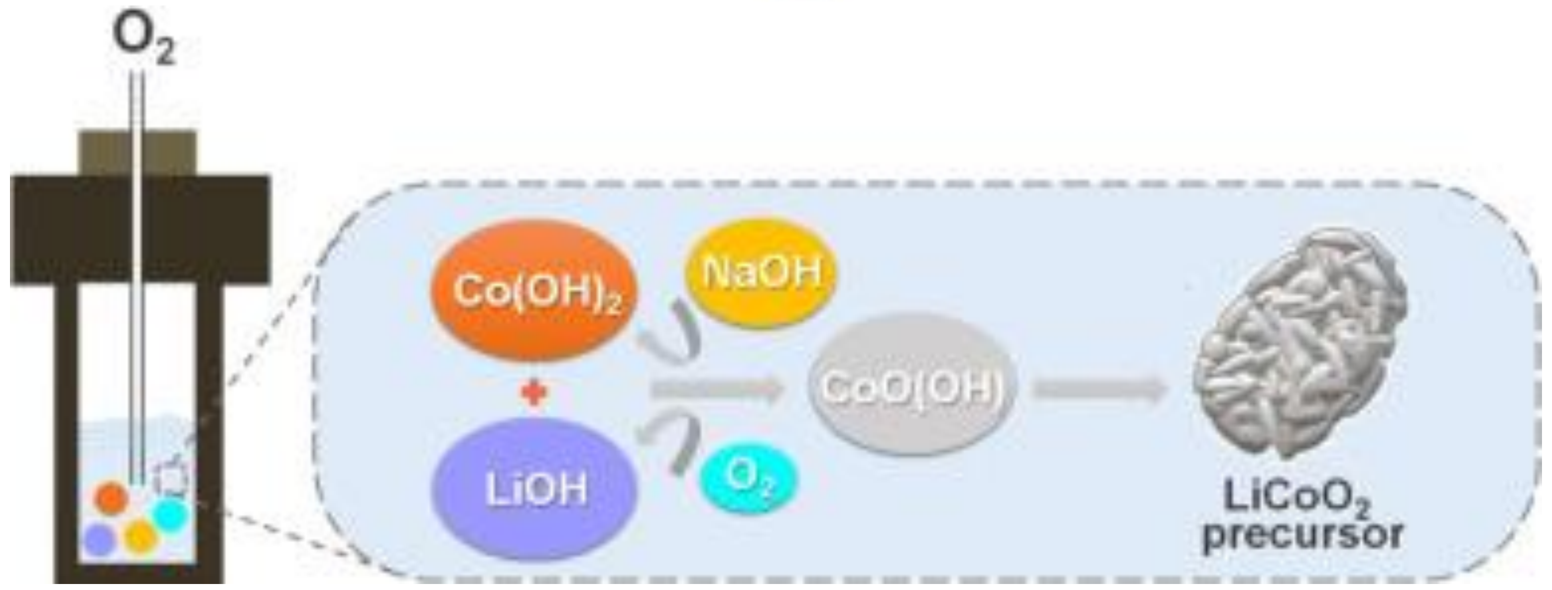

4. Enjoy your result!

How can modeling help you with each of these steps?

Step 1. Determine the desired composition and crystal structure

What material needs to be synthesized?

Prof. **A. Abakumov**

Dr. **A. Savina**

Case 1. You need new material for any application

Answer: High-throughput DFT screening of new materials

General principle of screening methodology

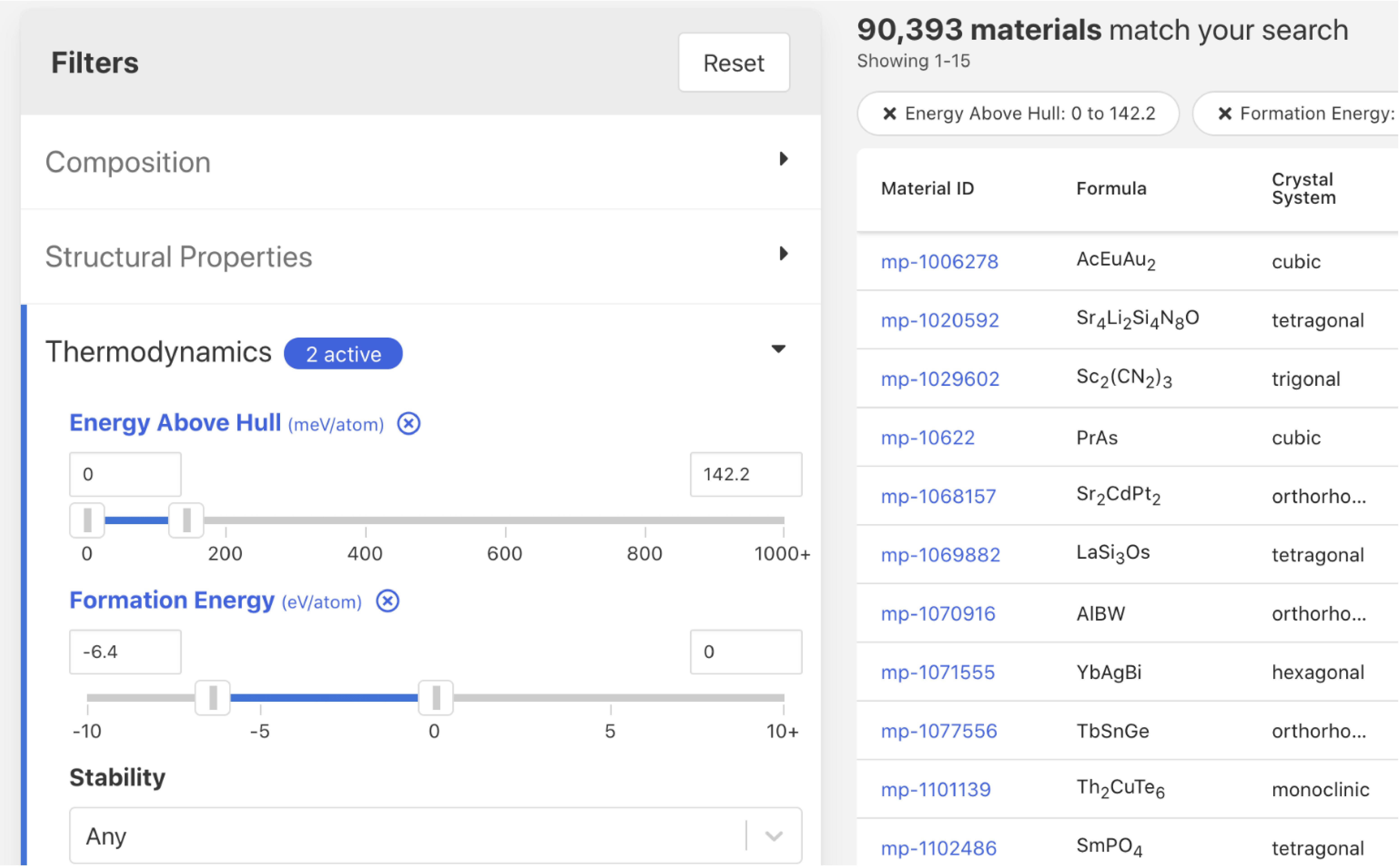

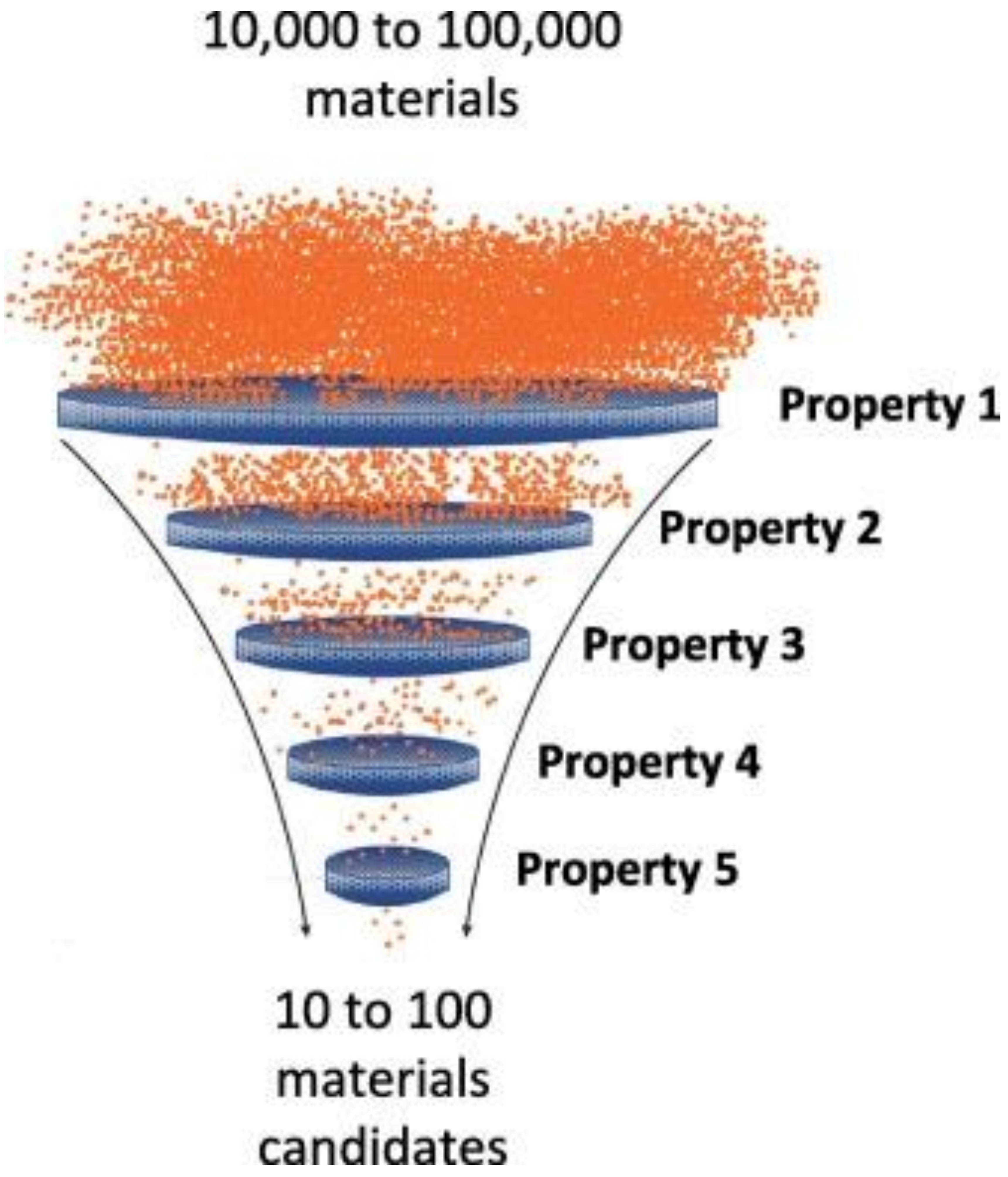

1. Take materials database

2. Set up a property funnel

Screening of new cathode materials for Li-O_2 batteries (Our)

Requirements to cathodes in Li-O_2:

- Good electronic conductivity
- Stability in highly porous form
- Stability of surface to oxidation and passivation

Our screening descriptors — **N_{AxBy} compounds**

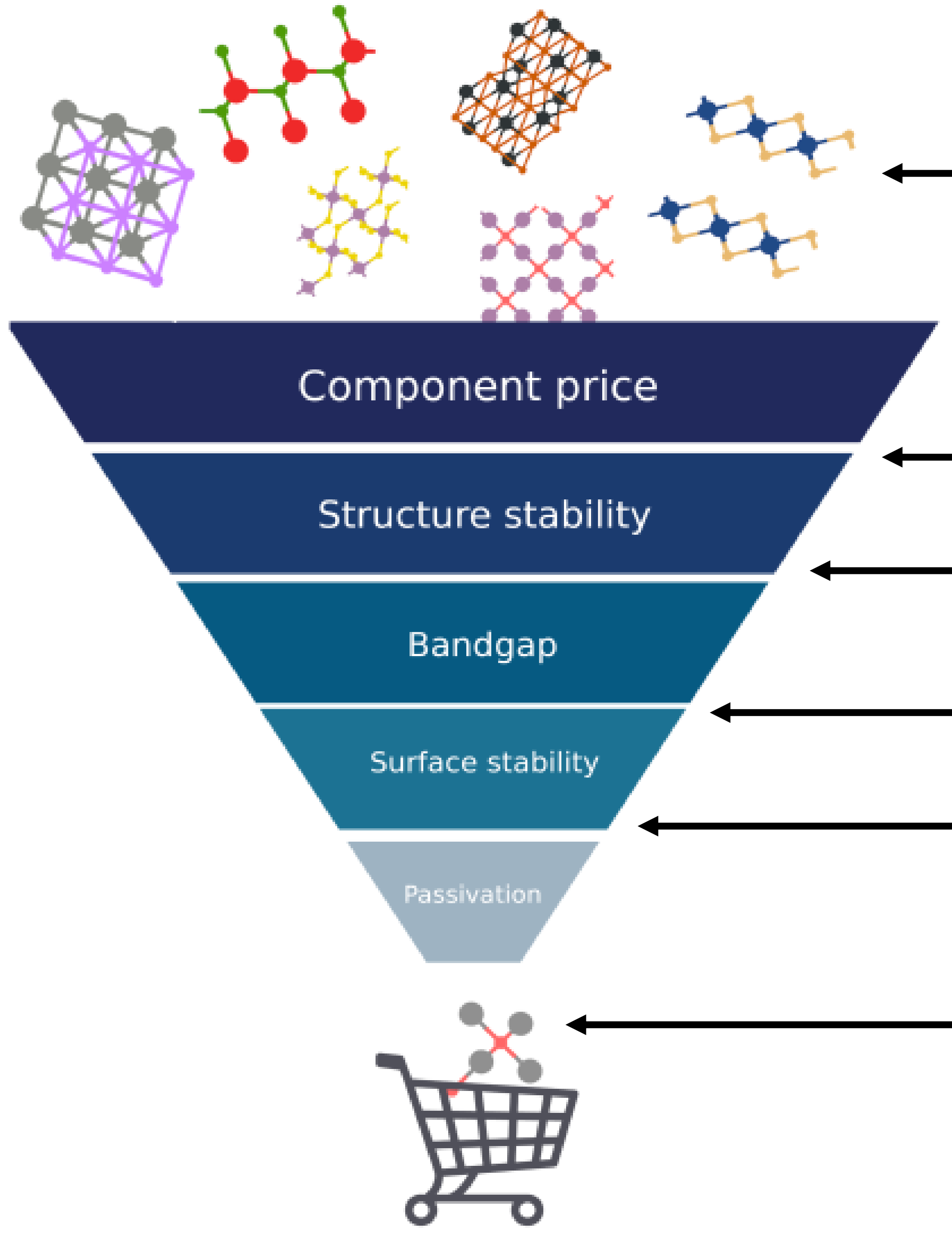

2755
242
230
99
33
5

VO$_2$ (P4$_2$/mnm,Tetragonal)

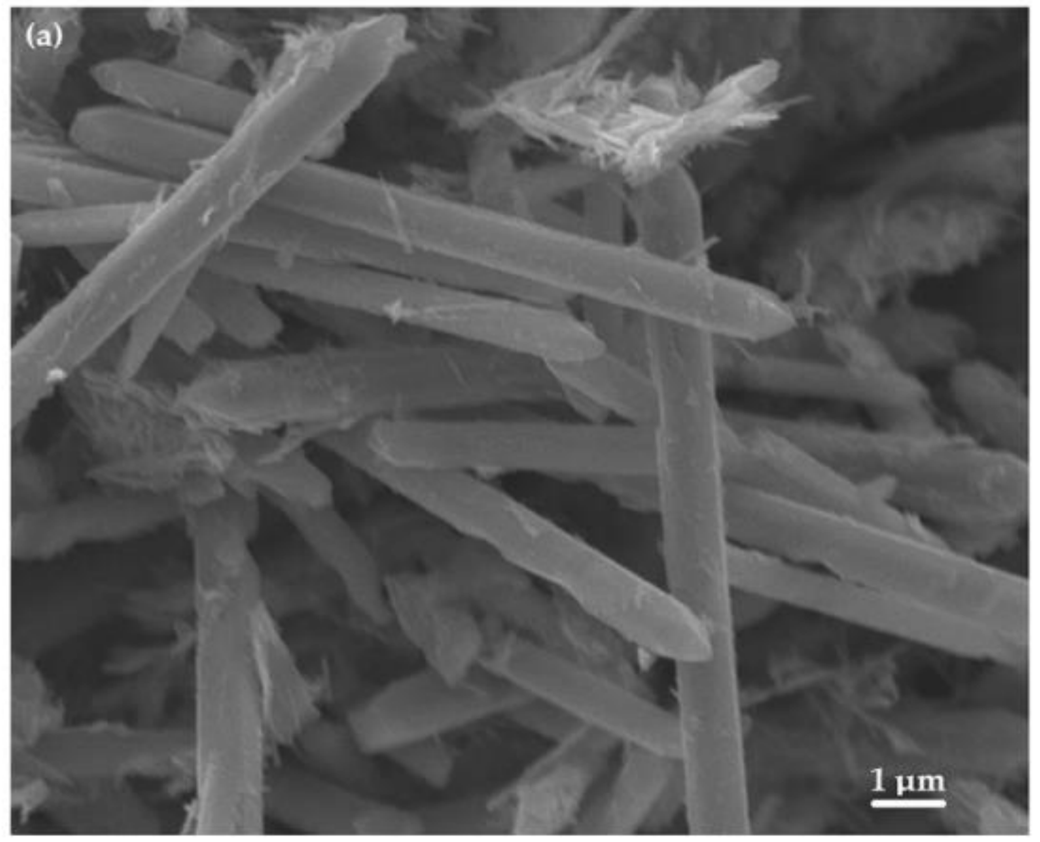

Mjejri, I. et. al. Ceramics International, 42(5), 2016

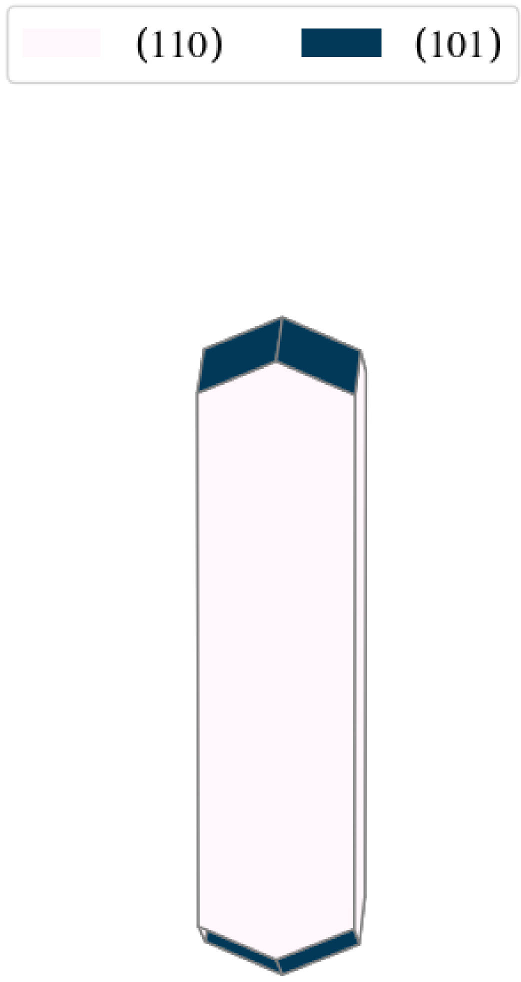

Passivation layer formation

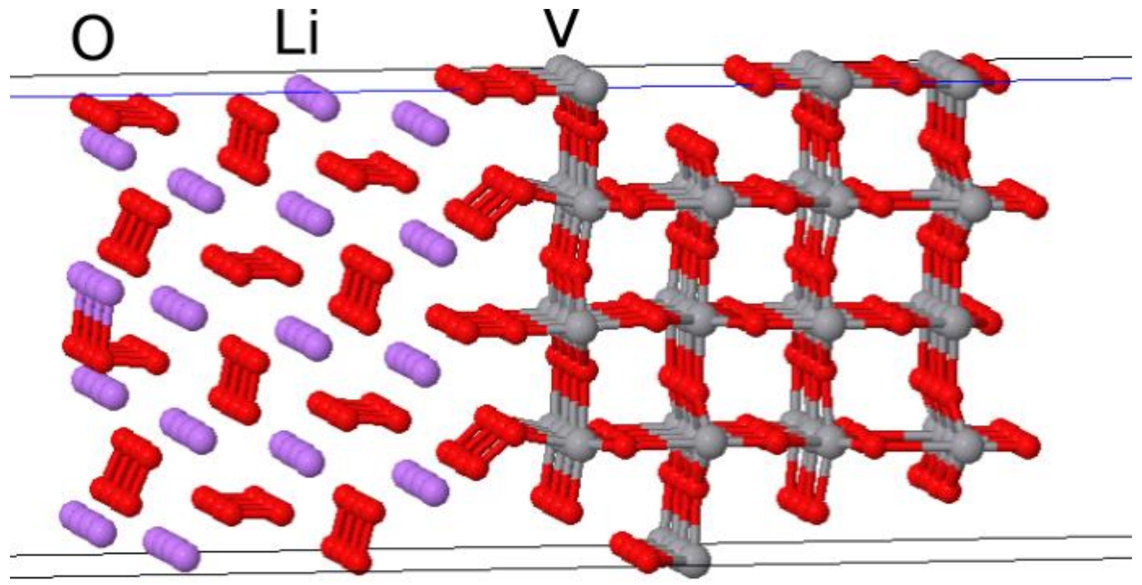

Boev A. O., Aksyonov D.A et al. // Comp.Mat. Sci. Volume 197, 2021, 110592

Screening for solid-state Li-ion conductors

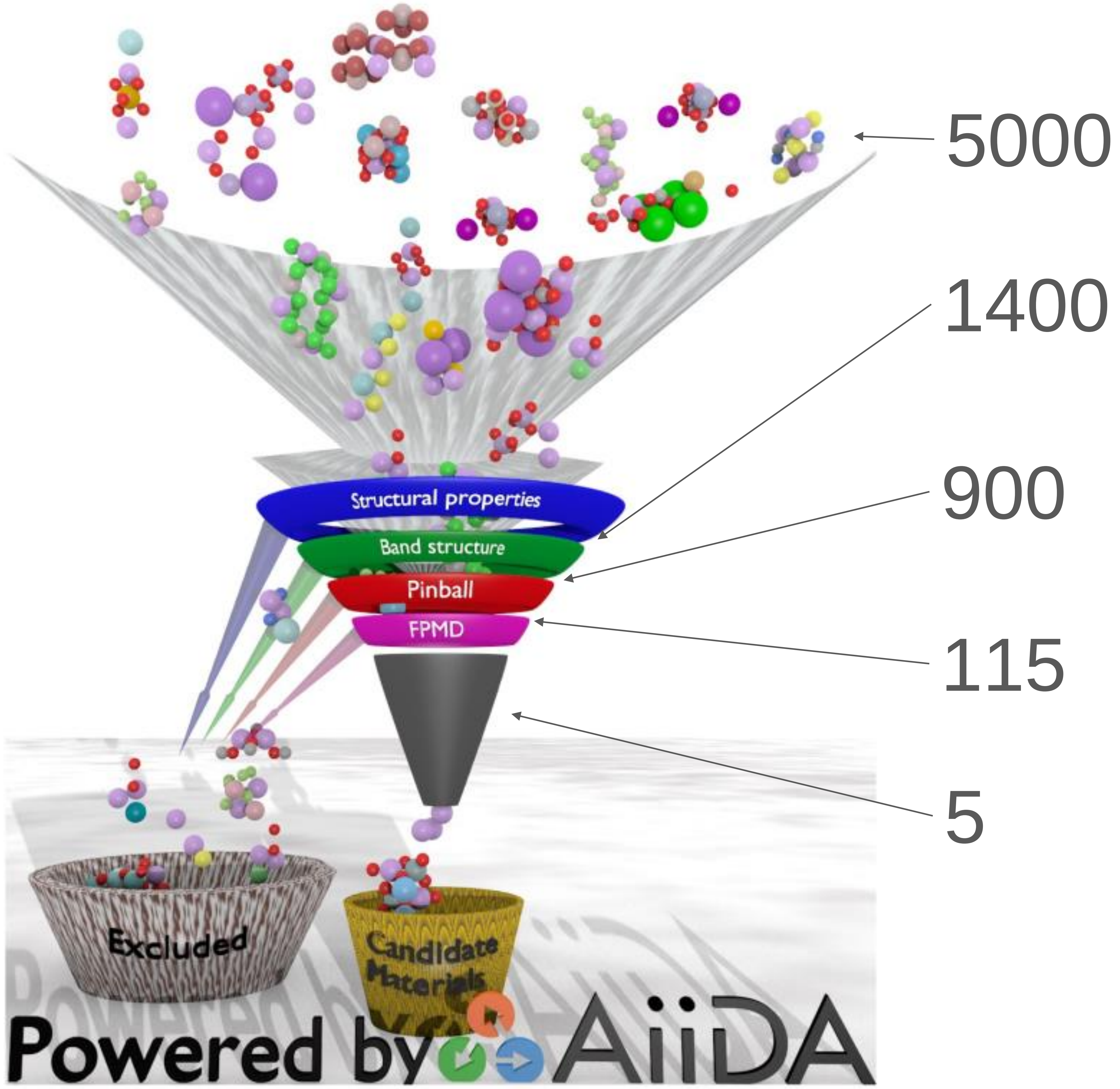

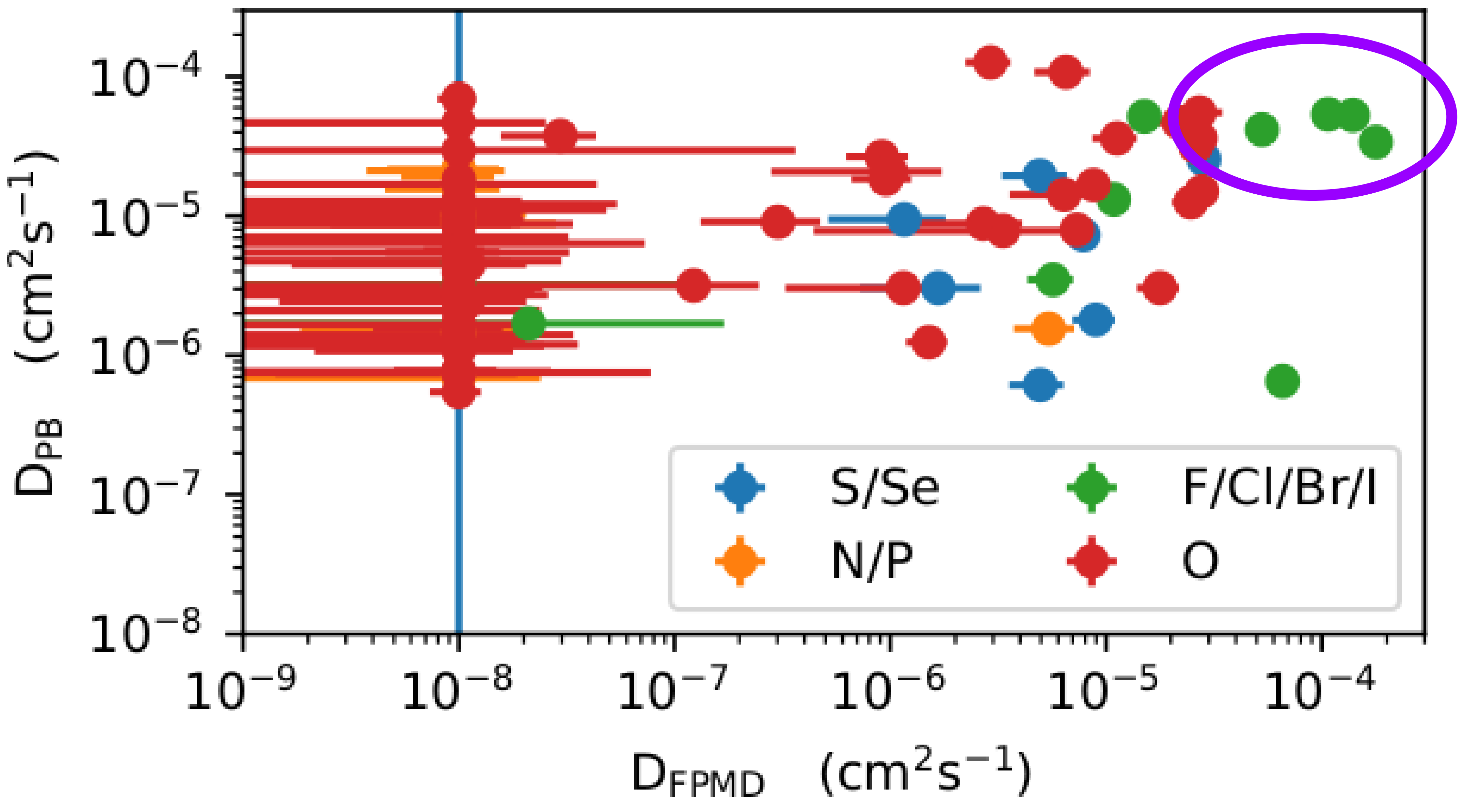

It was found five materials with fast ionic diffusion: Li-oxide chloride $\mathbf{Li_5Cl_3O}$, the doped halides $\mathbf{Li_2CsI_3}$, $\mathbf{LiGaI_4}$, and $\mathbf{LiGaBr_3}$, or the Li-tantalate $\mathbf{Li_7TaO_6}$.

Kahle L. et al. (2020). Energy & Environmental Science, 13(3), 928-948. IF = 32.4

Discovering a new class of fluoride solid-electrolyte

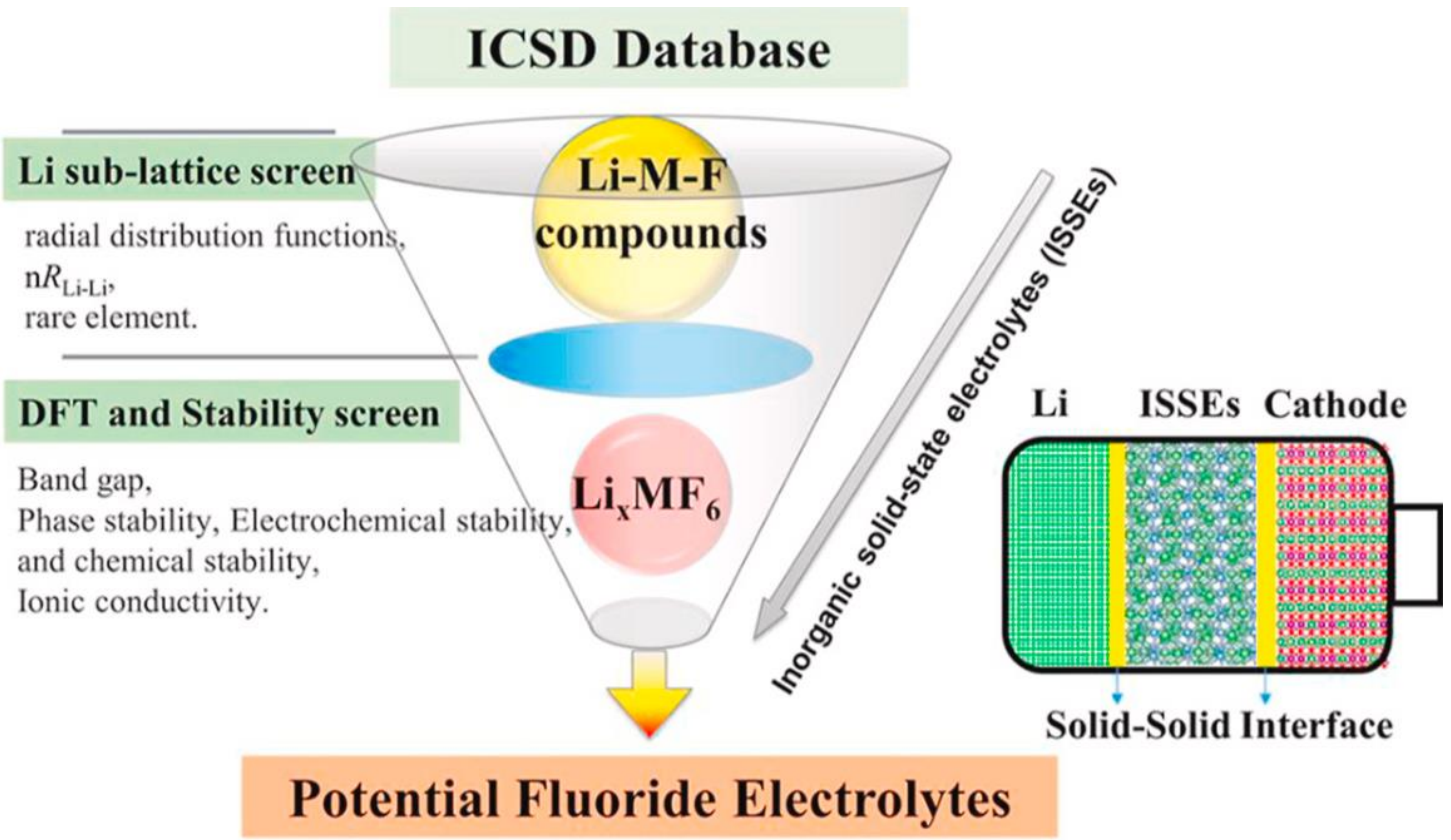

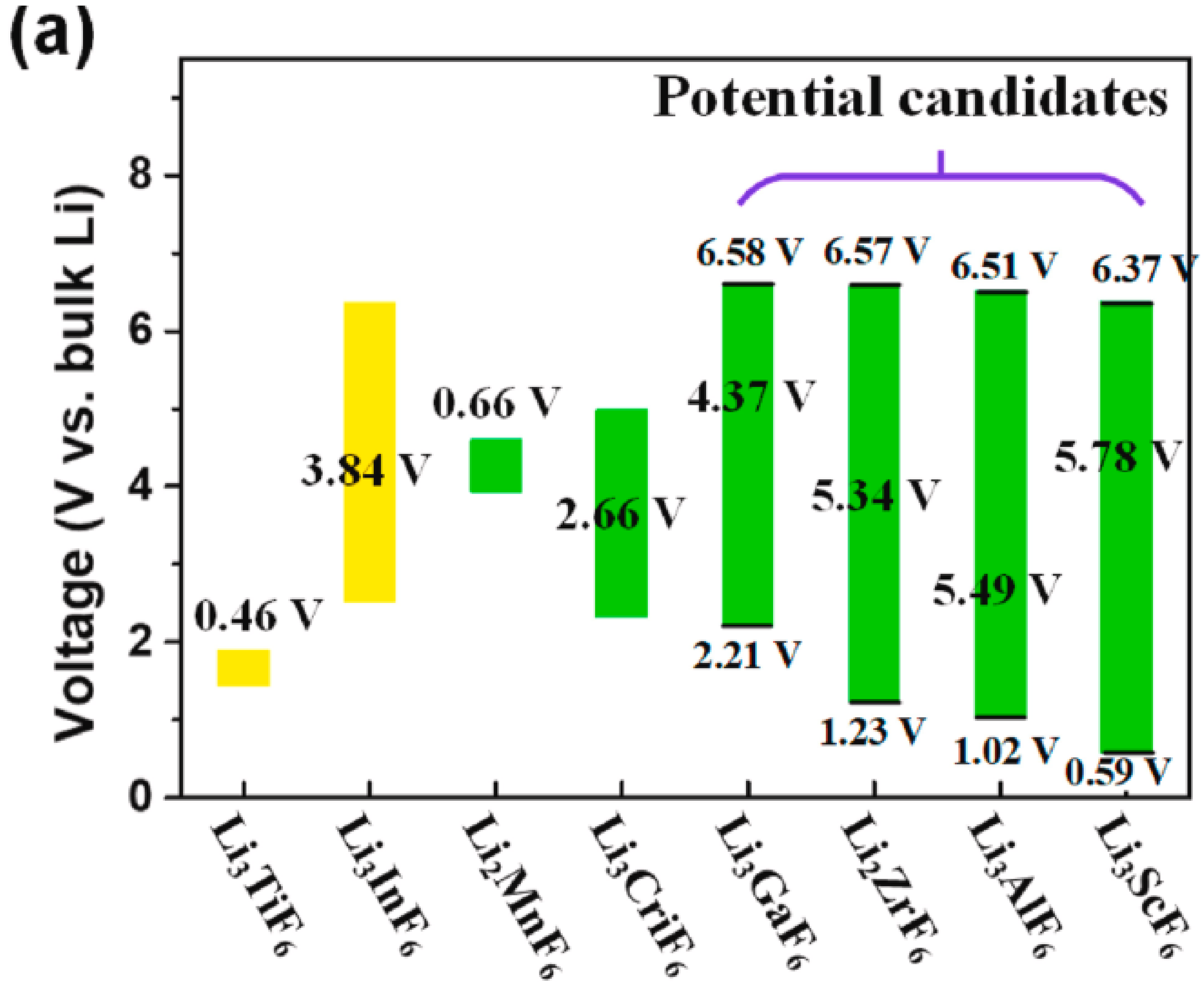

Zhang, B.et al. (2021). Nano Energy, 79, 105407.

Screening for new antiperovskite solid electrolytes

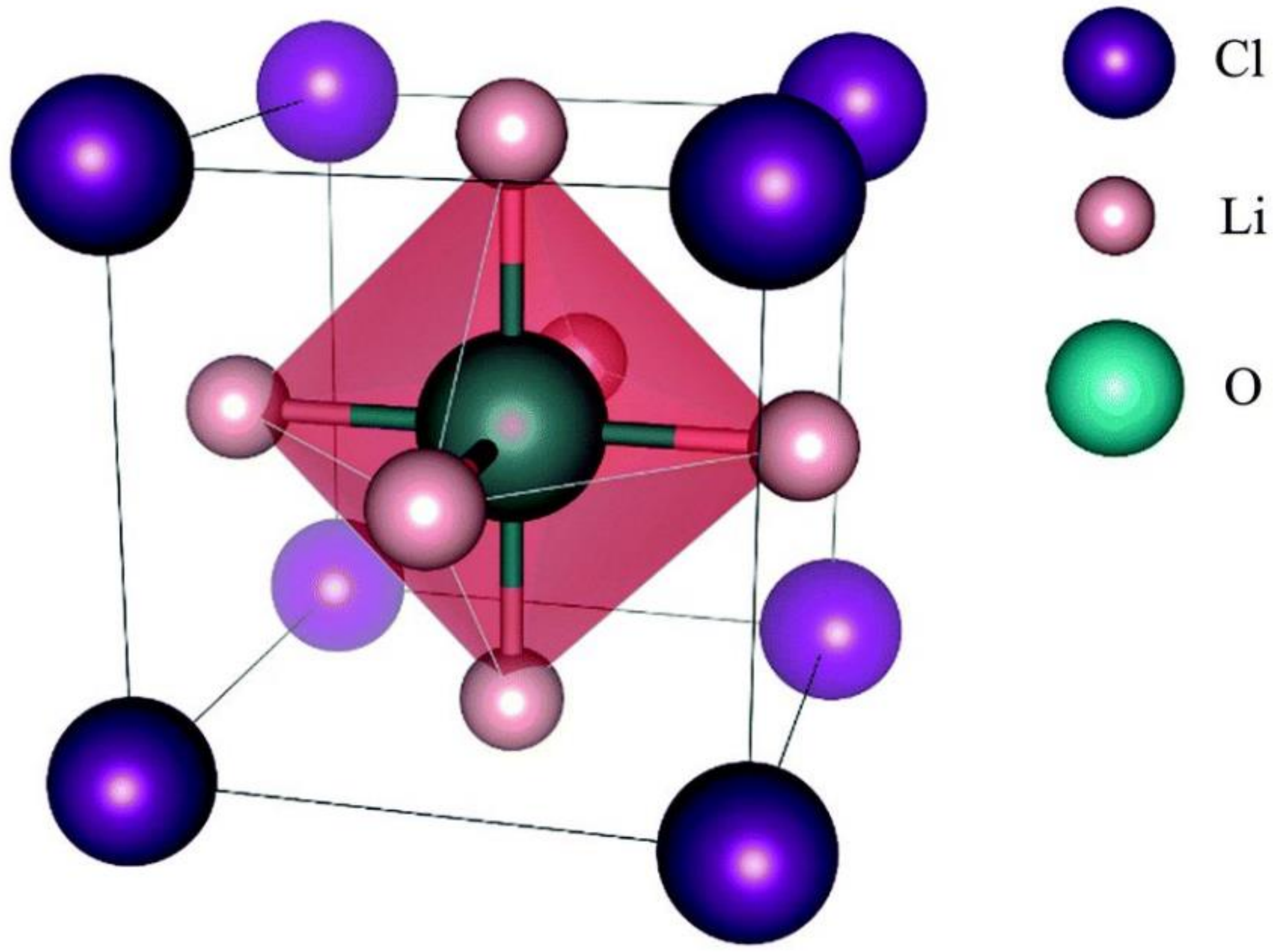

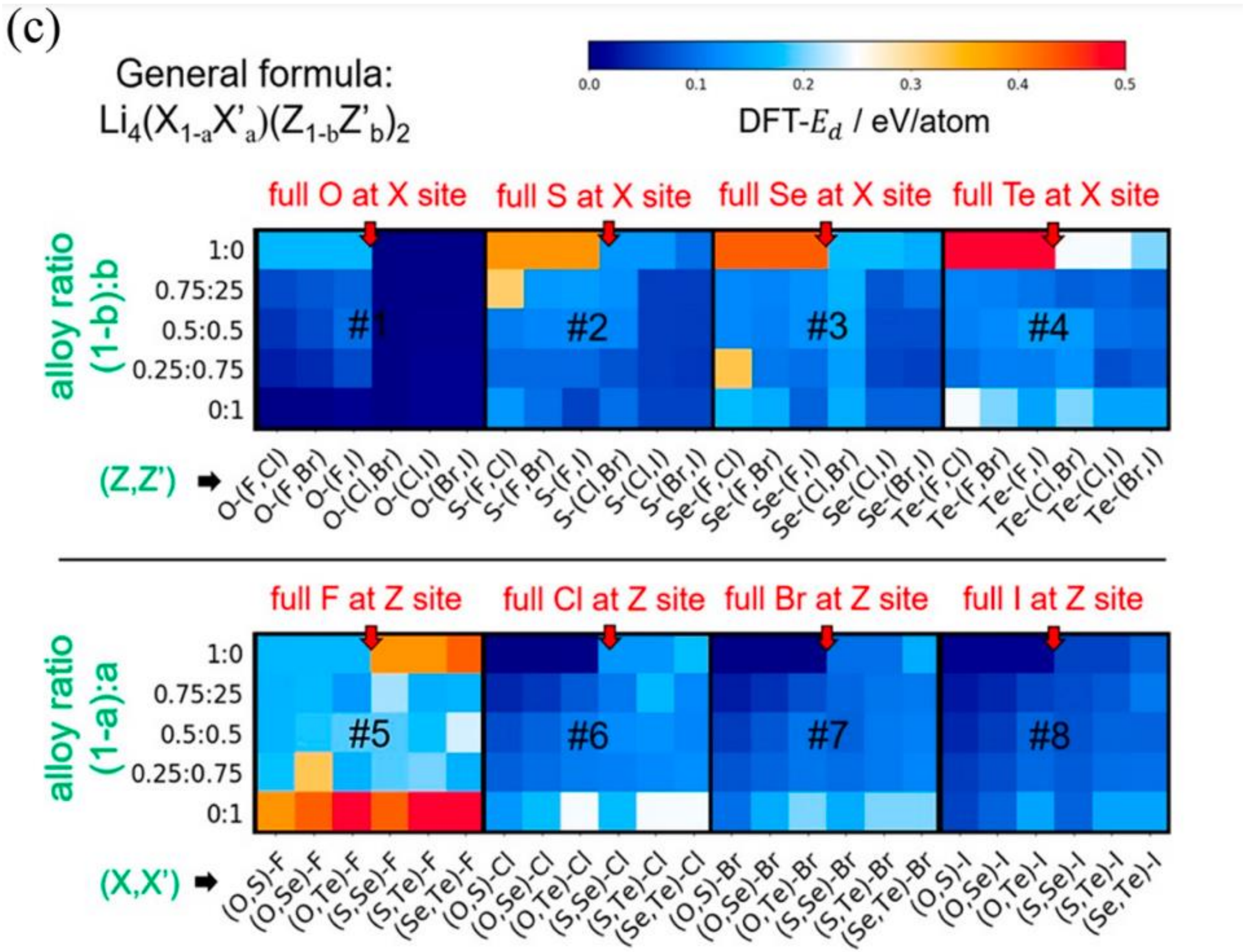

Jalem, R. et al. Chem. Mater. 2021, 33, 5859−5871.

What properties can be used for screening?

1. Composition or structure type
2. Phase stability
3. Bandgap
4. Ionic conductivity
5. Voltage window
6. Deintercalation potential (OCV)
7. Point defect energetics
8. And so on…

Case 2. You need to improve known material

Answer: DFT screening of dopants

Segregation dopants for $LiCoO_2$

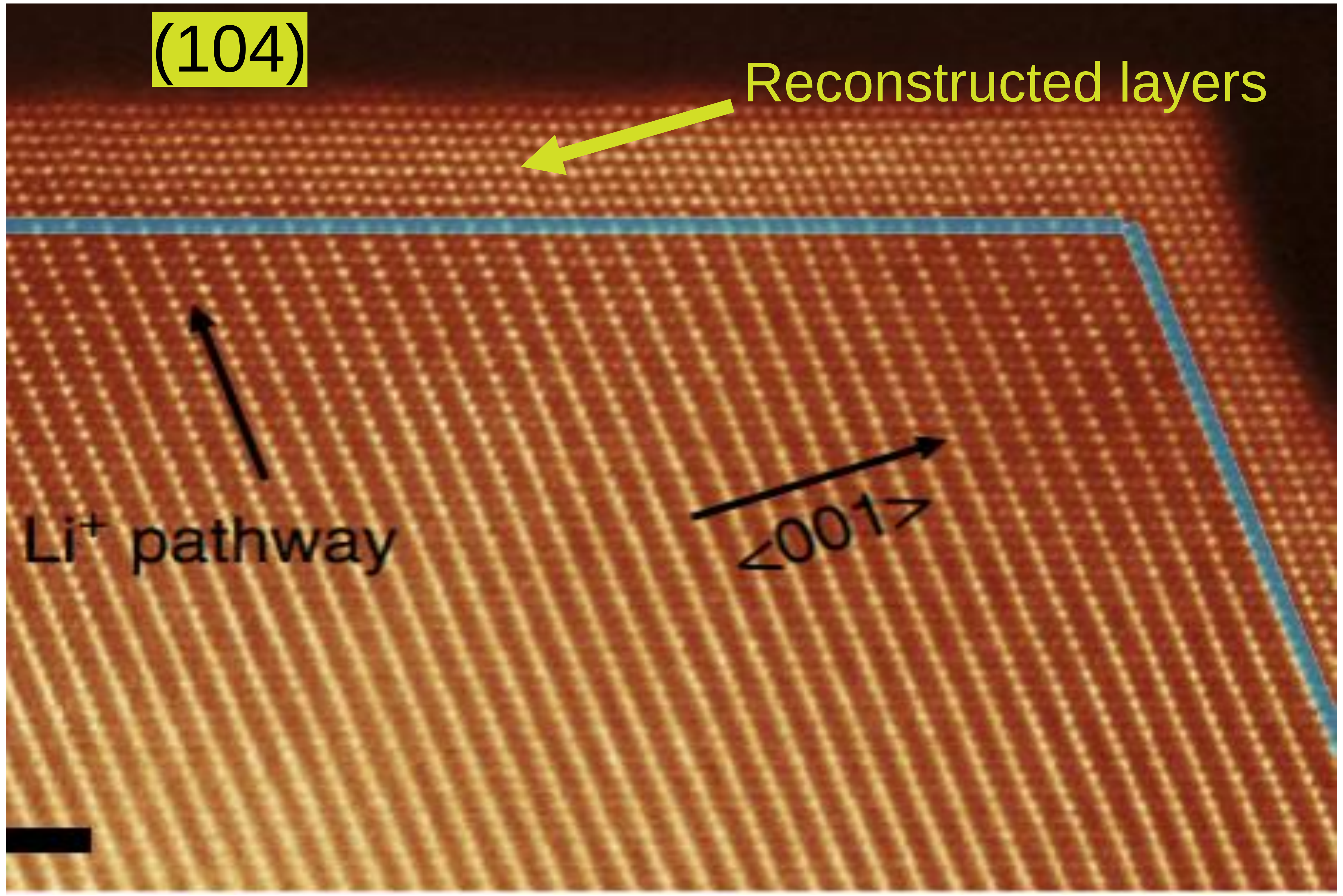

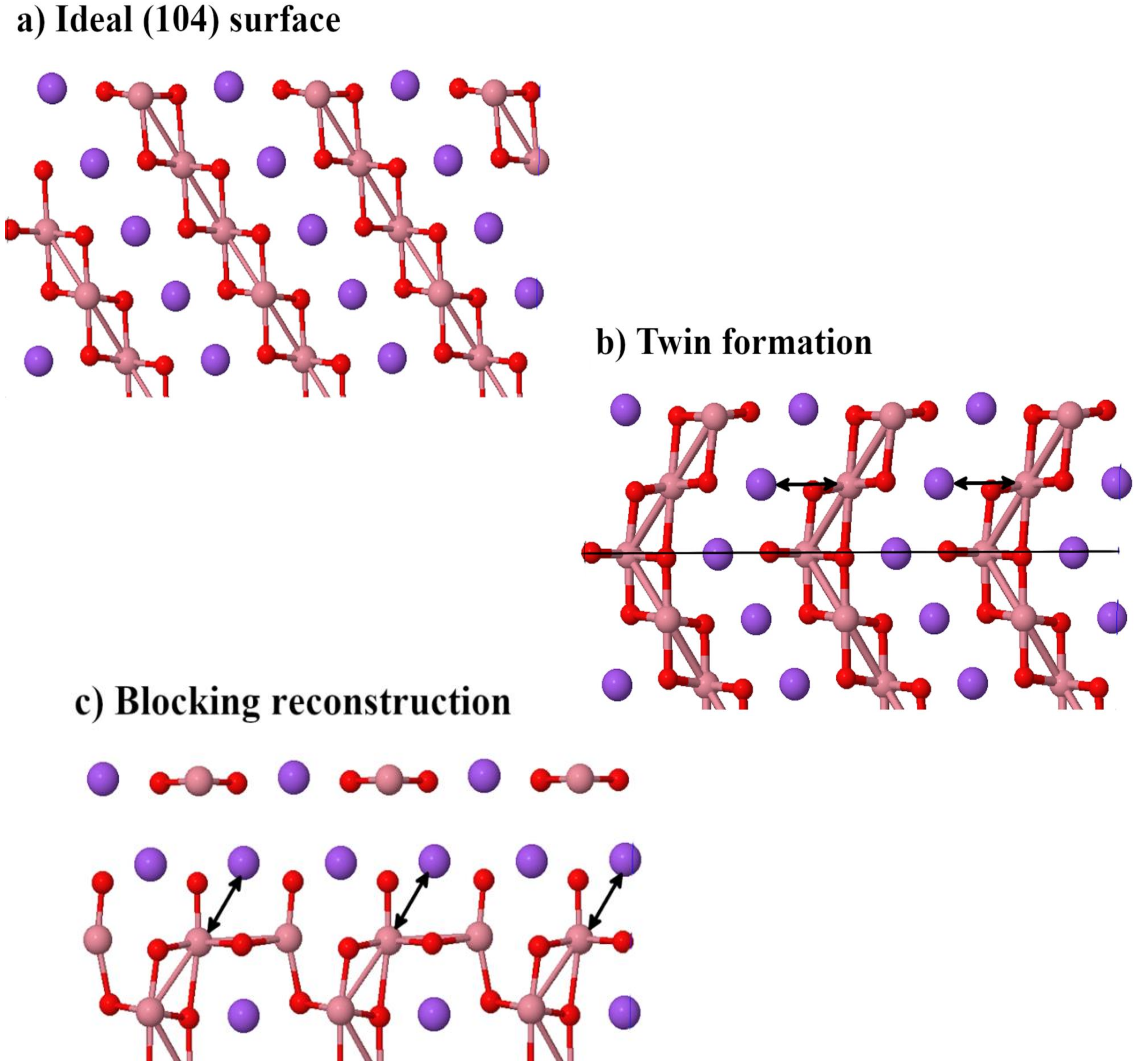

Segregation dopants for $LiCoO_2$

Schematic representation of a doped LCO particle,
where a surface enhancement takes place during annealing

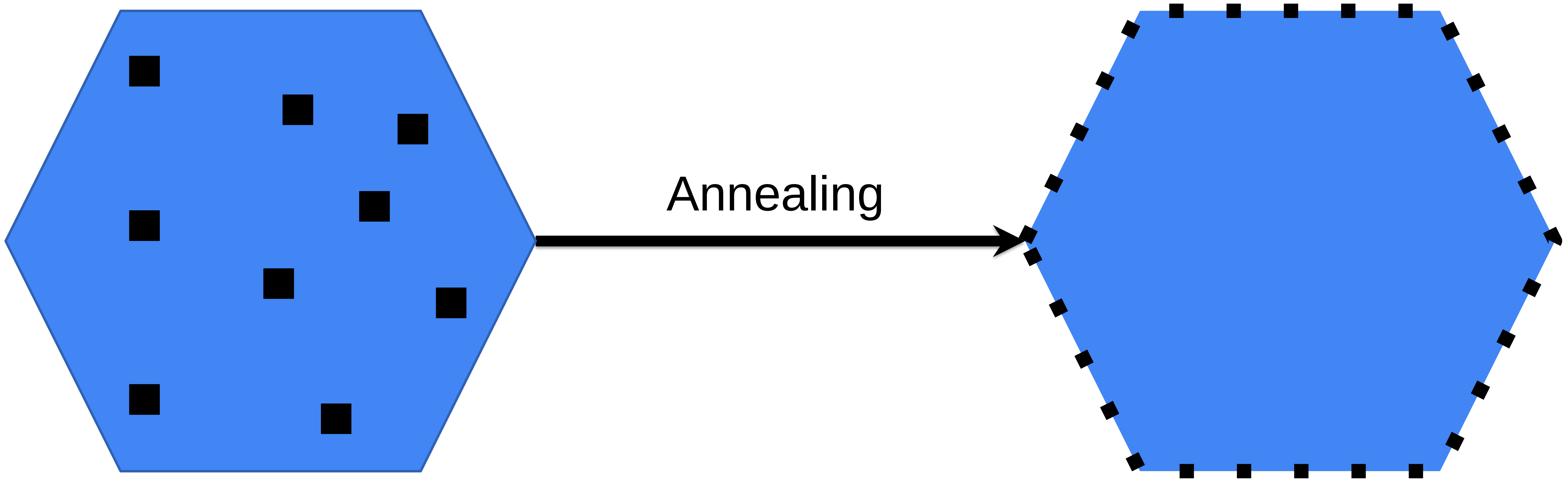

Segregation dopants for $LiCoO_2$

E_{seg} =

Surface position

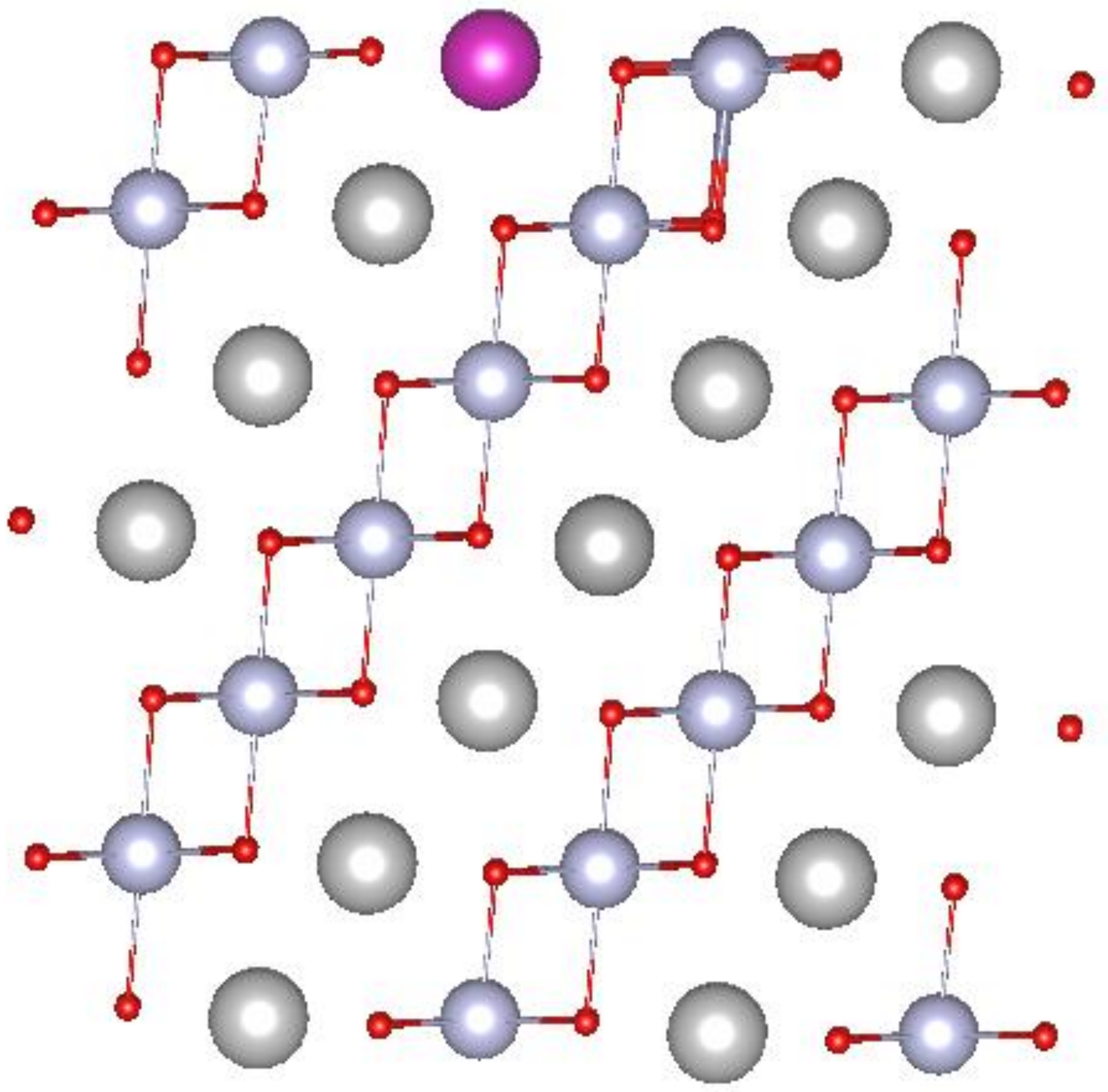

−

Bulk position

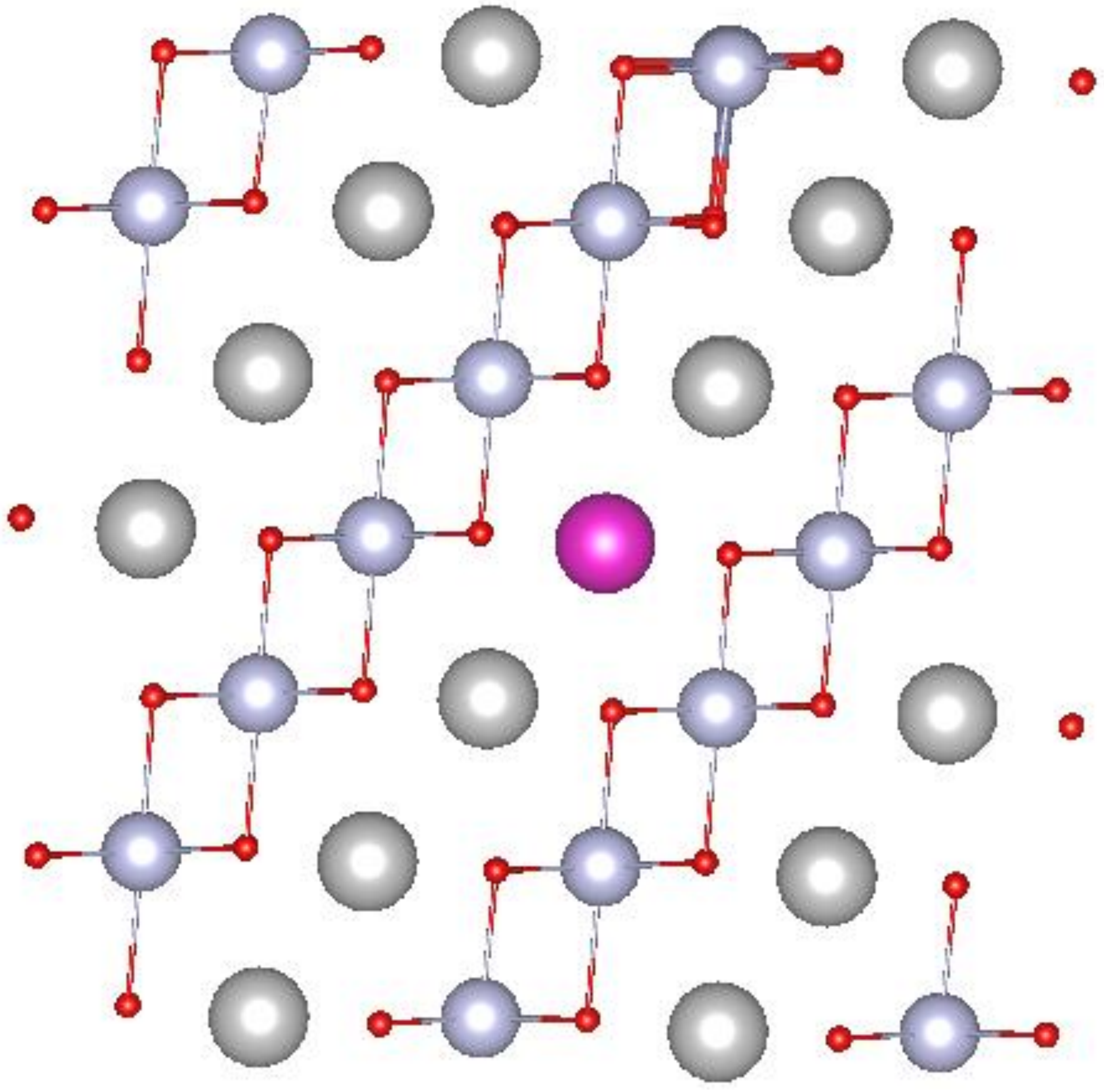

Segregation dopants for $LiCoO_2$

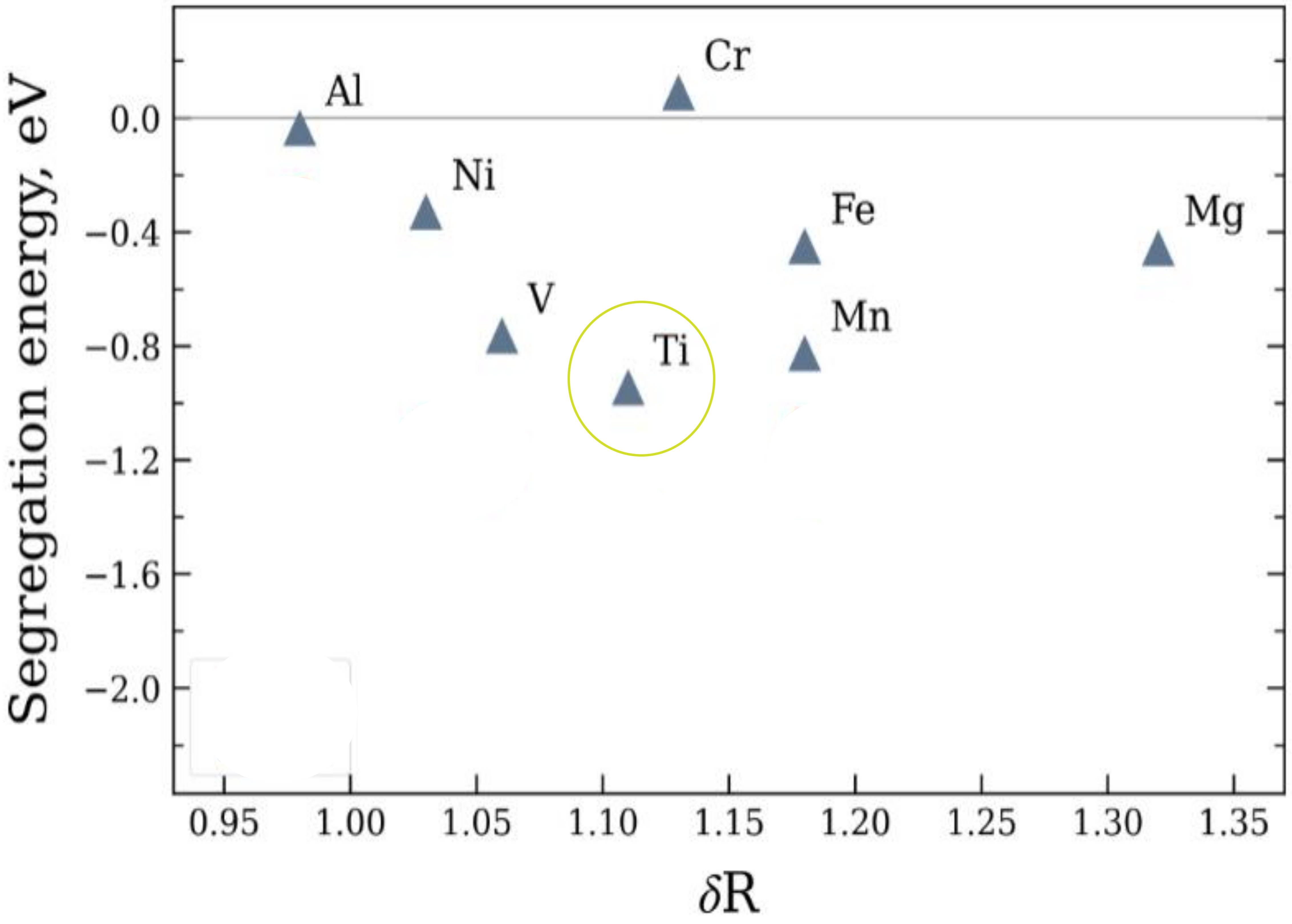

Boev, A. O. et al. *Phys. Rev. Mat.* **8**, 055403 (2024)

- Daheron et al. using XPS **does not detect Al surface segregation**, which agrees with 0 eV calculated segregation
- Li et al. shows with EDS mapping **monolayer Ti segregation** agreeing with strongly negative −0.94 eV energy
- Fe, Ni, Mn should segregate. What about experimental verification?

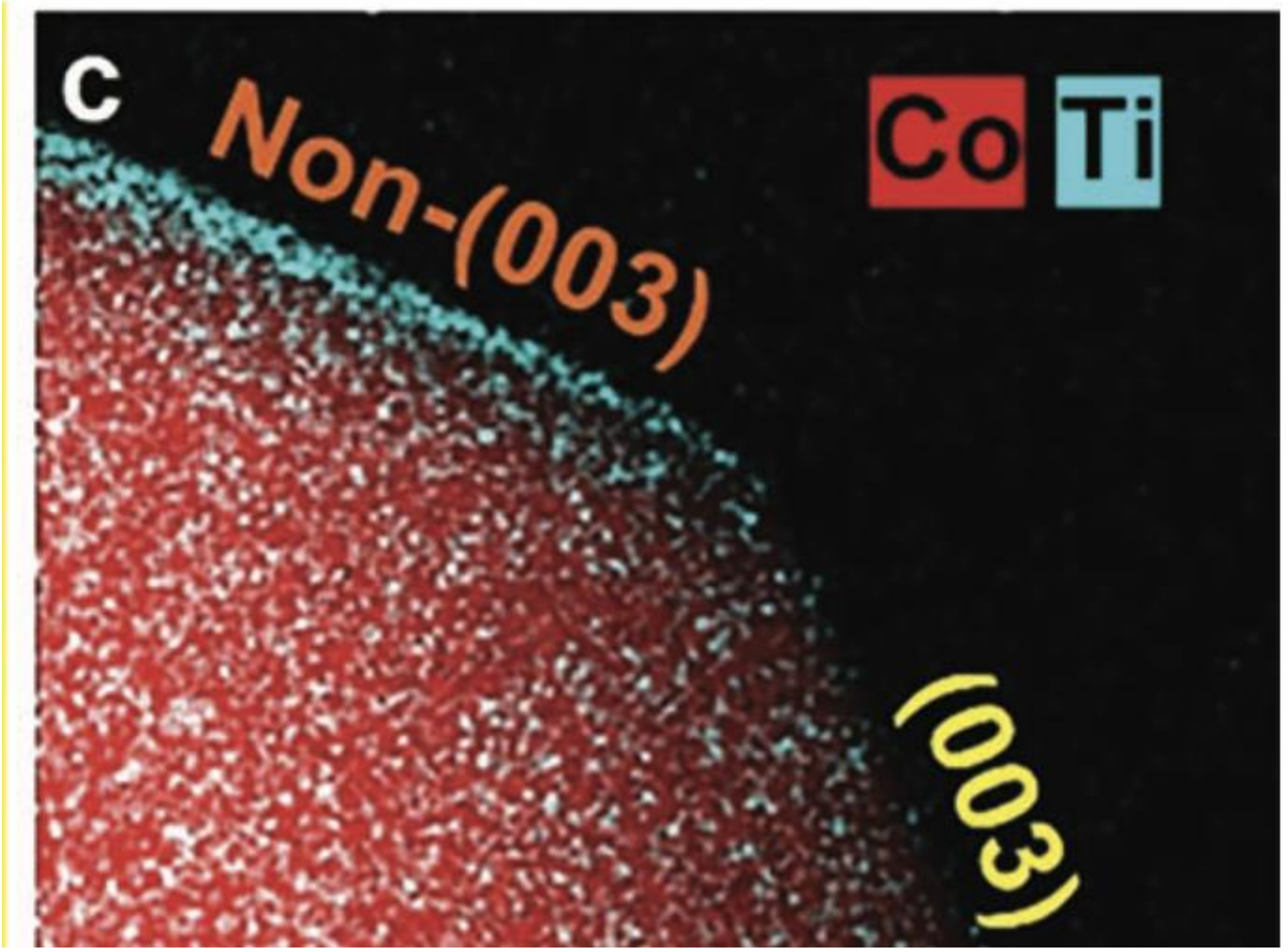

Li et al. *Small* **2023**, 2303474,
Daheron et al., *Chem. Mater*. 2009, 21, 5607–5616

Anomalous metal segregation in Li-rich material

“Ruthenium segregates out as metallic nanoclusters on the reconstructed surface. Our calculations show that the unexpected ruthenium metal segregation is due to its thermodynamic insolubility in the oxygen deprived surface.“

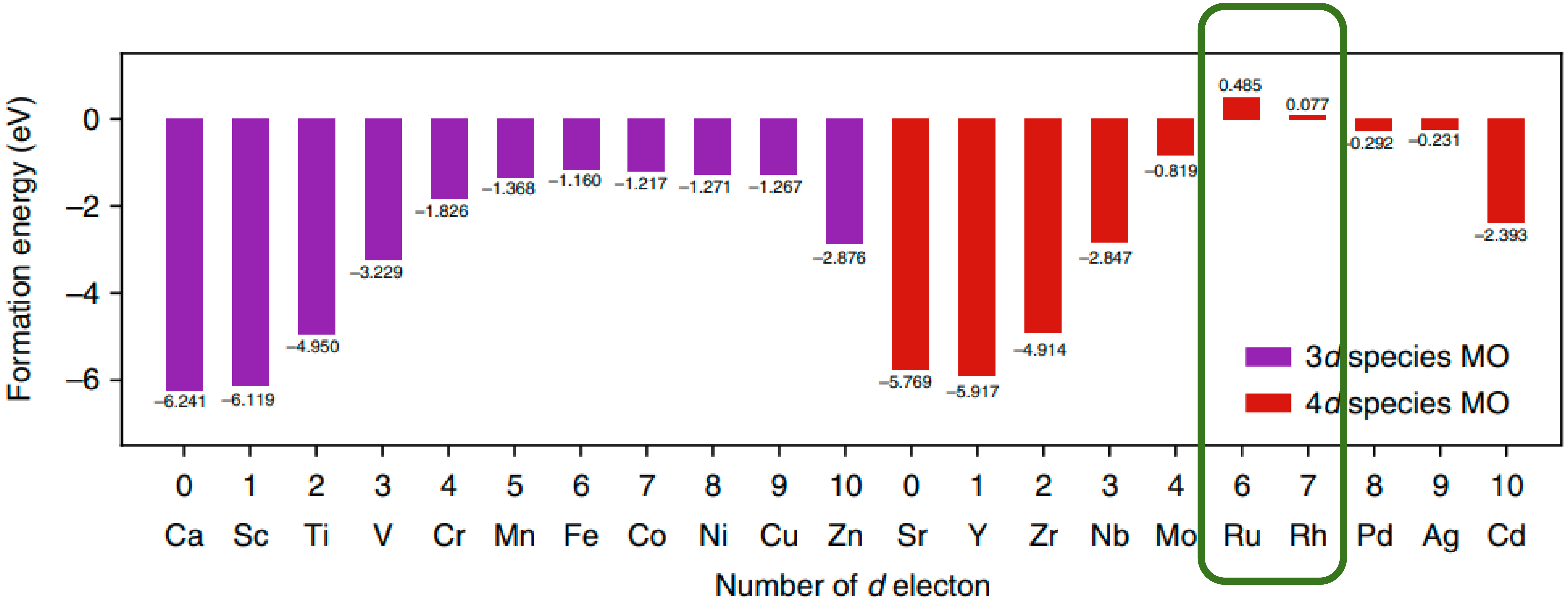

Burns, J ... & **Persson**, K. A. (2022). Chemistry of Materials, 34(16), 7210-7219.

Ru-doped Li-rich NMC

Кривые зависимости напряжения и скорости выделения O_2 от времени при проведении исследований методом дифференциальной электрохимической масс-спектрометрии

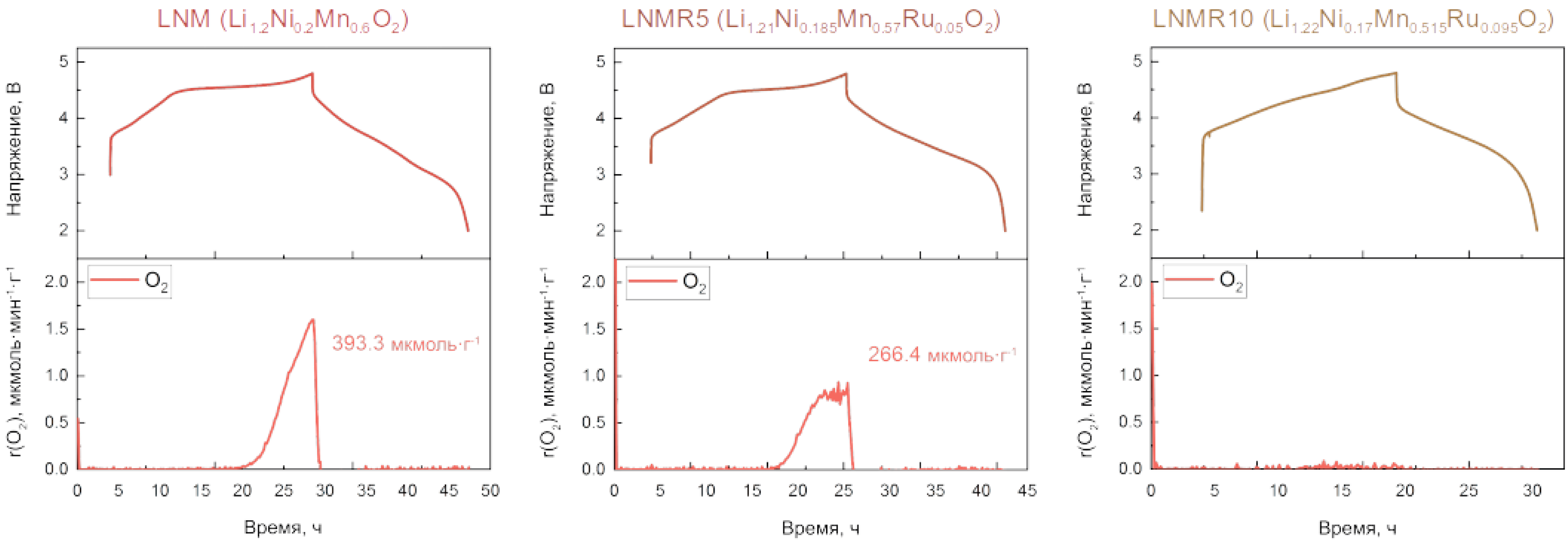

Morozov A. et al. (2022). Chem. Mater. 2022, 34, 6779−6791

Ru-doped Li-rich NMC

Зарядовая плотность (желтые области), соответствующая окисленным состояниям кислорода (чёрная стрелка) вблизи вакансии лития (пустой кружок) по результатам ТФП расчётов

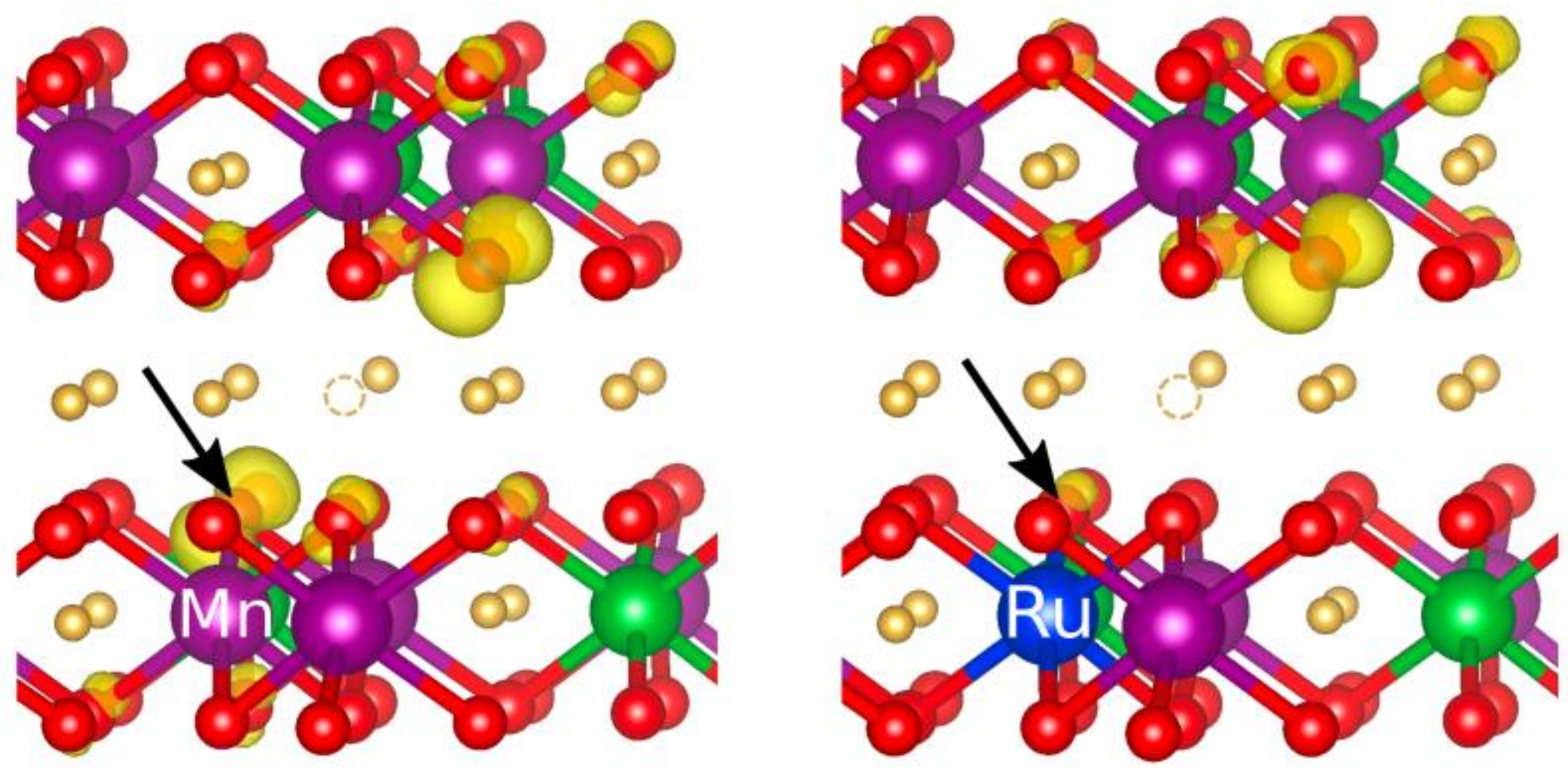

Зная этот эффект мы можем проверить хоть всю таблицу Менделеева и прогнозировать влияние допанта на окисление кислорода

Computational Screening of Cathode Coatings

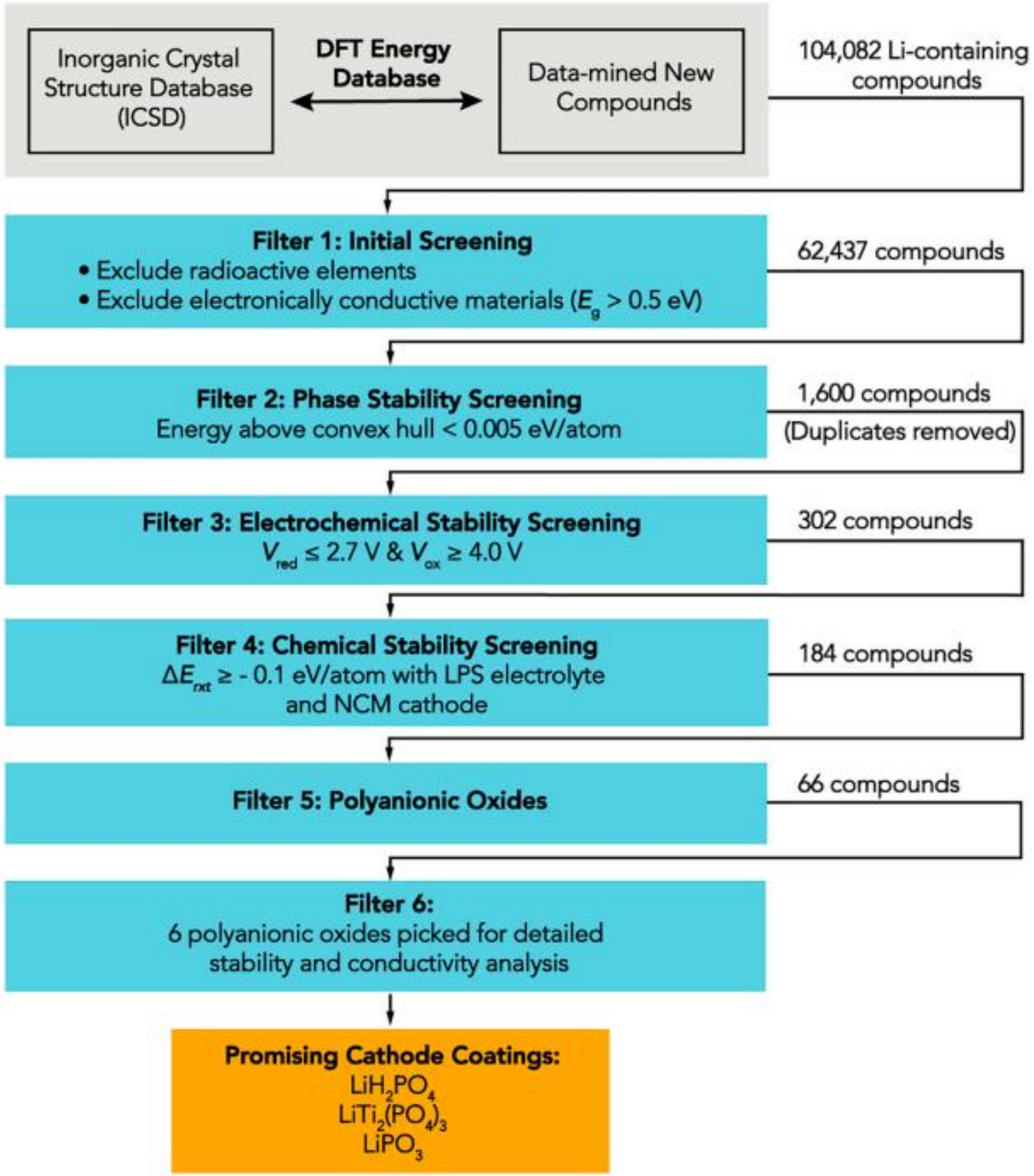

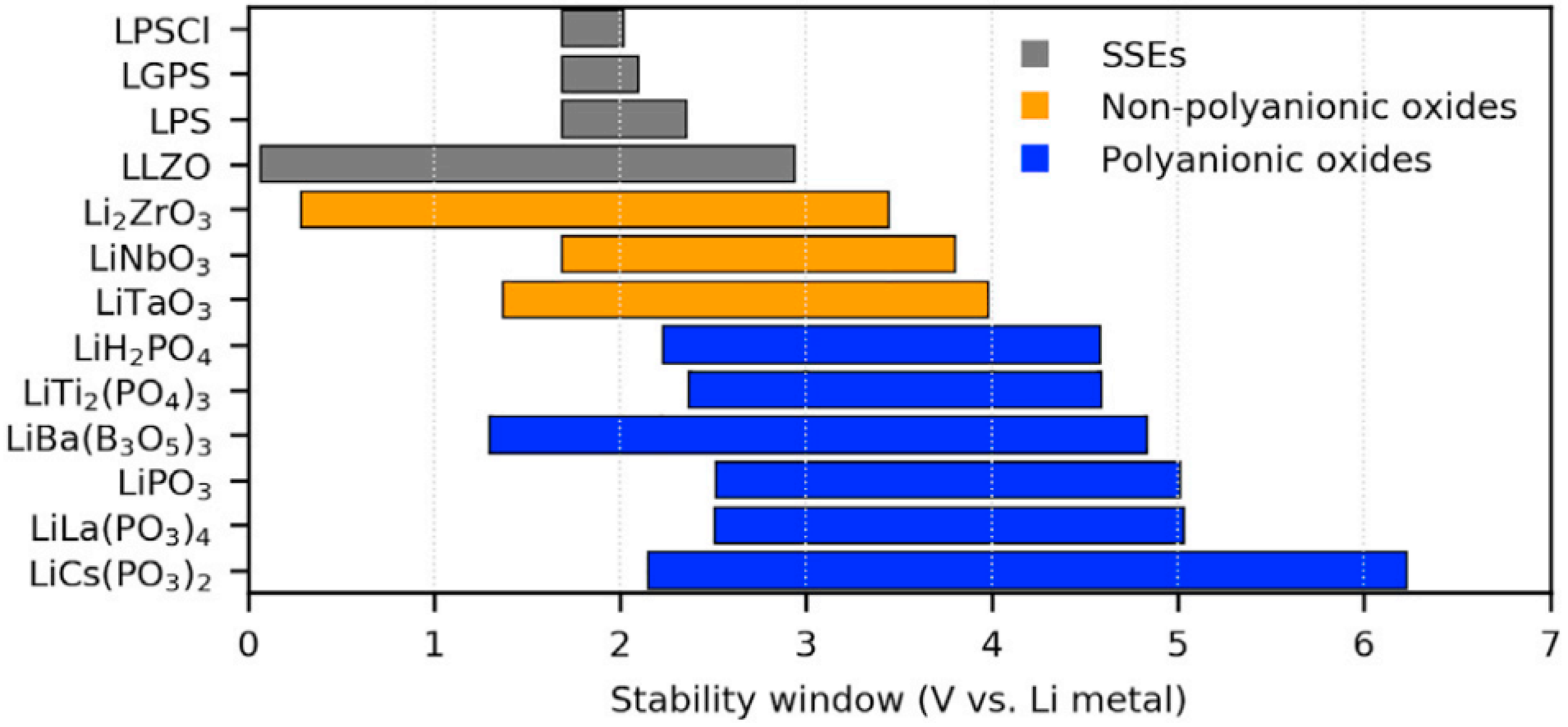

Table S4. Chemical reaction products from the most favorable reactions at cathodes/coating interfaces or cathode/SSE interfaces. Related to Figure 5.

Interfaces	Fully lithiated cathode	Half-lithiated cathode
NCM/Li_2ZrO_3	stable	$LiNiO_2$, NiO, Li_2MnO_3, ZrO_2, $Li_2Co_3NiO_8$
$LiCoO_2/ Li_2ZrO_3$	stable	Li_2CoO_3, $LiCoO_2$, ZrO_2
$LiMn_2O_4/Li_2ZrO_3$	$LiMnO_2$, Li_2MnO_3, ZrO_2	Li_2MnO_3, $LiMnO_2$, ZrO_2
$LiFePO_4/Li_2ZrO_3$	Li_3PO_4, FeO, ZrO_2	ZrO_2, Li_3PO_4, Fe_3O_4, FeO
$NCM/LiNbO_3$	Li_3NbO_4, $LiMnCoO_4$, NiO	stable
$LiCoO_2/LiNbO_3$	stable	stable
$LiMn_2O_4/LiNbO_3$	stable	Mn_2O_3, $Li_5Mn_7O_{16}$, Nb_2O_5
$LiFePO_4/LiNbO_3$	Nb_2FeO_6, Li_3PO_4	Li_3PO_4, Nb_2FeO_6, Fe_2O_3, Nb_2O_5
$NCM/LiTaO_3$	stable	stable
$LiCoO_2/LiTaO_3$	stable	stable
$LiMn_2O_4/LiTaO_3$	stable	$Li_5Mn_7O_{16}$, $LiTa_3O_8$, Mn_2O_3
$LiFePO_4/LiTaO_3$	Ta_2FeO_6, Li_3PO_4	Li_3PO_4, $TaFeO_4$, Ta_2FeO_6, $TaPO_5$
NCM/LiH_2PO_4	$HCoO_2$, Li_3PO_4, $Li_2Mn_3NiO_8$, $Ni(HO)_2$	$Ni_3P_2(HO)_{16}$, O_2, Li_3PO_4, $LiMnCoO_4$, $Ni_3(PO_4)_2$
[illegible]	[illegible]	[illegible]

Coatings	ICSD #	Calculated Migration Barrier (eV)
Li_2ZrO_3	31941	0.48
LiH_2PO_4	100200	0.33
$LiTi_2(PO_4)_3$	95979	0.42
$LiBa(B_3O_5)_3$	93013	1.96
$LiPO_3$	51630	0.40
$LiLa(PO_3)_4$	416877	1.39
$LiCs(PO_3)_2$	62514	1.27

Xiao, Y., … **Ceder**, G. (2019). Joule, 3(5), 1252-1275. **IF = 38.6**

Computational Screening of Cathode Coatings

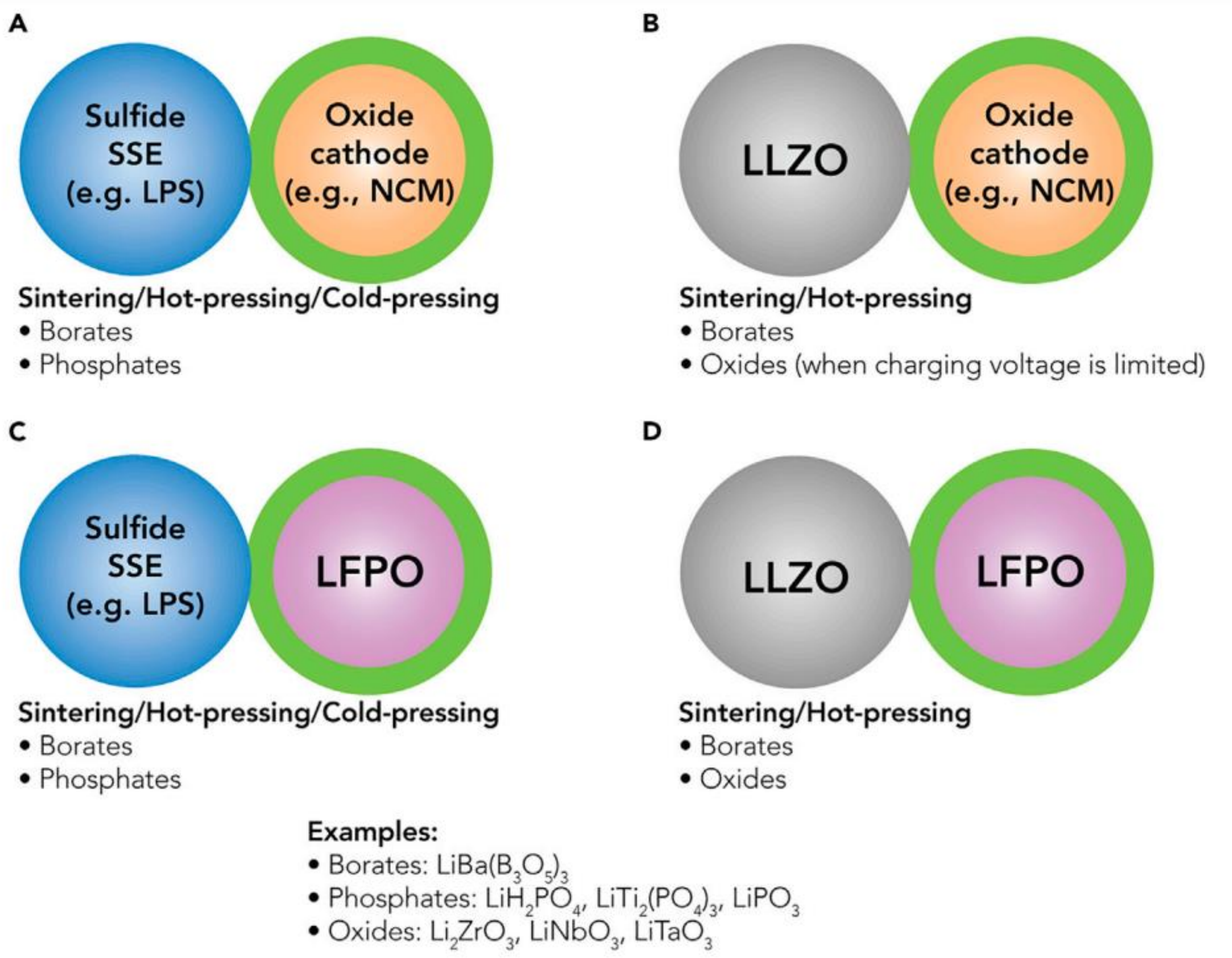

Xiao, Y., … **Ceder, G**. (2019). Joule, 3(5), 1252-1275.

Step 2. Determine the recipe

Case 1. Recipe is absolutely unknown

Answer: Use database of recipes

Materials Project

Materials Project

TARGET MATERIAL

$LiCoO_2$

PRECURSOR MATERIALS

Li_2CO_3 Co_3O_4

PARAGRAPH EXCERPT

"Reference Co3O4 and LiCoO2 phases were obtained by a classical ceramic method. Co3O4 was ..."

REACTION EQUATION

$0.333\ Co_3O_4 + 0.5\ Li_2CO_3 + 0.083\ O_2 \rightarrow LiCoO_2 + 0.5\ CO_2$

SYNTHESIS PROCEDURES

1. synthesized
2. calcination at 450 °C, for 15 h, in oxygen
3. heated at 850 °C, for 2 day, in oxygen

SYNTHESIS TYPE

solid-state

See less

Extracted from Publication

TARGET MATERIAL

$LiCoO_2$

PRECURSOR MATERIALS

Li_2O $Co(NO_3)_2$ $H_4N_2O_3$

PARAGRAPH EXCERPT

"LiCoO2 was prepared as support material by solid-state reaction of Li2O and Co(NO3)2·6H2O. ..."

REACTION EQUATION

$Co(NO_3)_2{\cdot}6H_2O + 0.5\ Li_2O + 0.25\ O_2 + 2\ [OH-] \rightarrow LiCoO_2 + 7\ H_2O + 2\ [NO3-]$

SYNTHESIS PROCEDURES

1. prepared
2. mixed
3. heated
4. prepared
5. prepared
6. calcined at 300 °C, for 3 h
7. heated at 900, 800, 700, 600, 500 °C

SYNTHESIS TYPE

solid-state

See less

Extracted from Publication

TARGET MATERIAL

$LiCoO_2$

PRECURSOR MATERIALS

Co LiHO

PARAGRAPH EXCERPT

"The LiNi0.5-yMn0.5-yCo2yO2 samples with 0 ≤ 2y ≤ 0.58 were prepared by firing the coprecipitated ..."

REACTION EQUATION

$0.5\ Co_2 + LiOH + 0.75\ O_2 \rightarrow LiCoO_2 + 0.5\ H_2O$

SYNTHESIS PROCEDURES

1. prepared
2. firing at 900 °C, for 24 h, in air, air
3. adding
4. washing using water
5. prepared
6. synthesized

SYNTHESIS TYPE

solid-state

See less

Extracted from Publication

TARGET MATERIAL

$LiCoO_2$

PRECURSOR MATERIALS

$Co(HO)_2$ LiHO H_5NO

PARAGRAPH EXCERPT

"The metal oxides LiMO2 (M = Co, Ni) and Li2MO3 (M = Mn, Mo, Sn) were synthesized directly by solid-..."

REACTION EQUATION

$Co(OH)_2 + LiOH.H_2O + 0.25\ O_2 \rightarrow LiCoO_2 + 2.5\ H_2O$

SYNTHESIS PROCEDURES

1. synthesized
2. cooling
3. synthesized
4. drying
5. heating at 900 °C, for 12 h

SYNTHESIS TYPE

solid-state

See less

Extracted from Publication

Ion exchange reaction

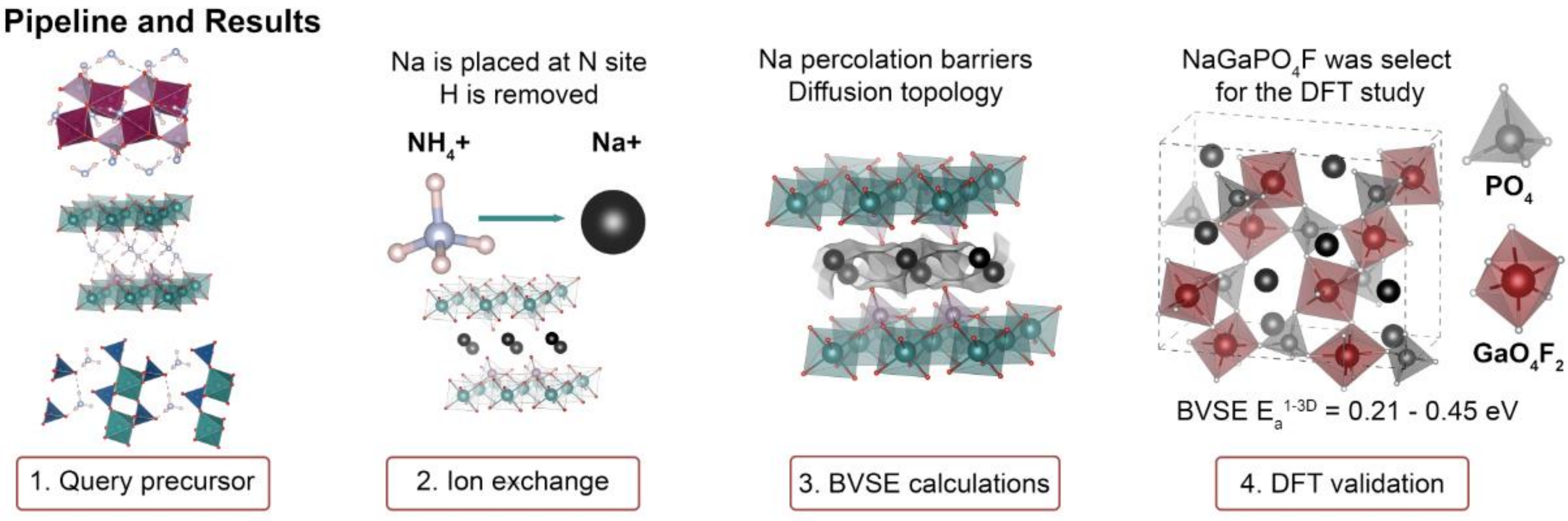

Dembitskiy, A. D., Aksyonov, D. A., Abakumov, A. M., & Fedotov, S. S. (2022). *Solid State Ionics*, *374*, 115810.

Case 2. Recipe is known but the conditions are not suitable

Answer: Use DFT phase diagrams

Pourbaix diagram

Home / Apps / Pourbaix Diagram

Pourbaix Diagram

References | Documentation

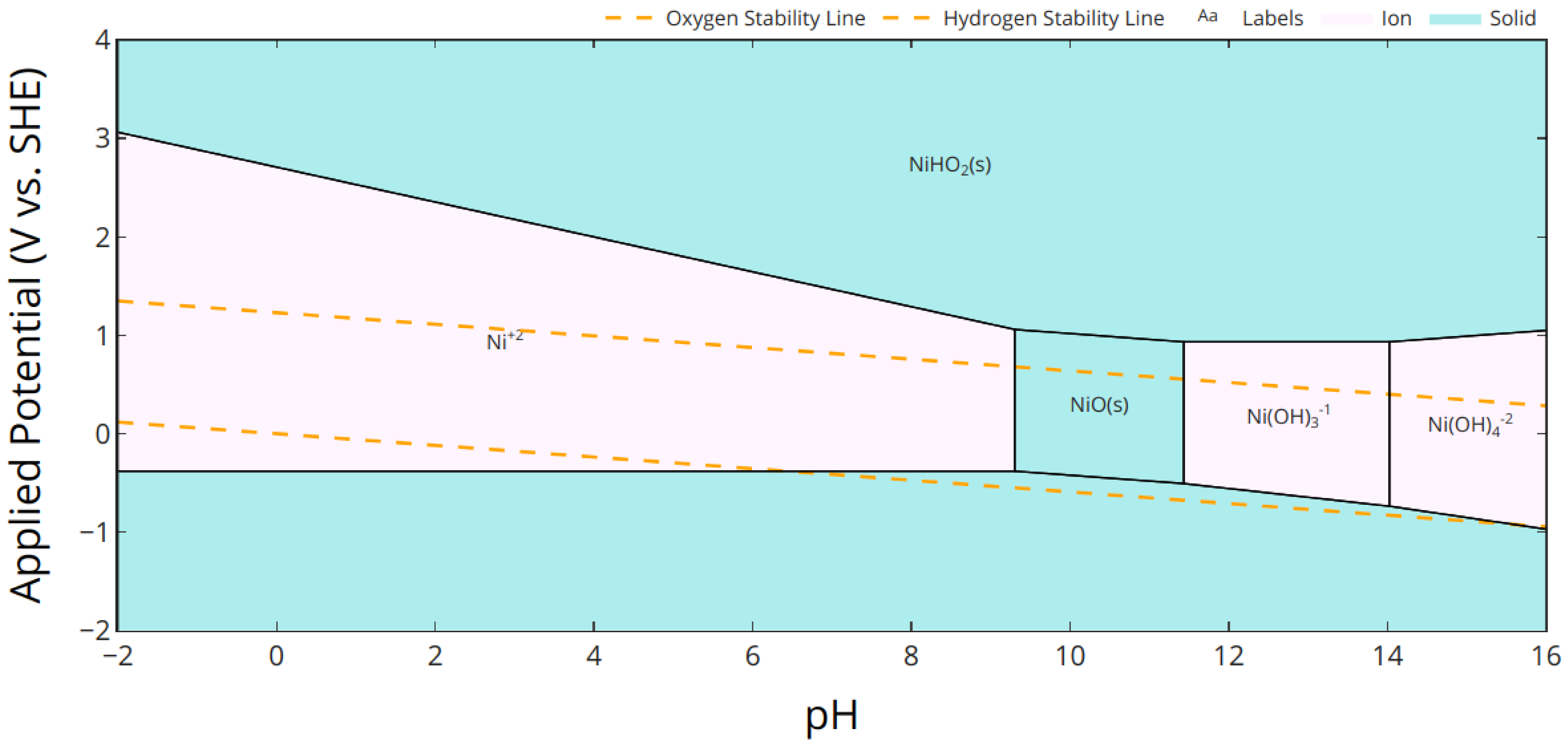

Pourbaix diagram

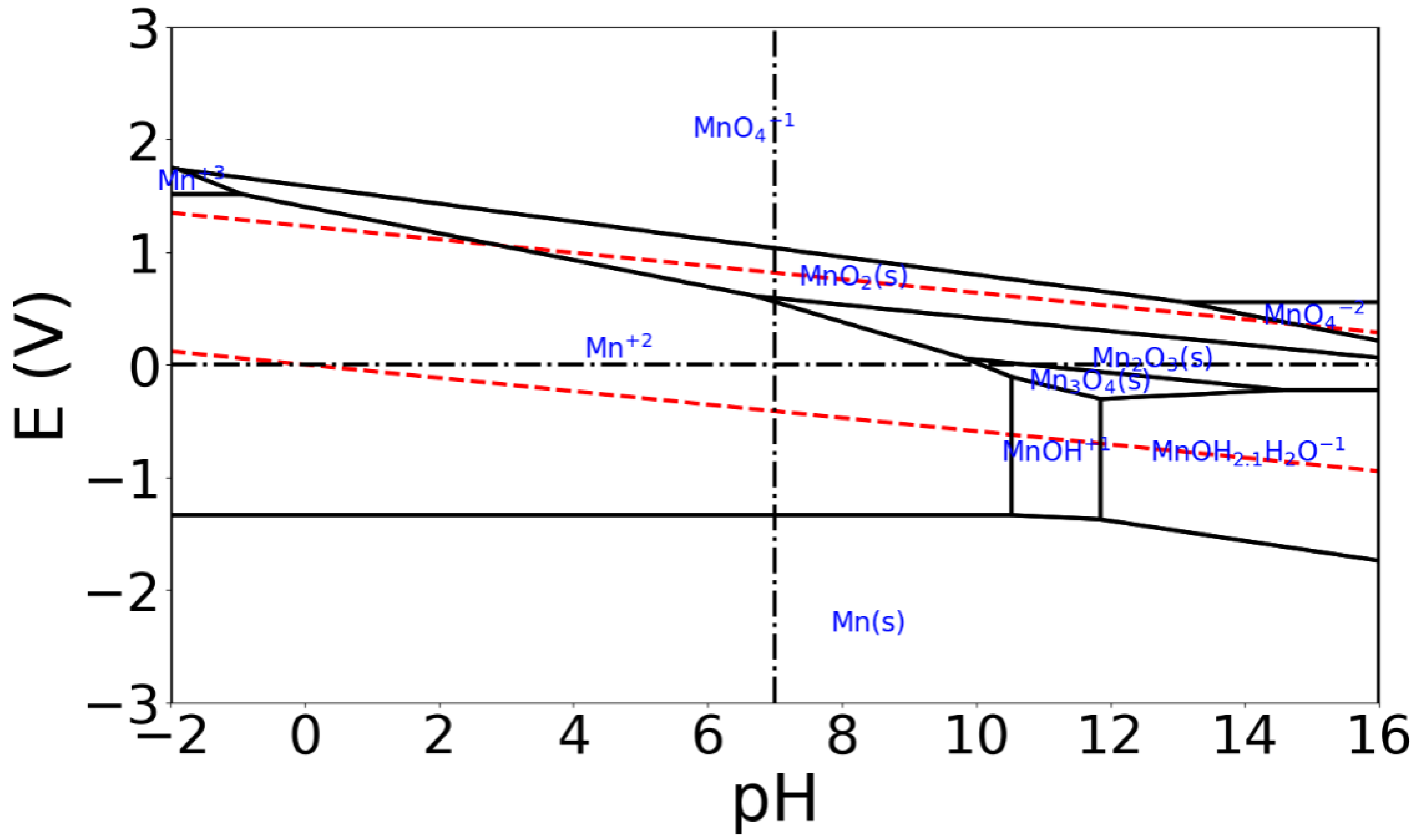

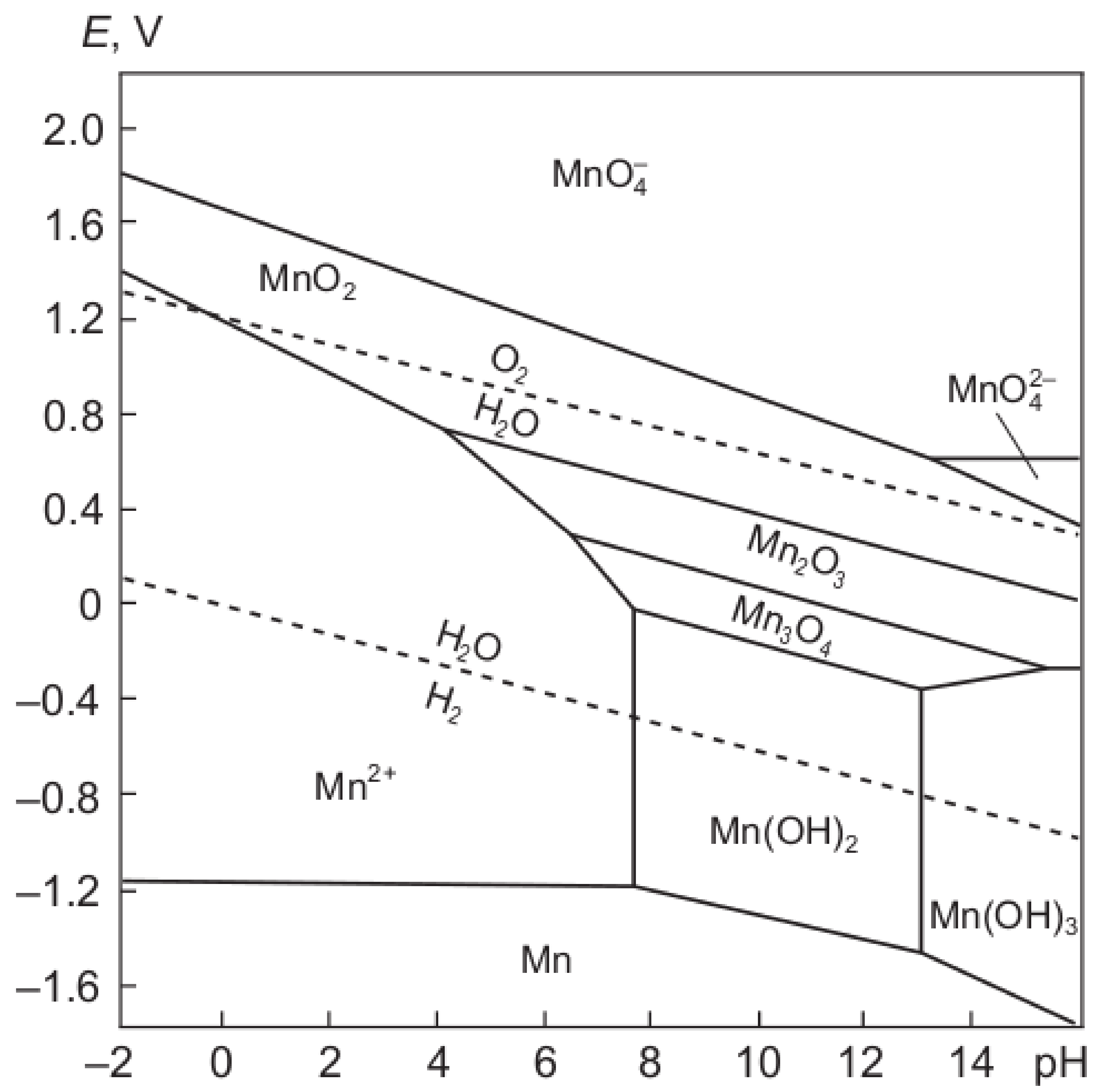

Figure 34. Pourbaix diagram for the Mn–H_2O system (without taking into account the formation of Mn^{II} amminocomplexes). Dashed lines define E–pH dependences for the reactions $O_2 + 2H_2O + 4e^- \rightarrow 4OH^-$ and $2H_2O + 2e^- \rightarrow H_2 + 2OH^-$. The figure was created by the authors of the review based on data from the Ref. 205.

Convex hull

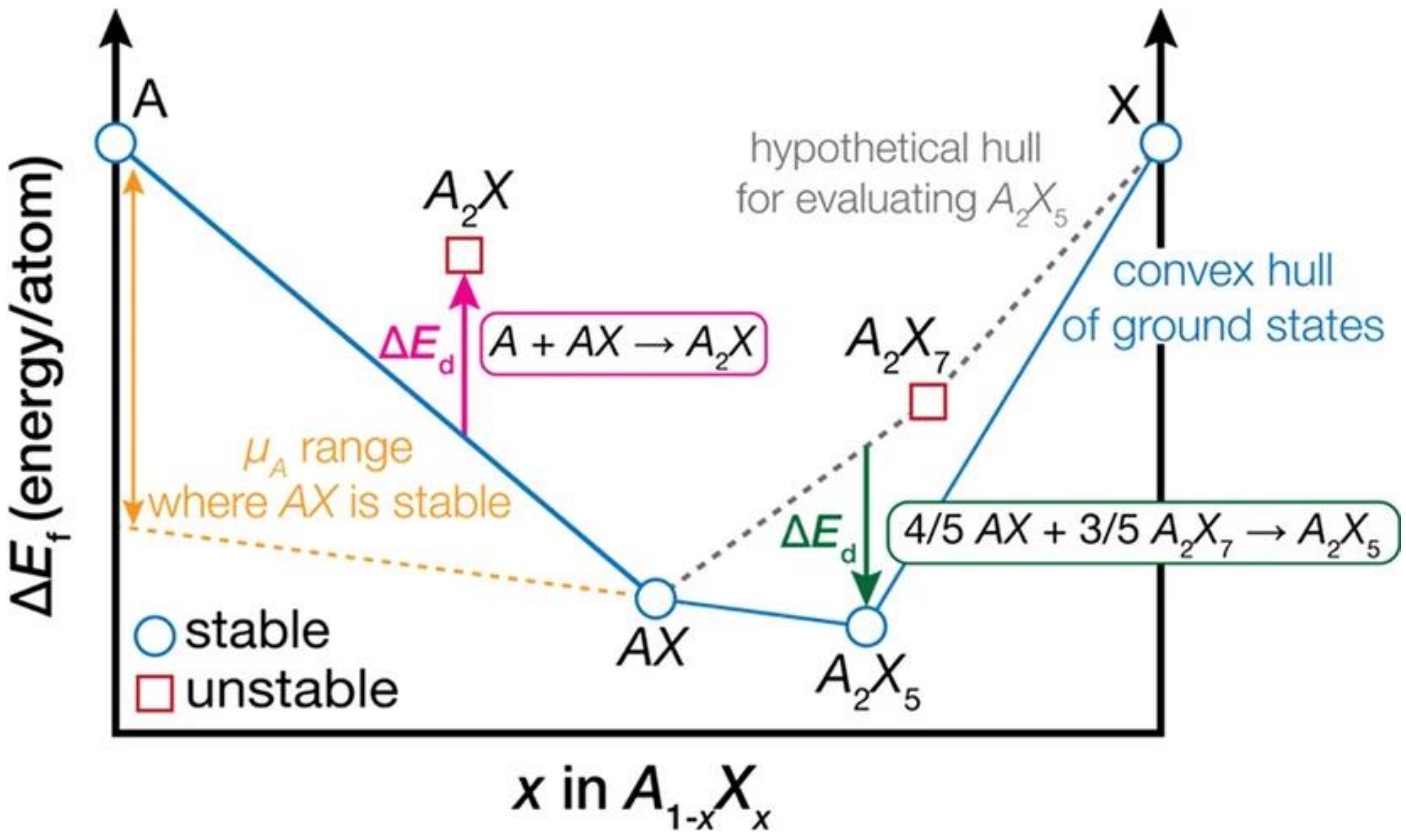

Phase diagram at 0 K and 0 atm.
For systems comprising primarily of condensed phases, the PV term can be neglected and at 0K, the expression for G simplifies to just E.

Source

Convex hull (Binary)

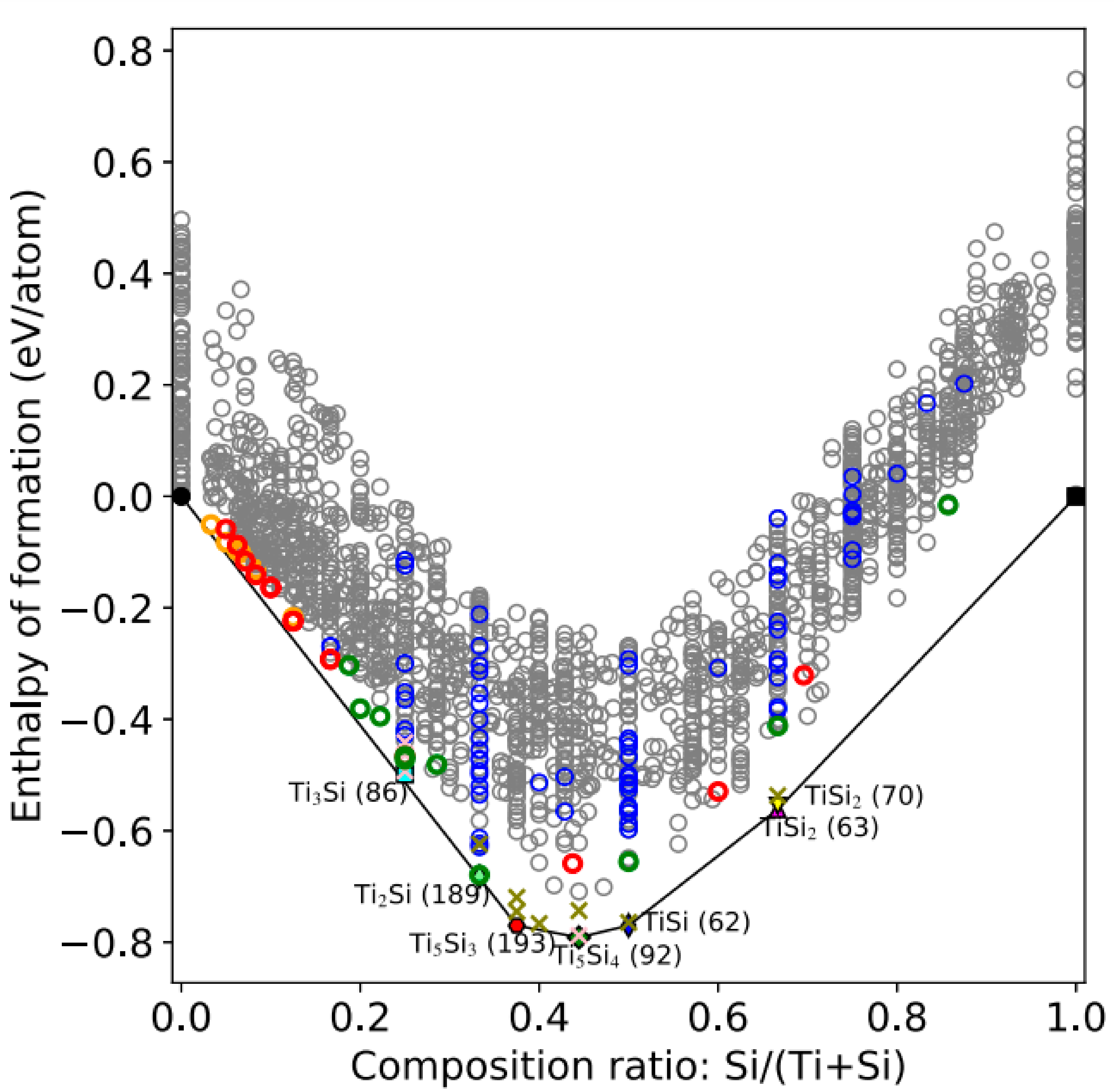

Poletaev, D. O., Aksyonov, D. A., & Lipnitskii, A. G. (2020) CALPHAD, 71, 102201.

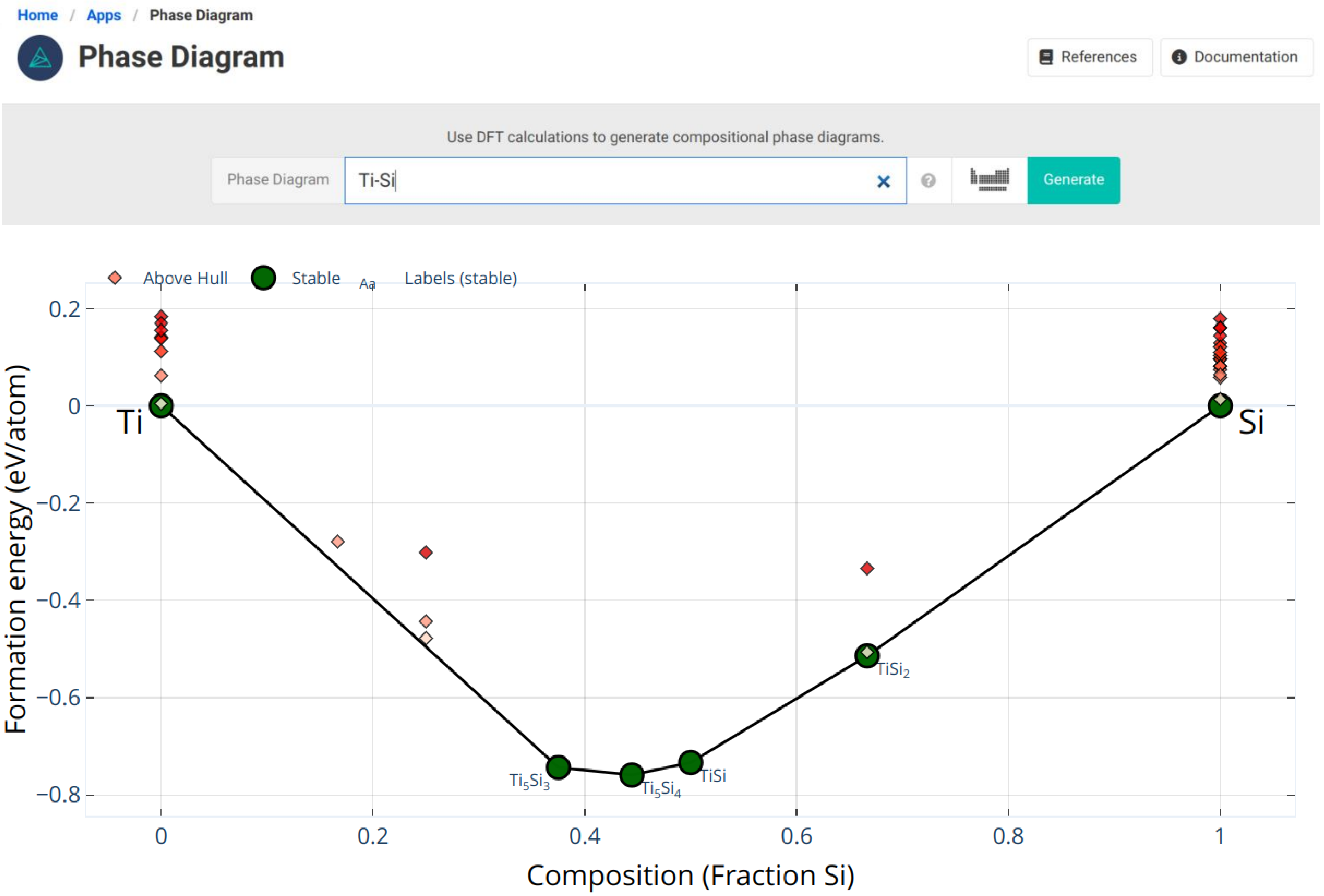

Materials Project

Convex hull (Ternary)

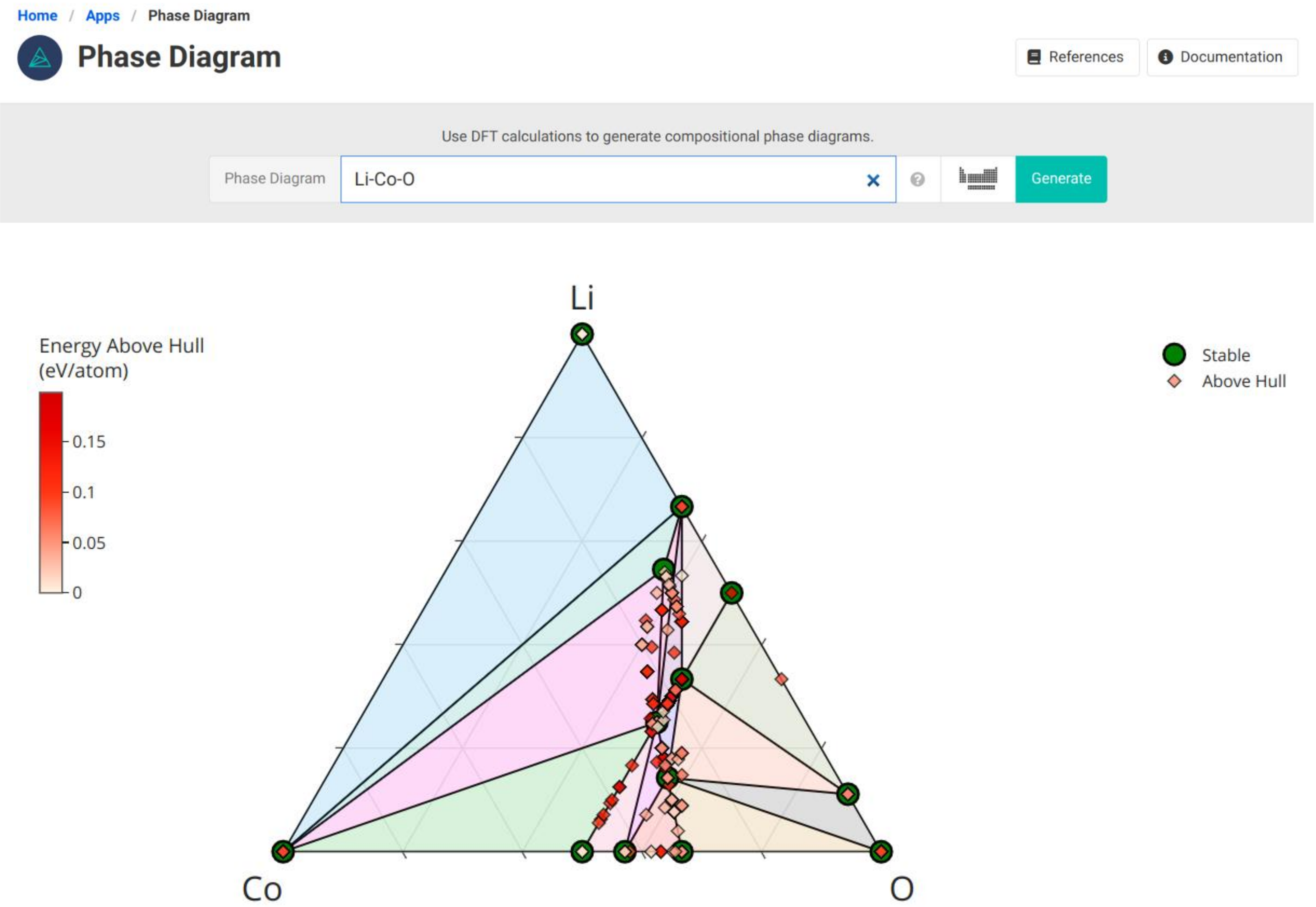

Chemical potential space diagram

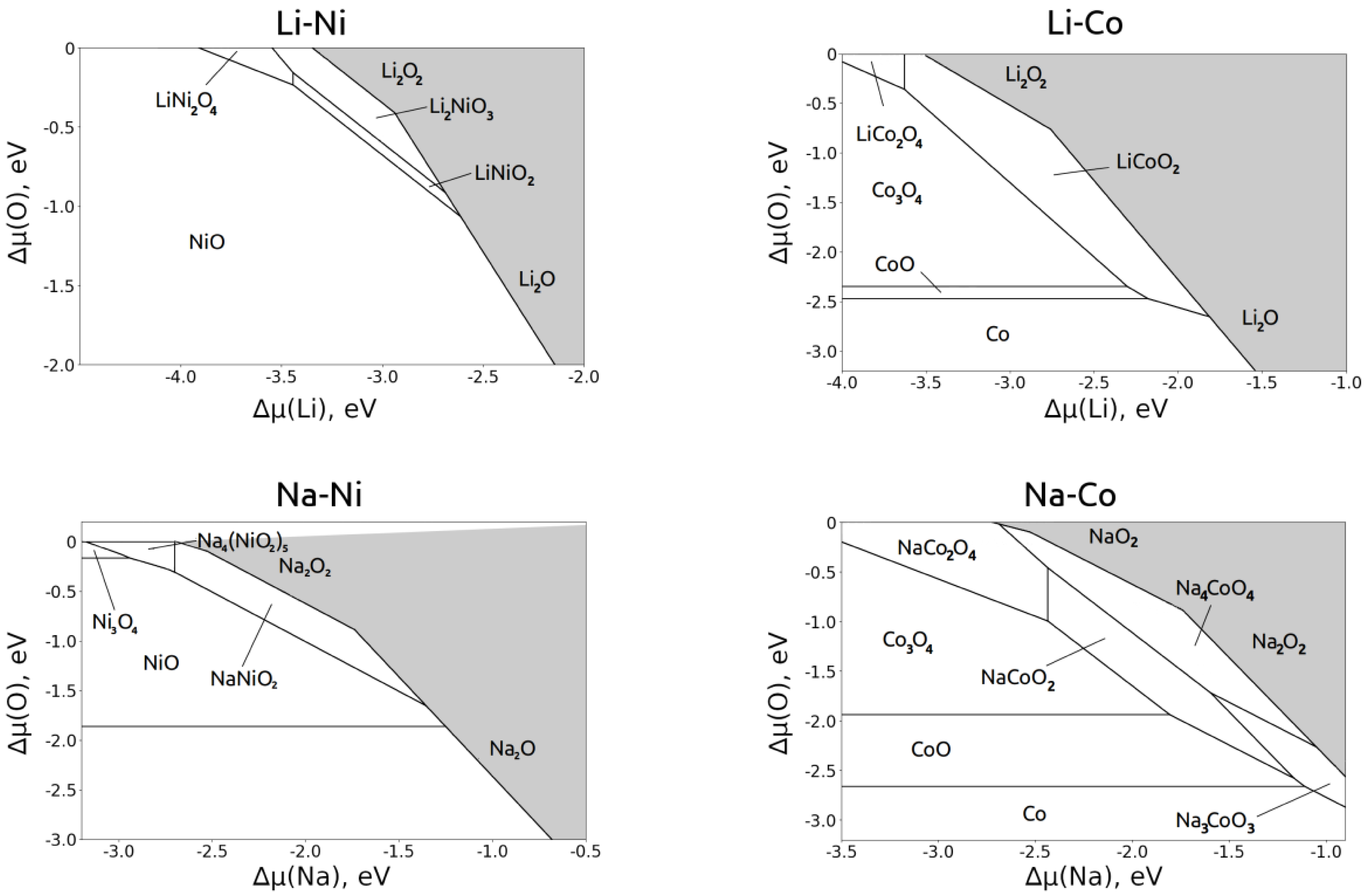

Boev, A. O., et al. *Applied Surface Science* 537 (2021): 147750.

Oxygen chemical potential

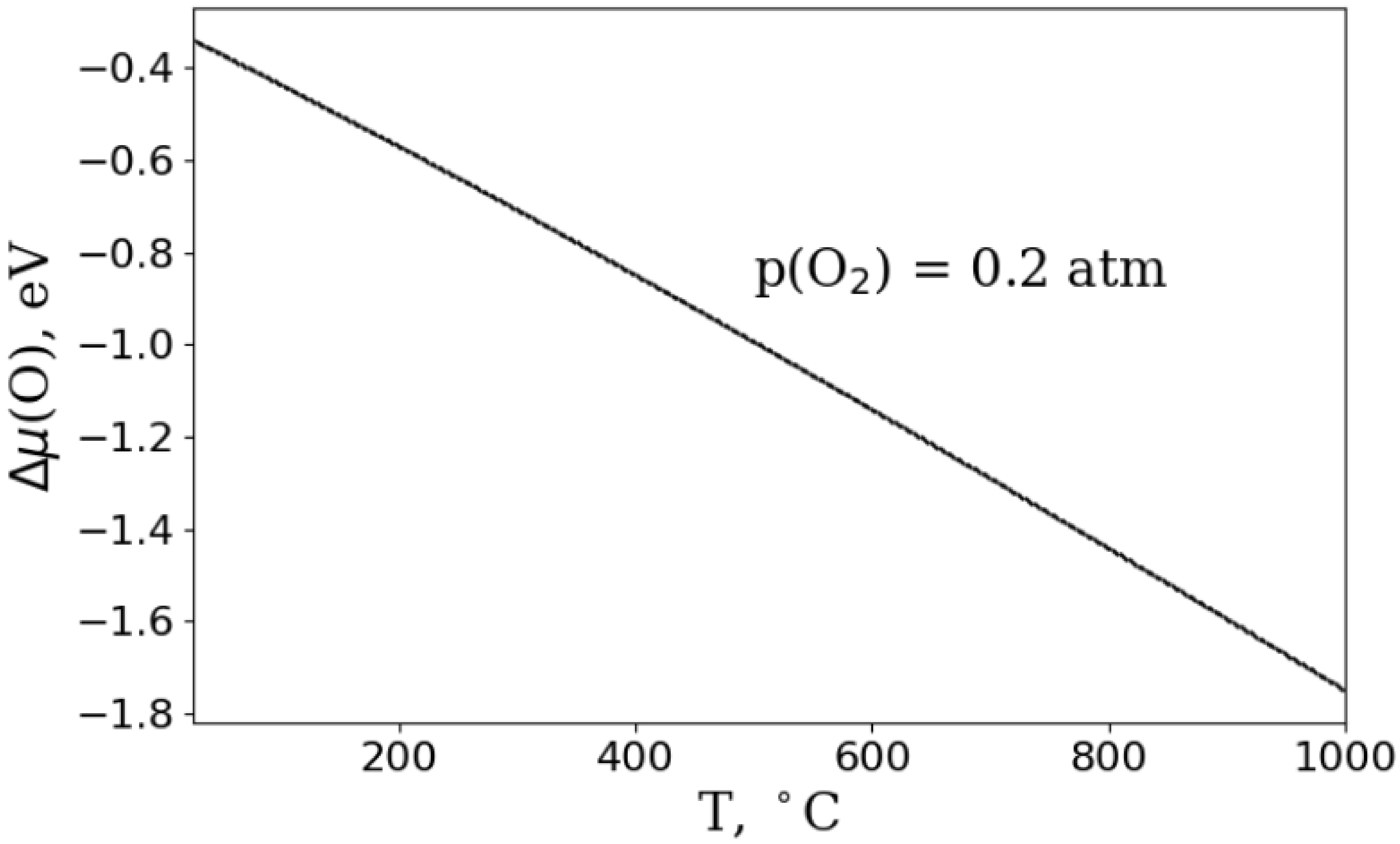

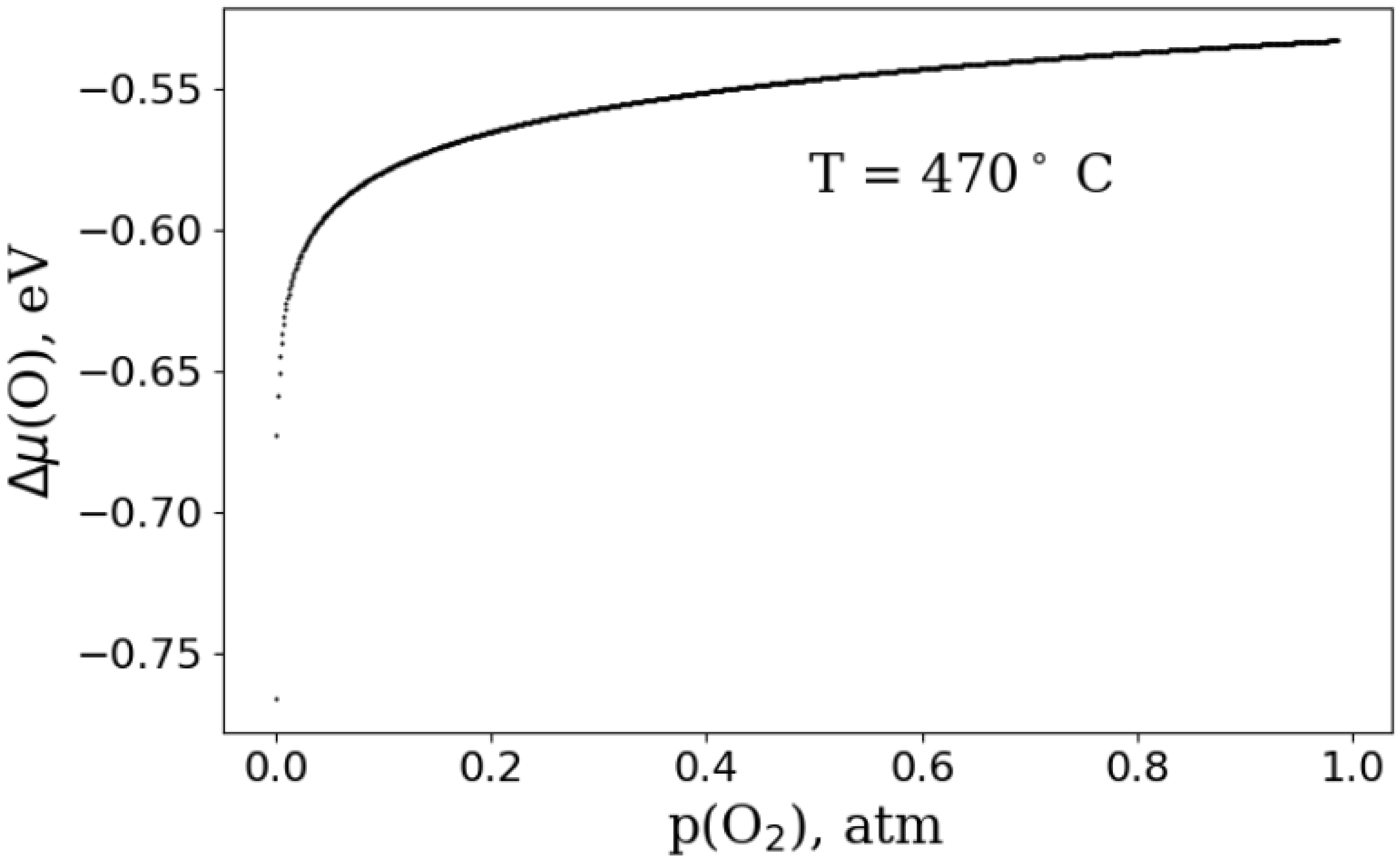

$$\mu(O_2;\ T, p) = \mu(O_2, 0\ K) + \Delta G^{\circ}(O_2,\ T) + RT \ln p(O_2)$$

Step 3. Follow the recipe

A computational dude has a rest

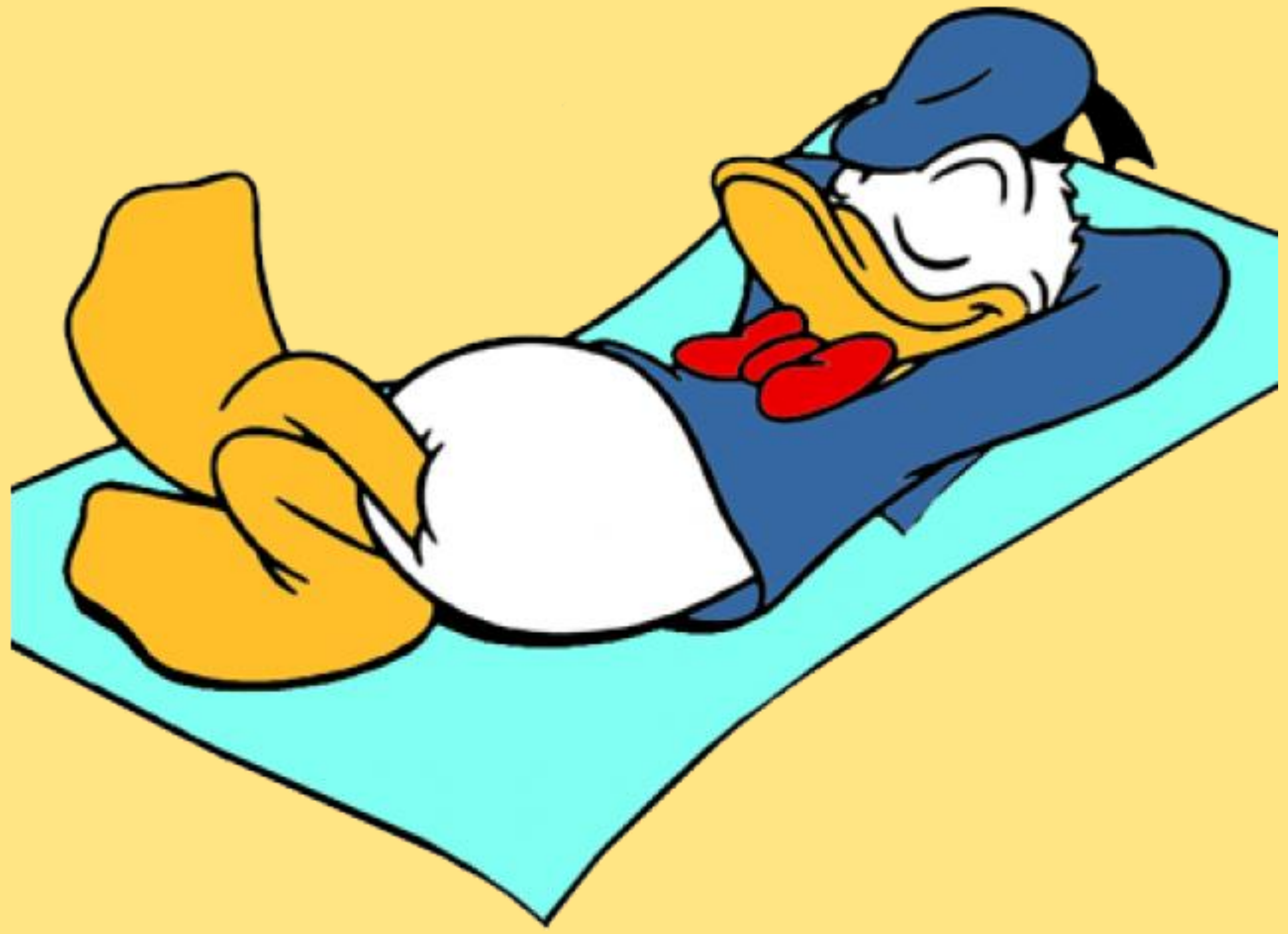

Step 4. Enjoy your result

Step 4. Enjoy your result

… Or not?

Resulting particle shape is not suitable

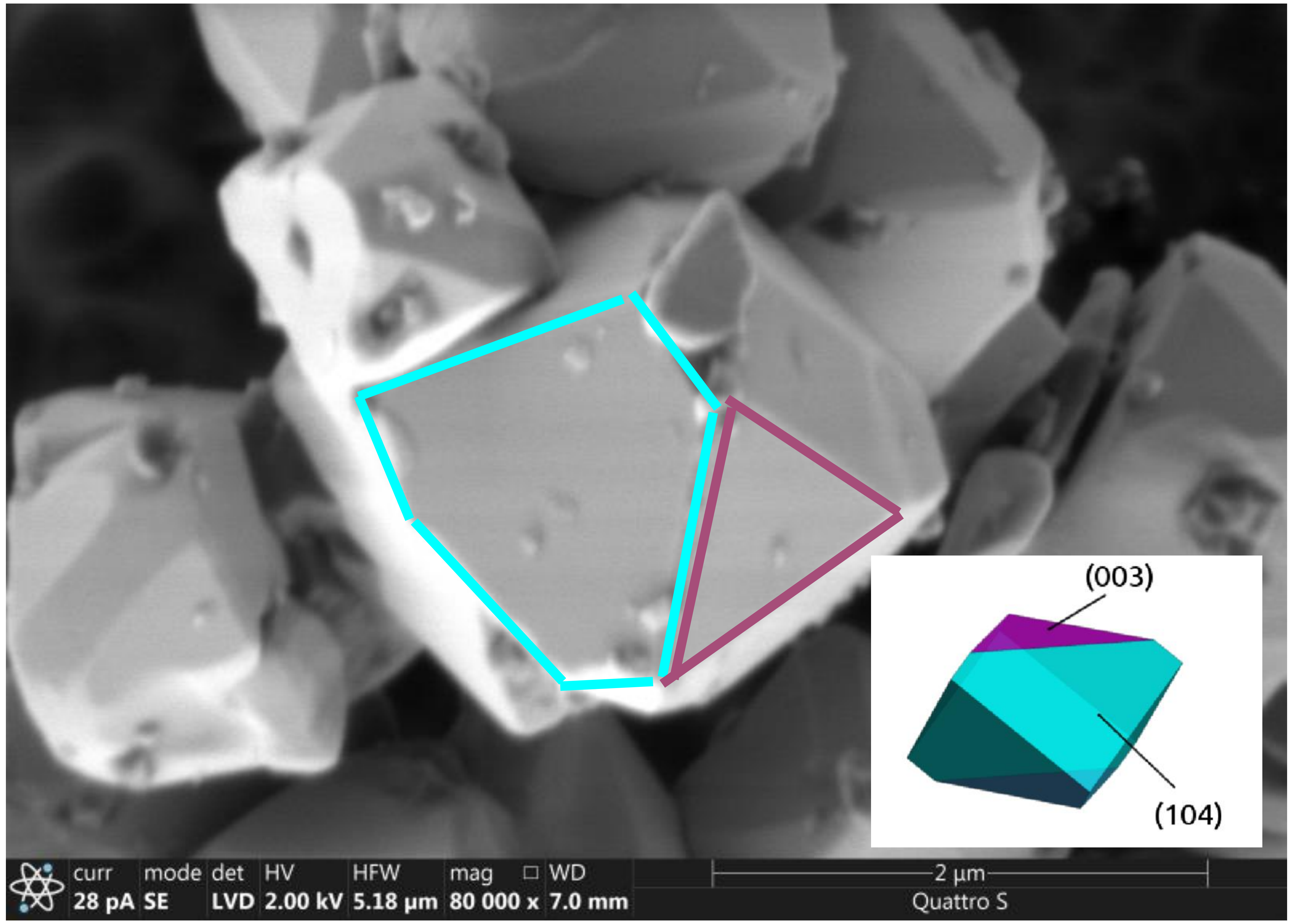

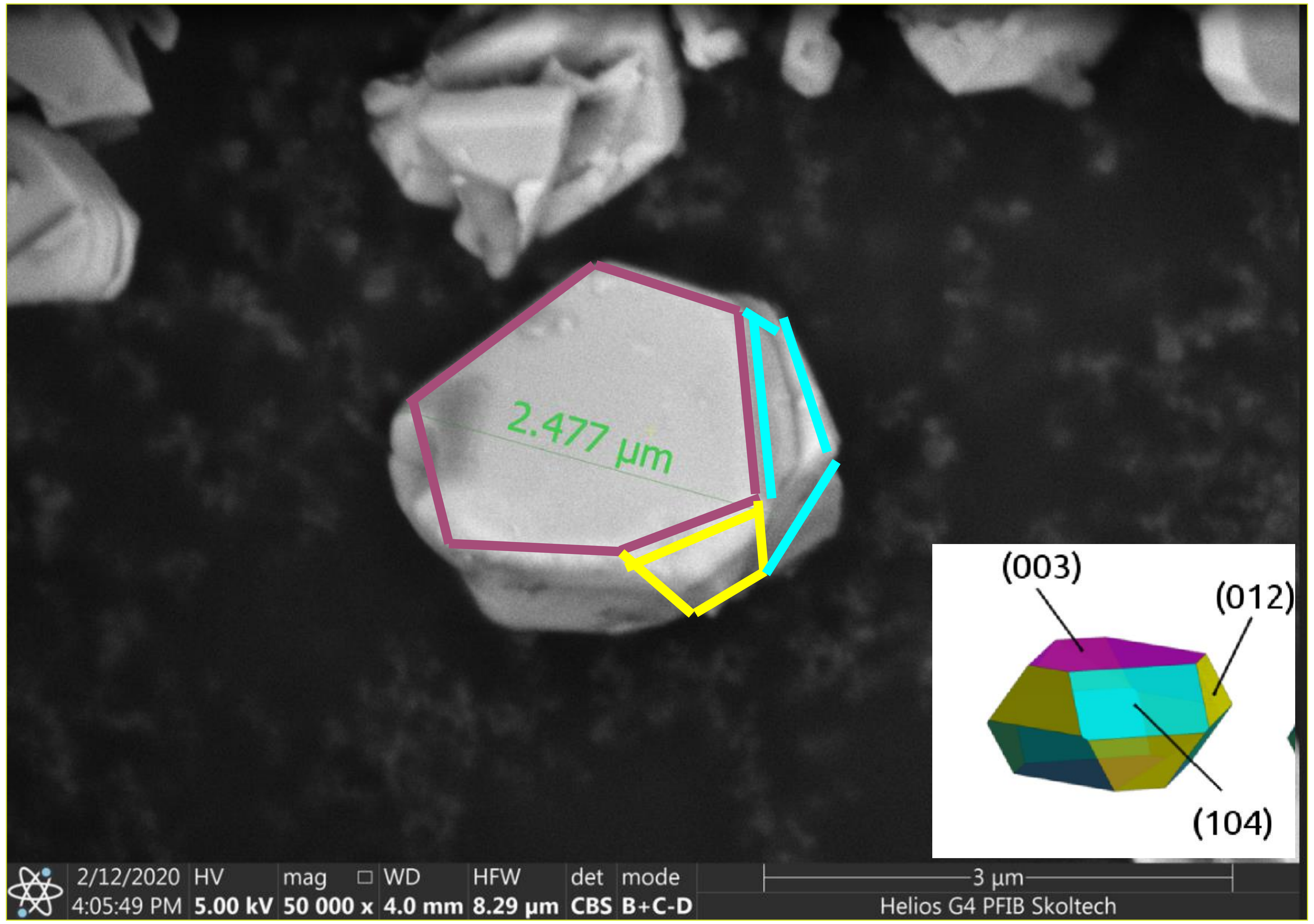

Li-Co-O phase diagram

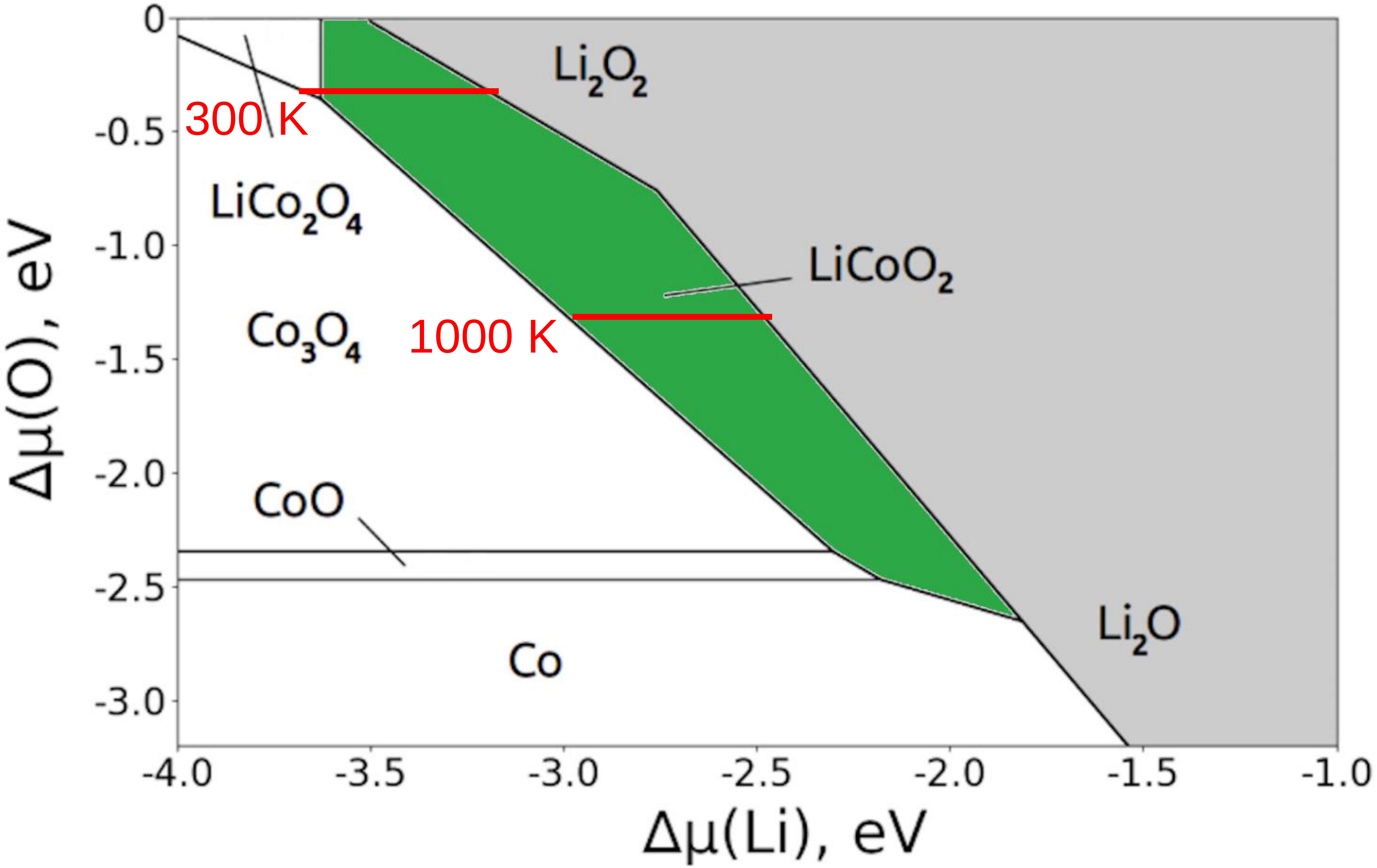

Wulff shapes. Examples

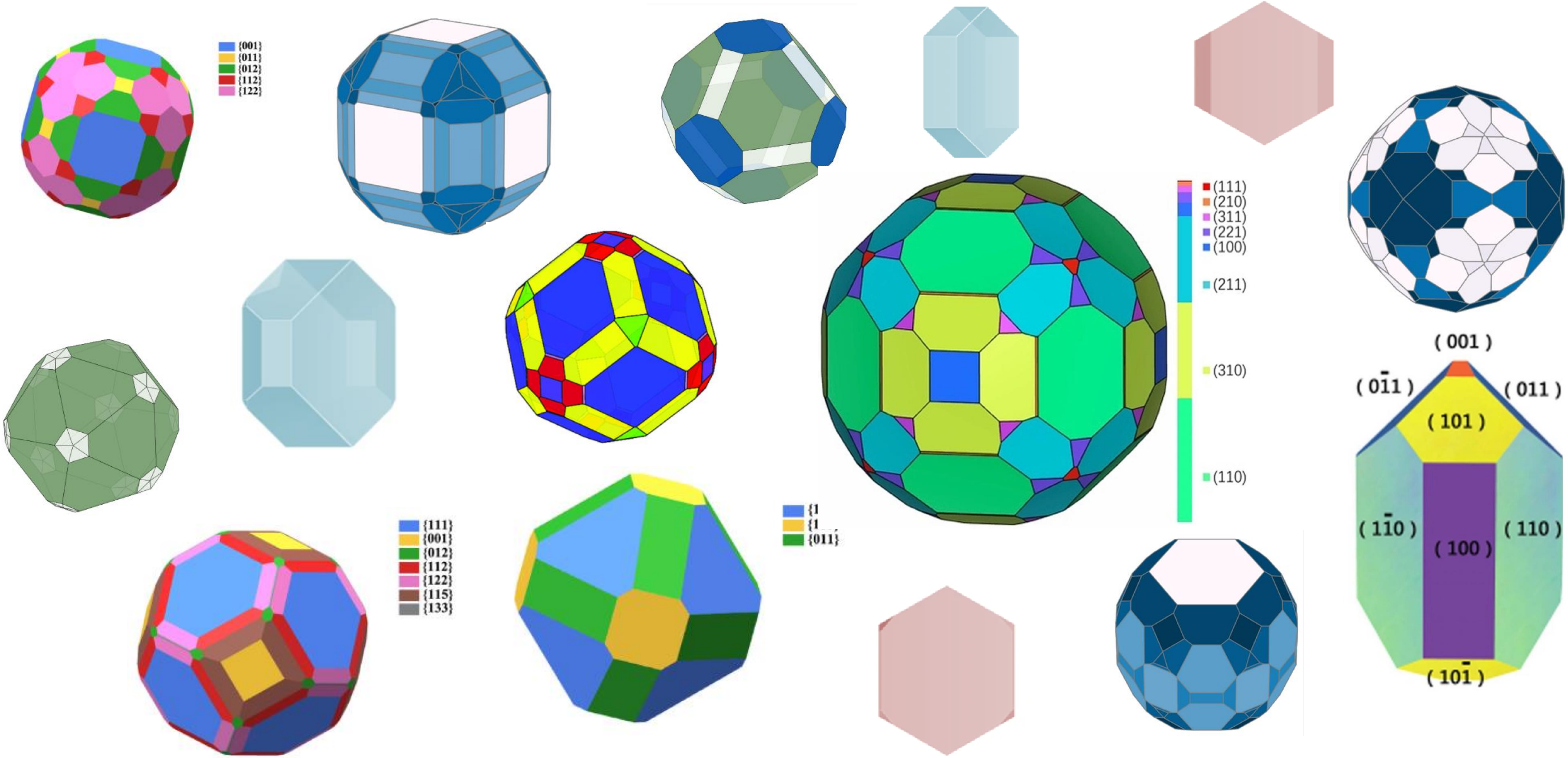

Main surfaces of layered oxides

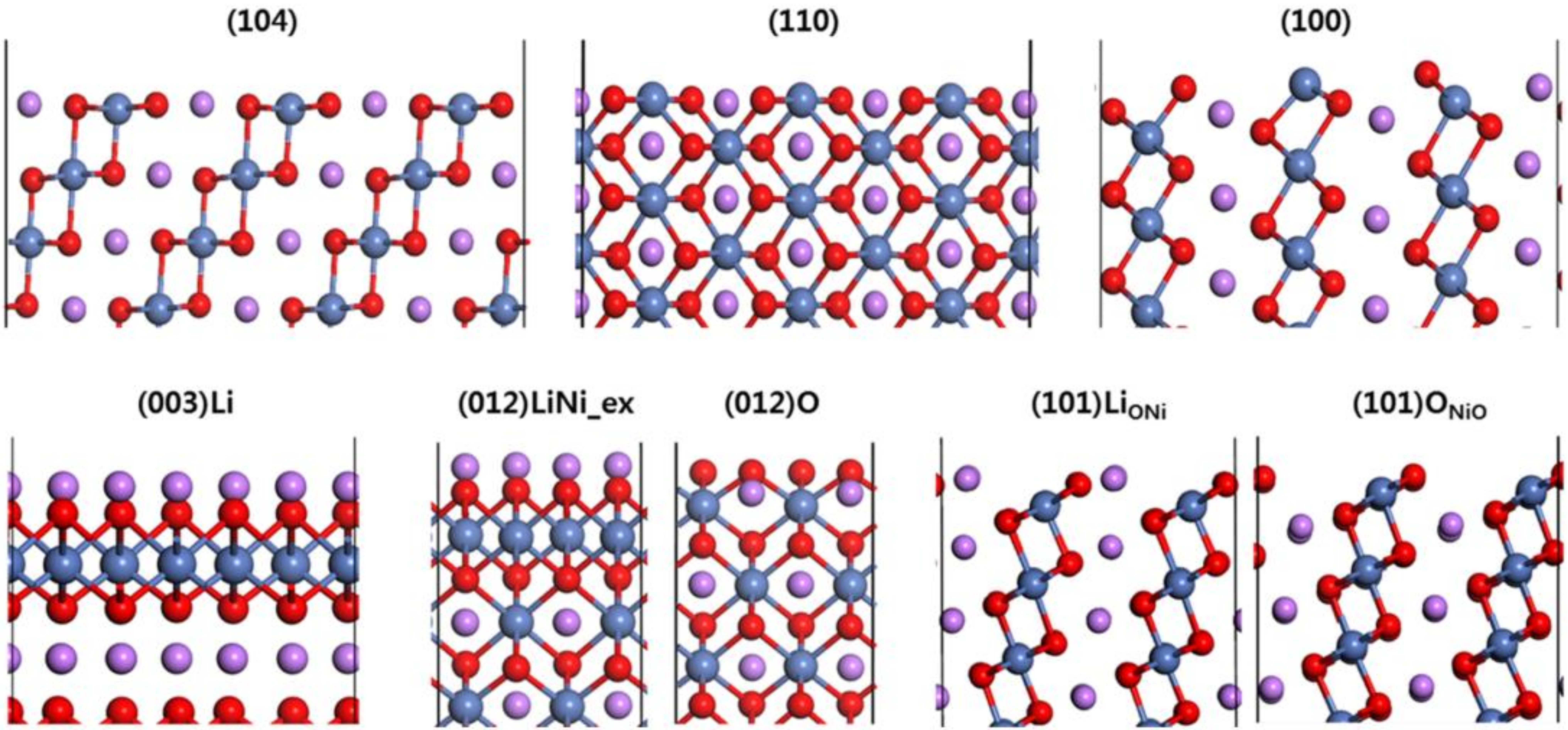

Figure 2. Relaxed surface geometries of nonpolar surfaces, (104), (110), and (100) facets, together with representative relaxed structures of polar surfaces, (003), (012), and (101) facets. Violet: Li, red: O, royal blue: Ni.

Effect of oxygen chemical potential on surface energy

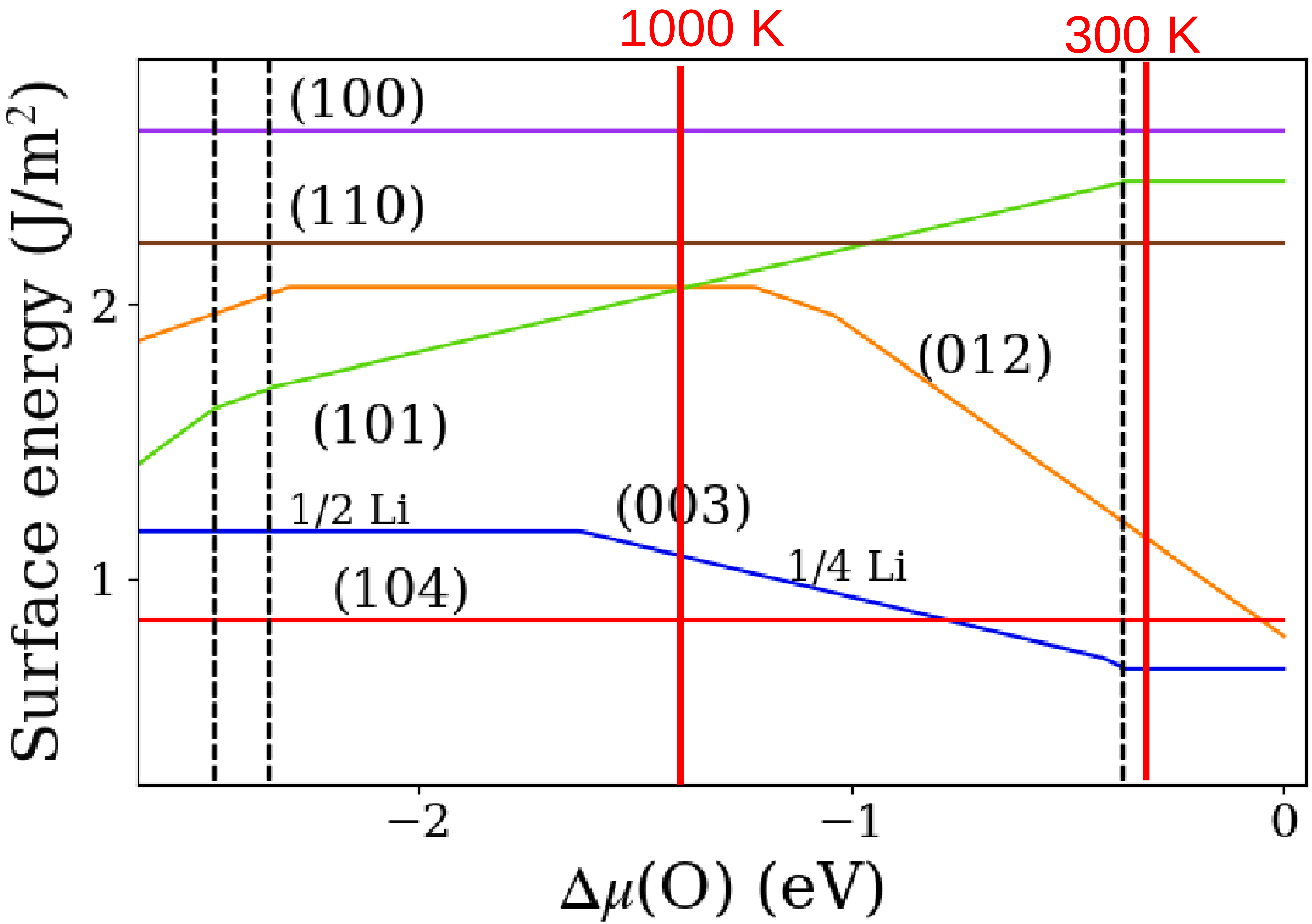

Effect on particle shape

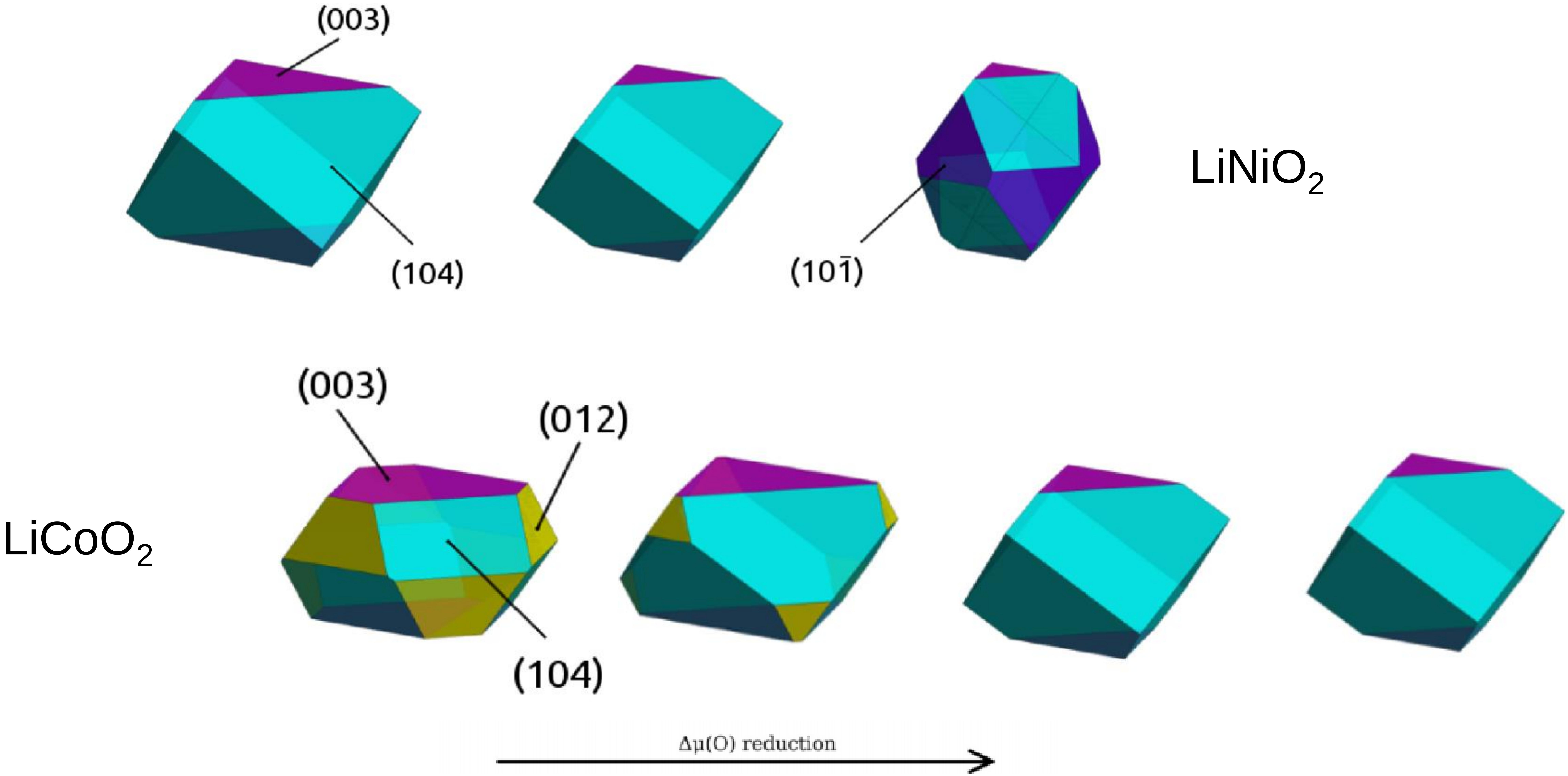

Couple of examples of particle shape prediction

VO_2

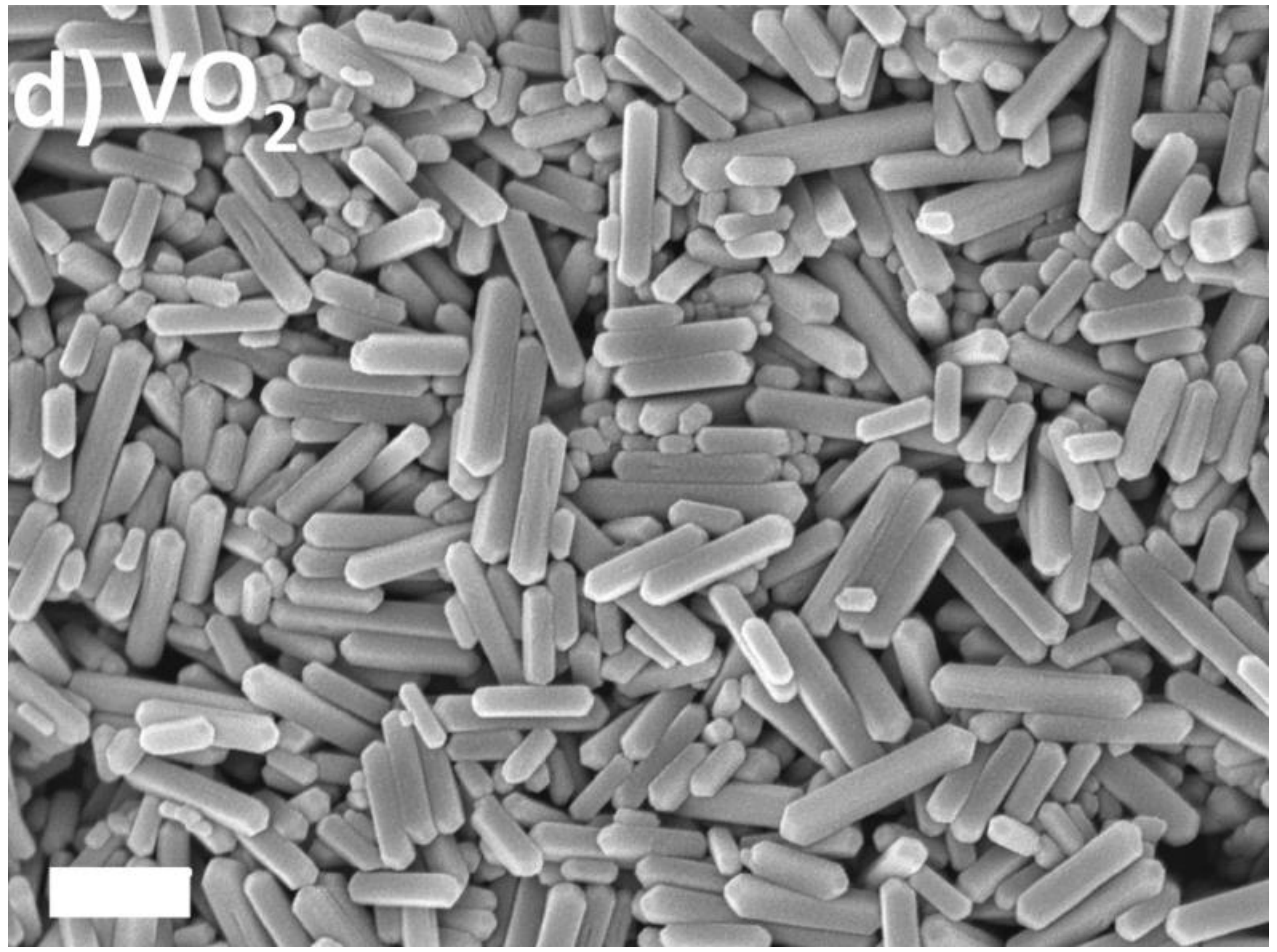

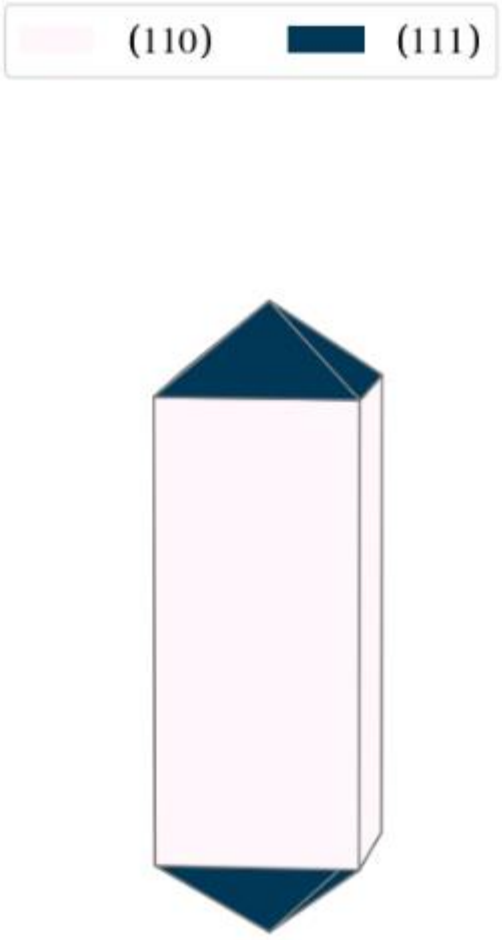

Wang, N., et al. *Advanced Materials Interfaces*, *3*(15), 1600164.

TiS_2

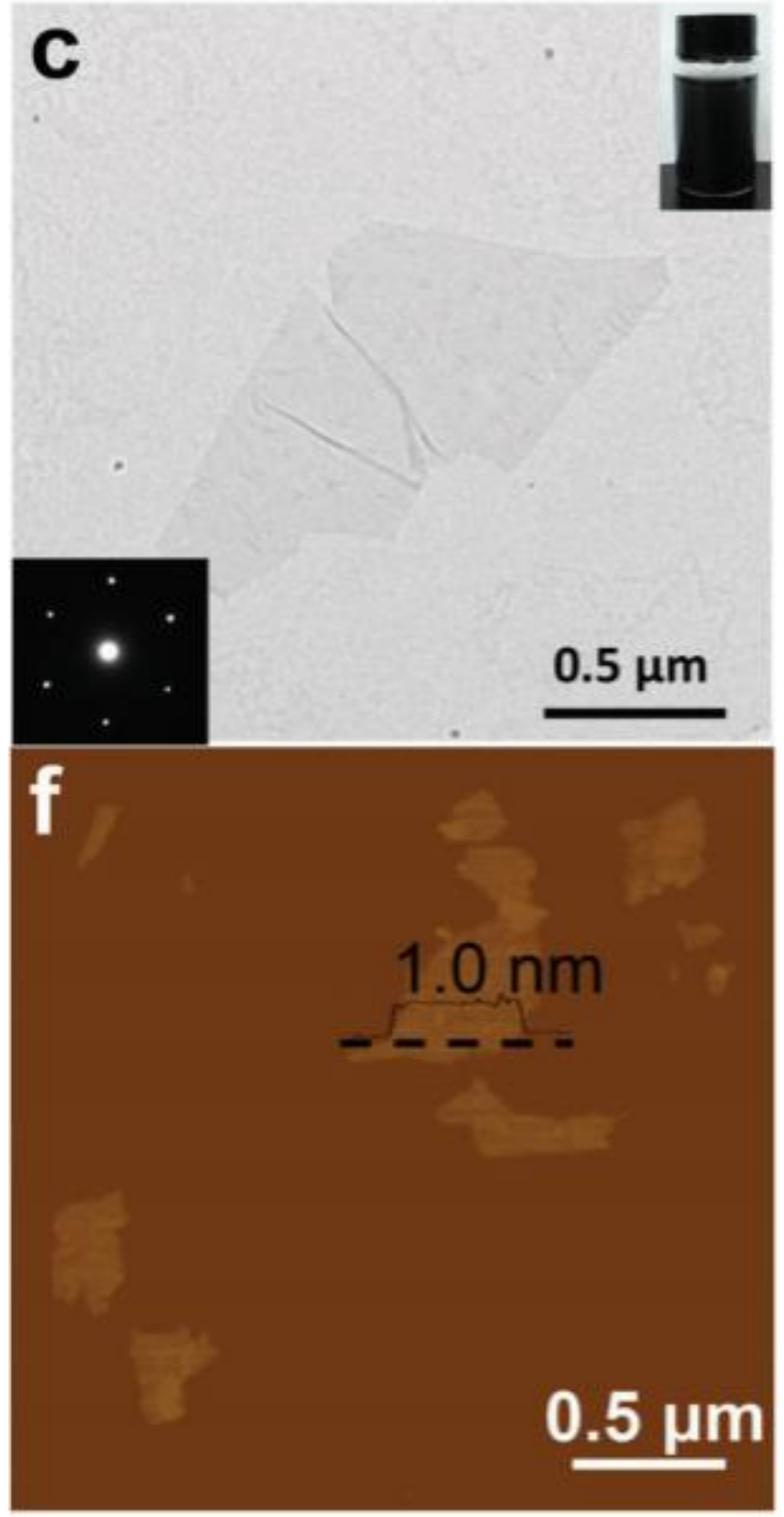

EM and (f) AFM of TiS_2 nanosheets.

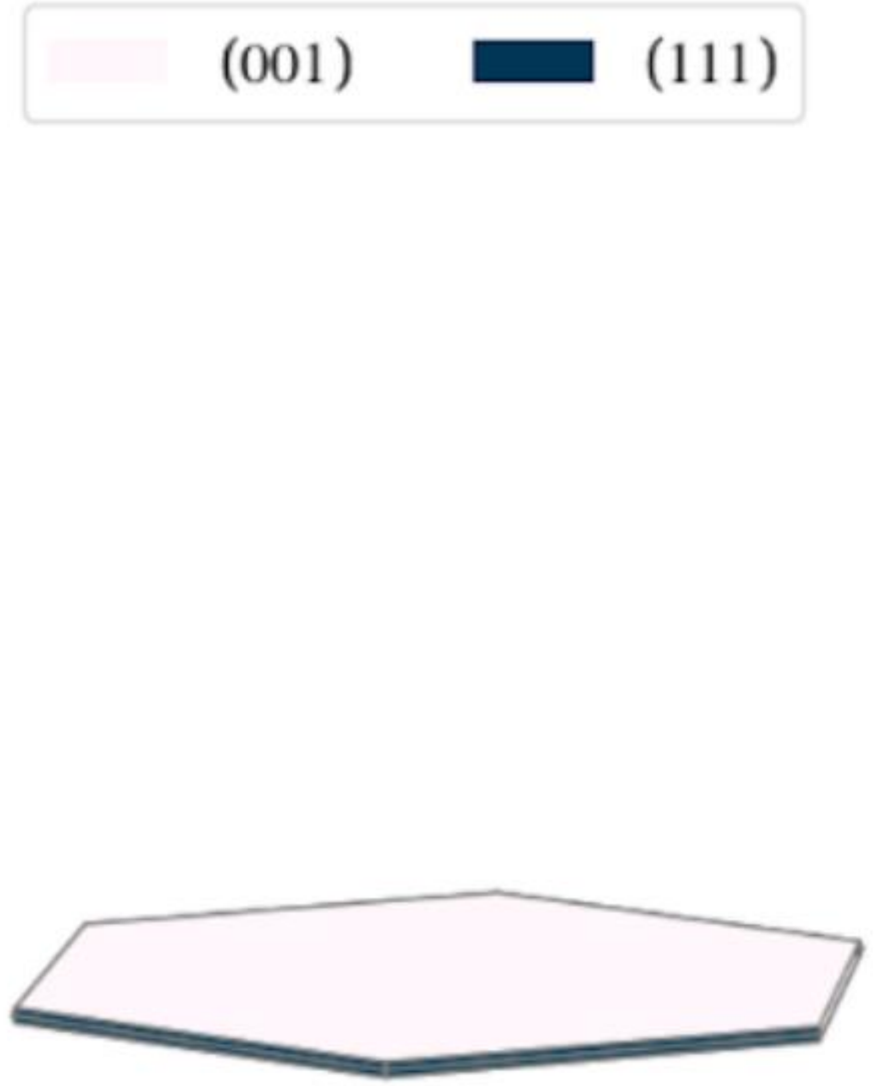

Example: LCO film growth

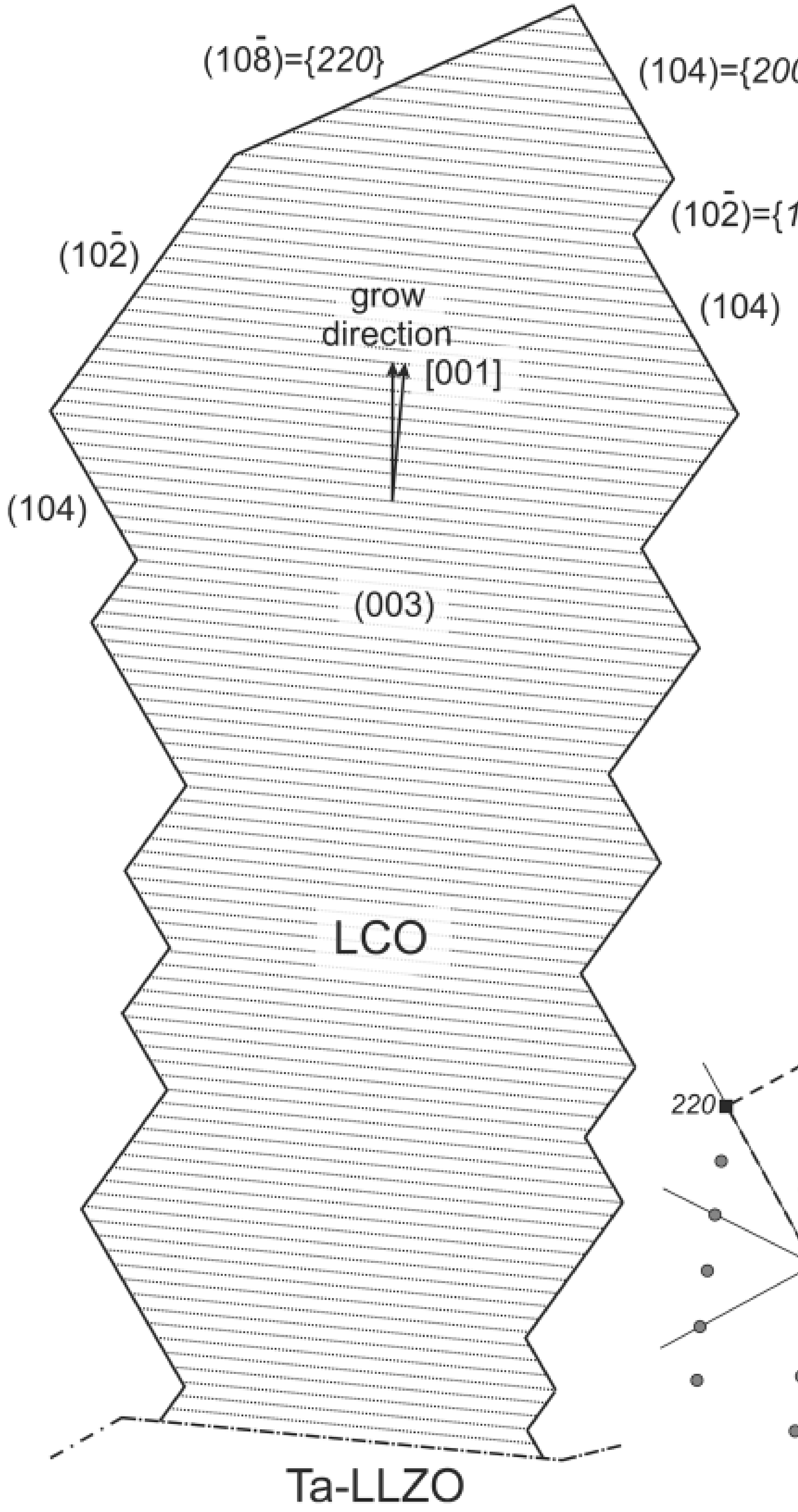

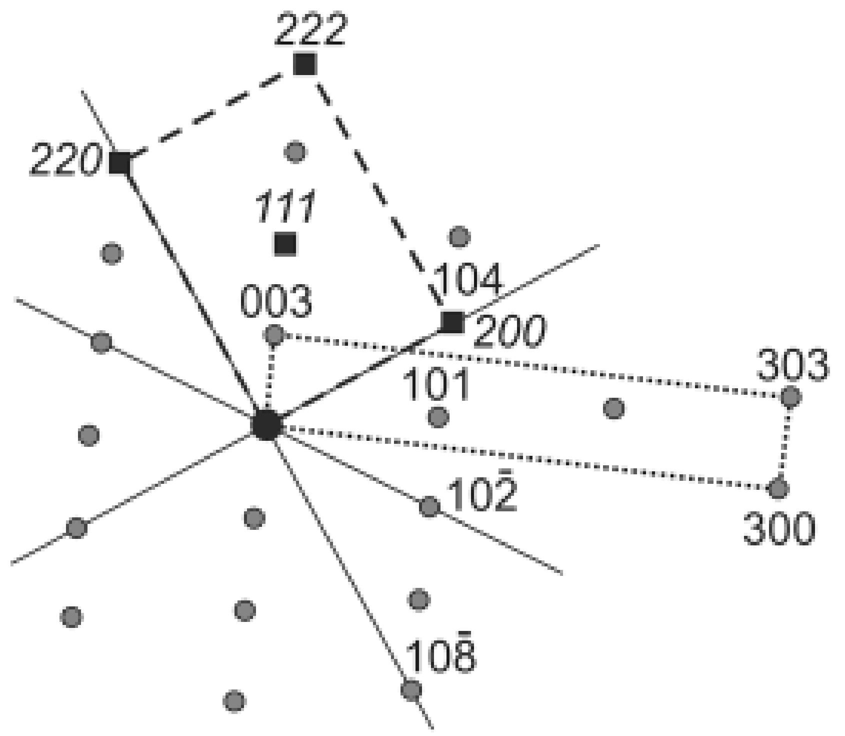

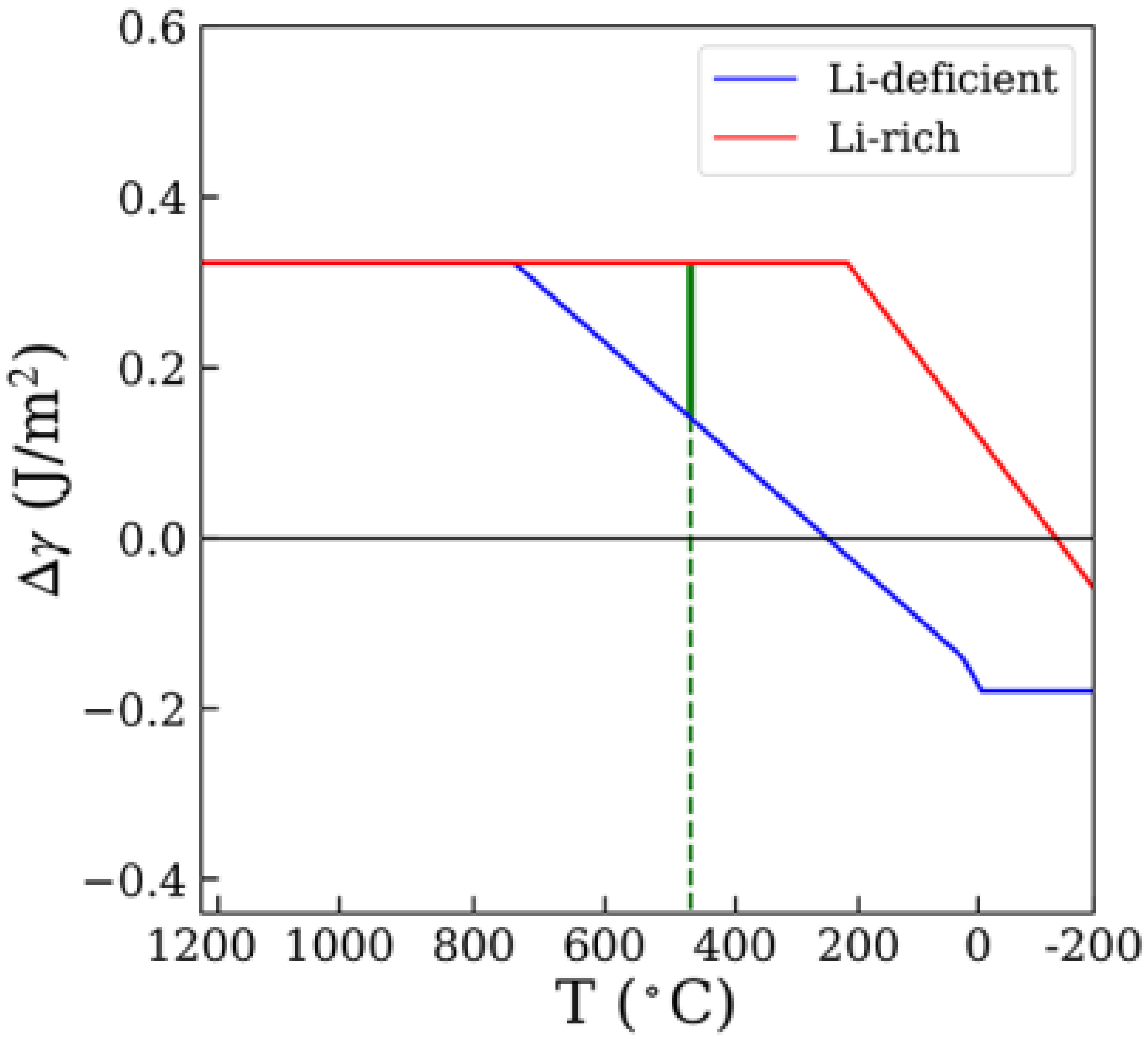

$$\Delta\gamma = \gamma(003) - \gamma\{104\}$$

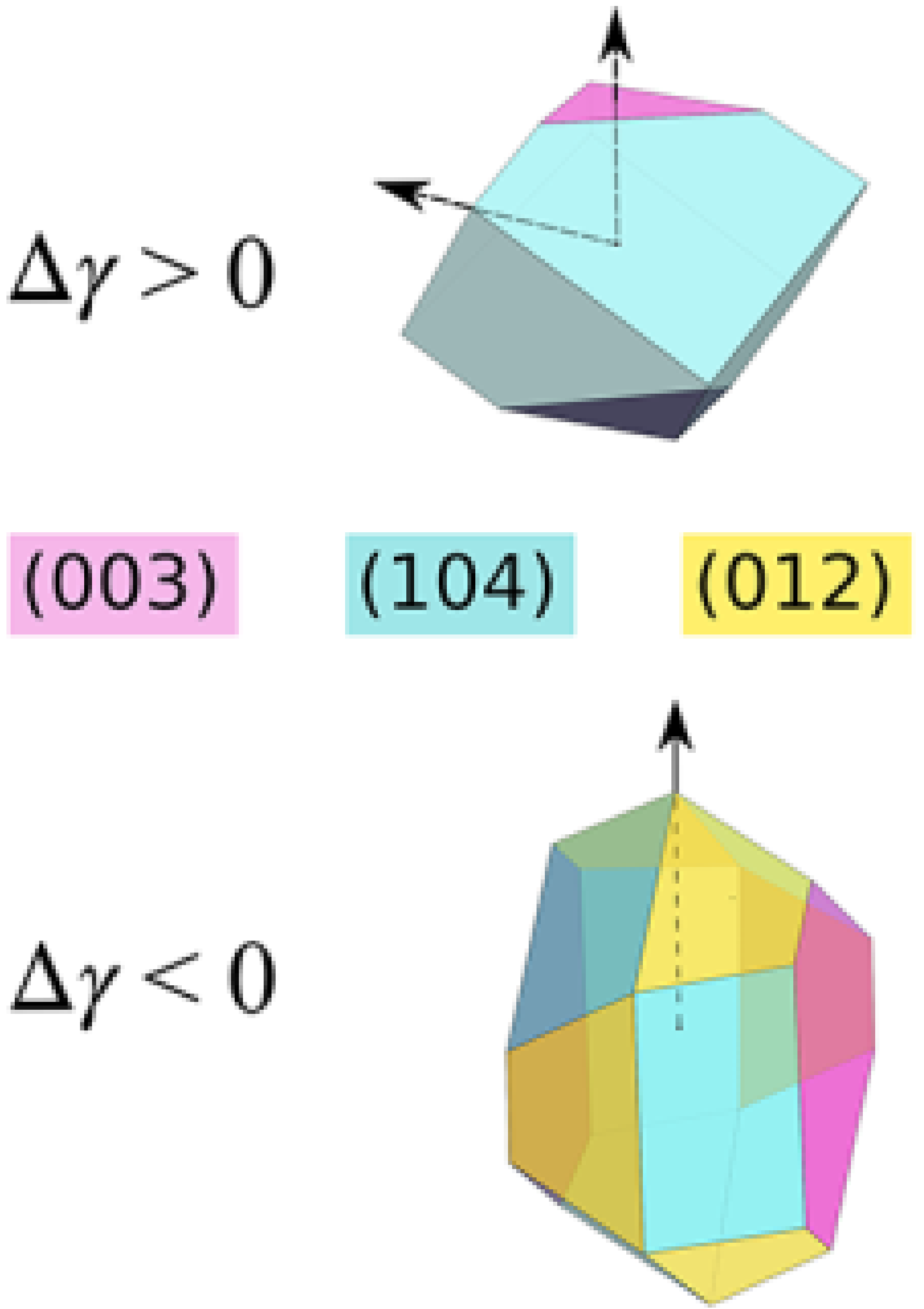

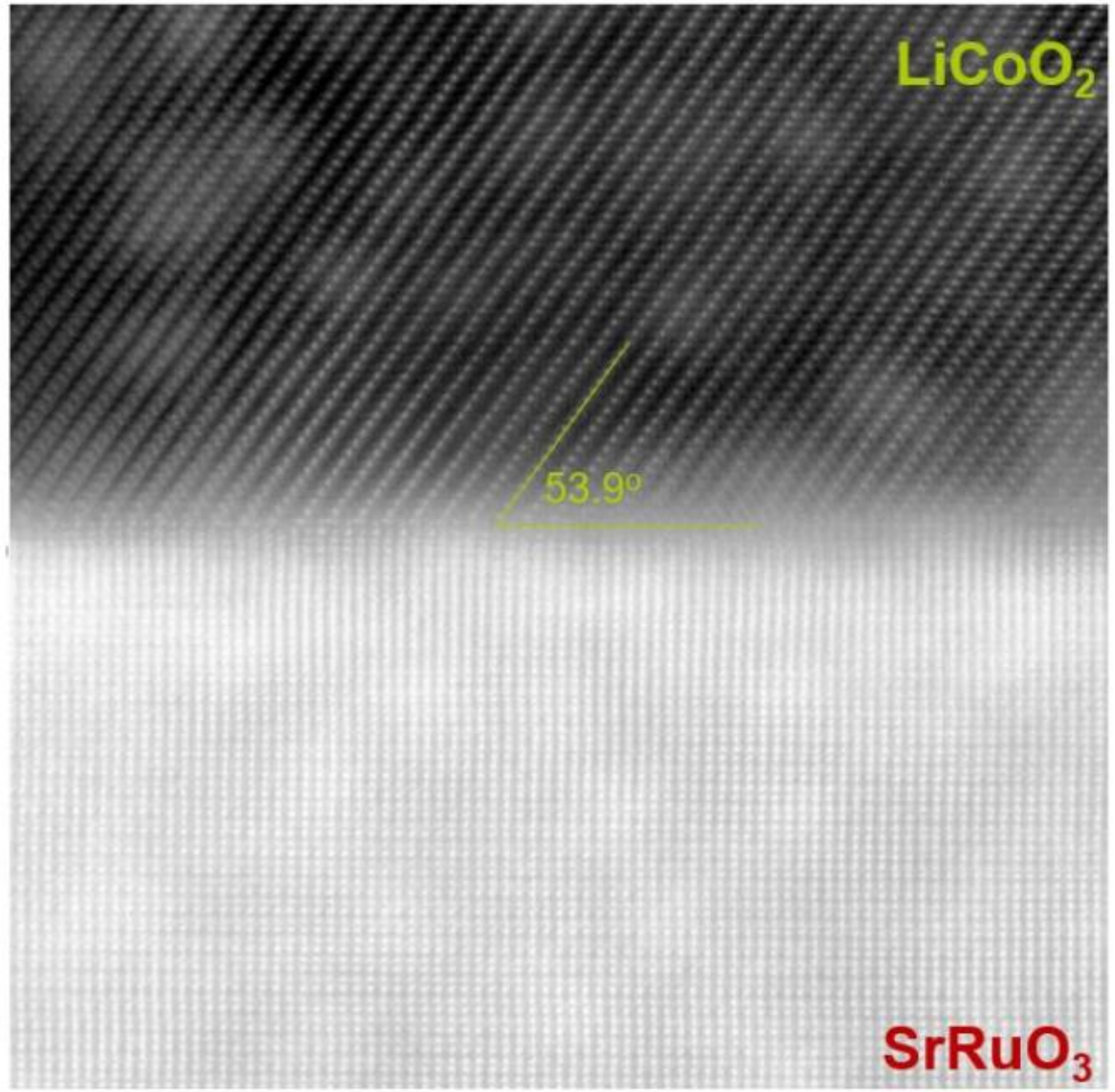

Figure S21. Atomic resolution HAADF-STEM image of the LCO/SRO interface in the LCO/SRO/STO sample obtained using optimized deposition conditions. The formation of {104}-oriented LCO layer is explicitly demonstrated.

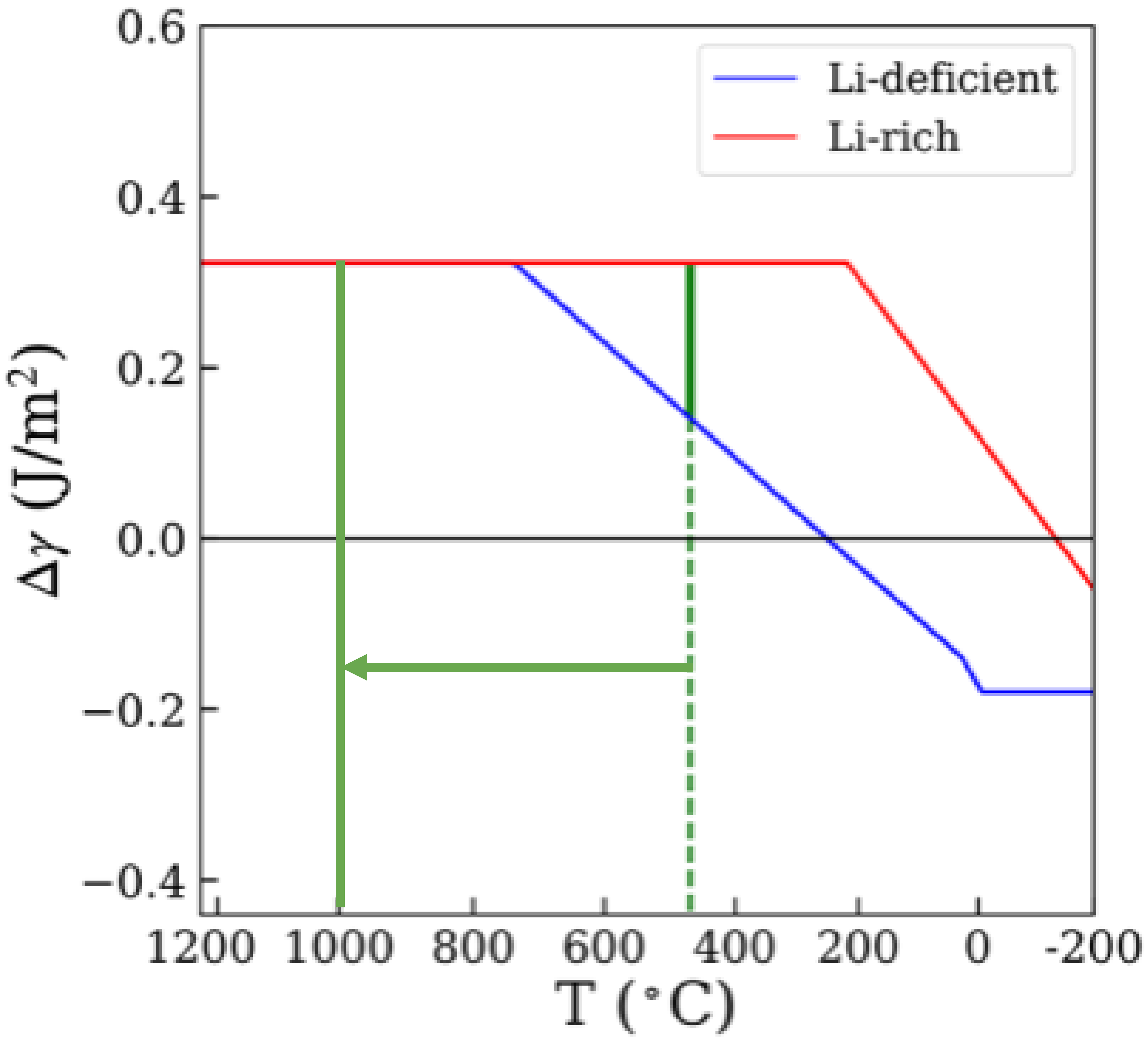

$$\Delta\gamma = \gamma(003) - \gamma\{104\}$$

Example: B solubility in NMC

B-doping of NMC

Task: We have no idea which position B takes in layered NMC structure. Help!

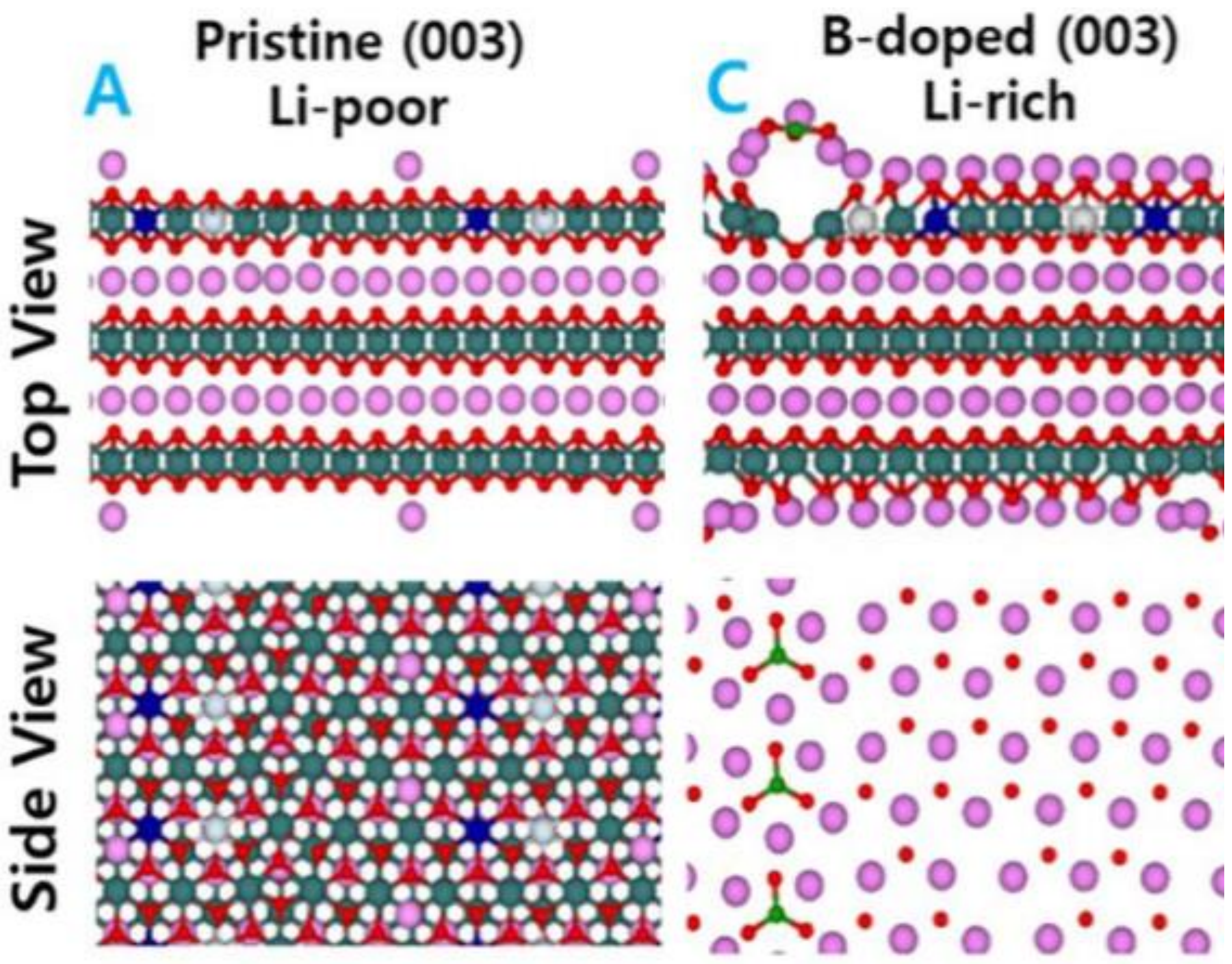

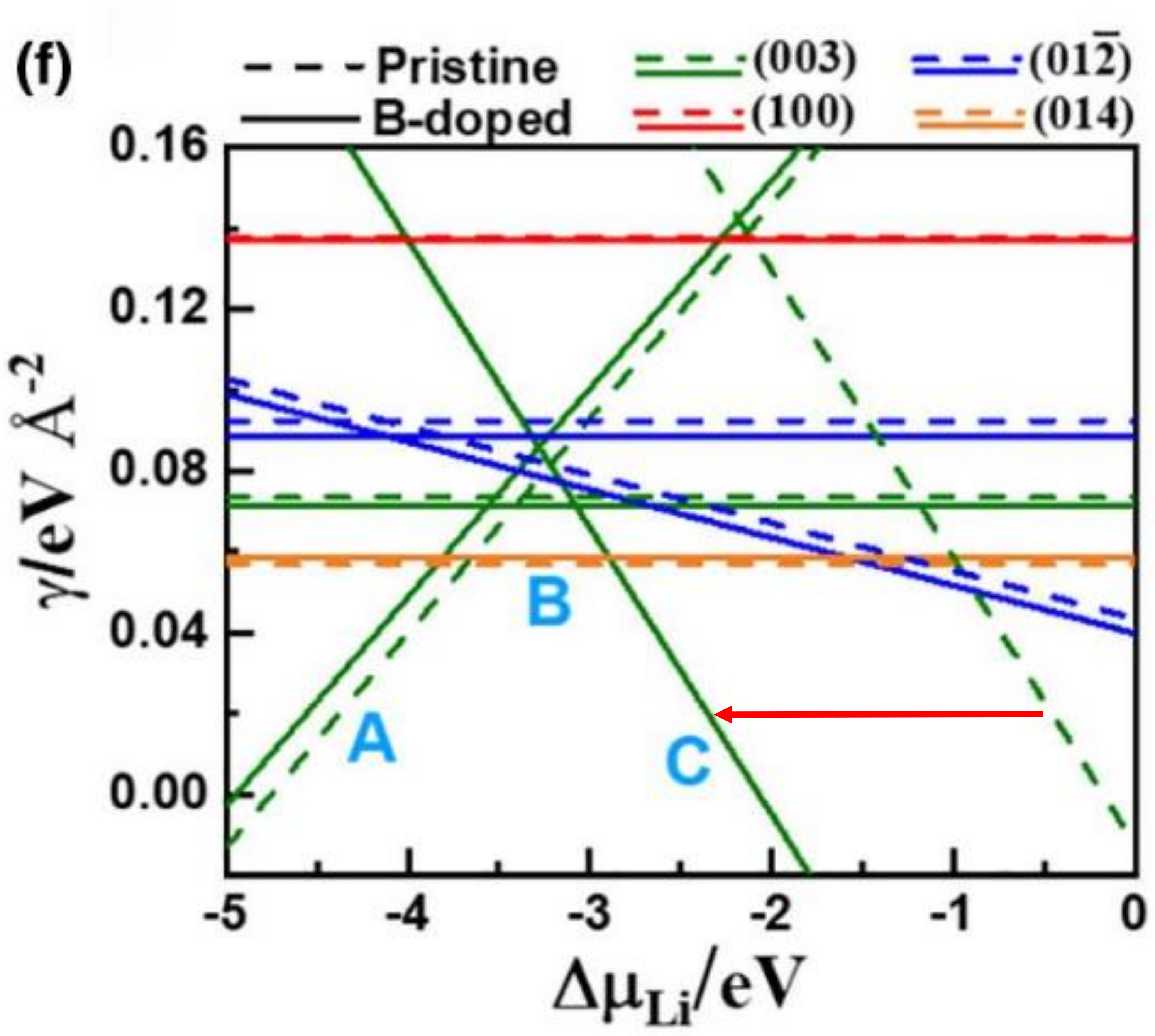

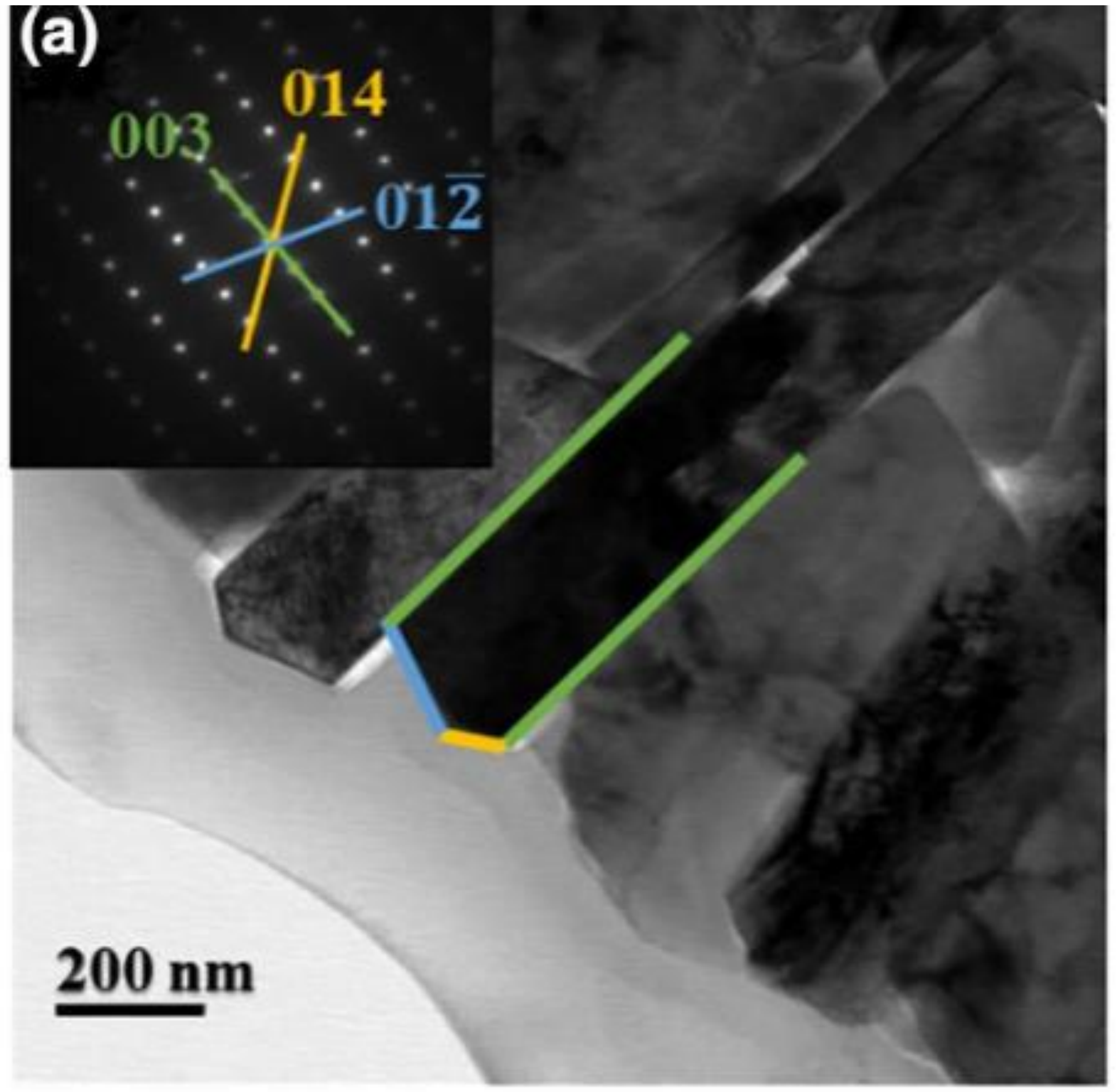

H.-H. Ryu et al. Mater. Today (2020)

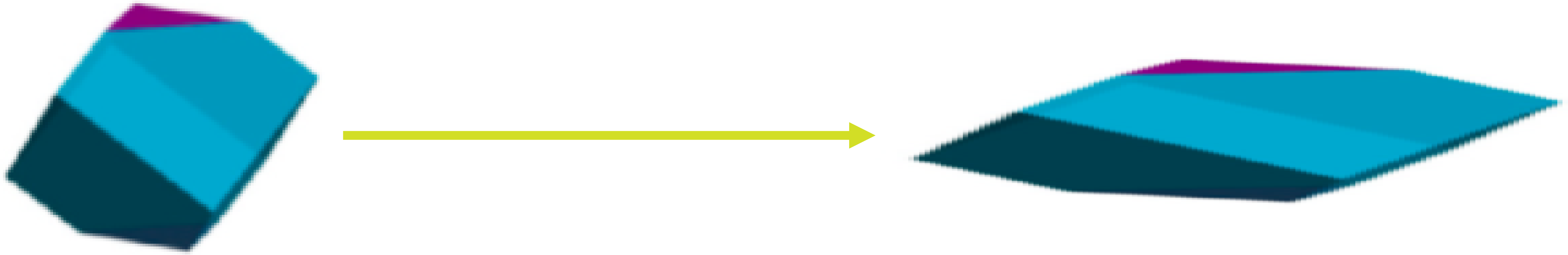

B-doping of NMC

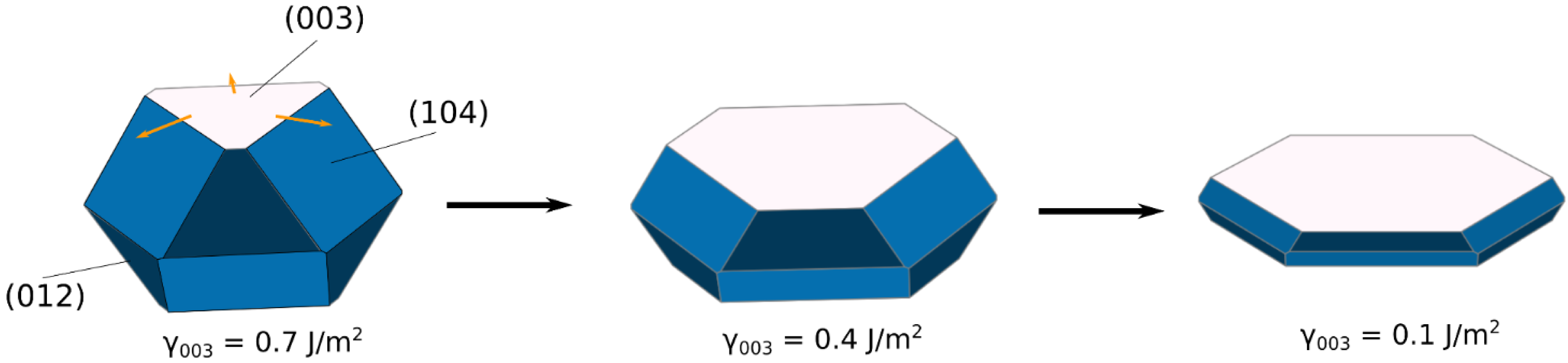

B-doping of NMC

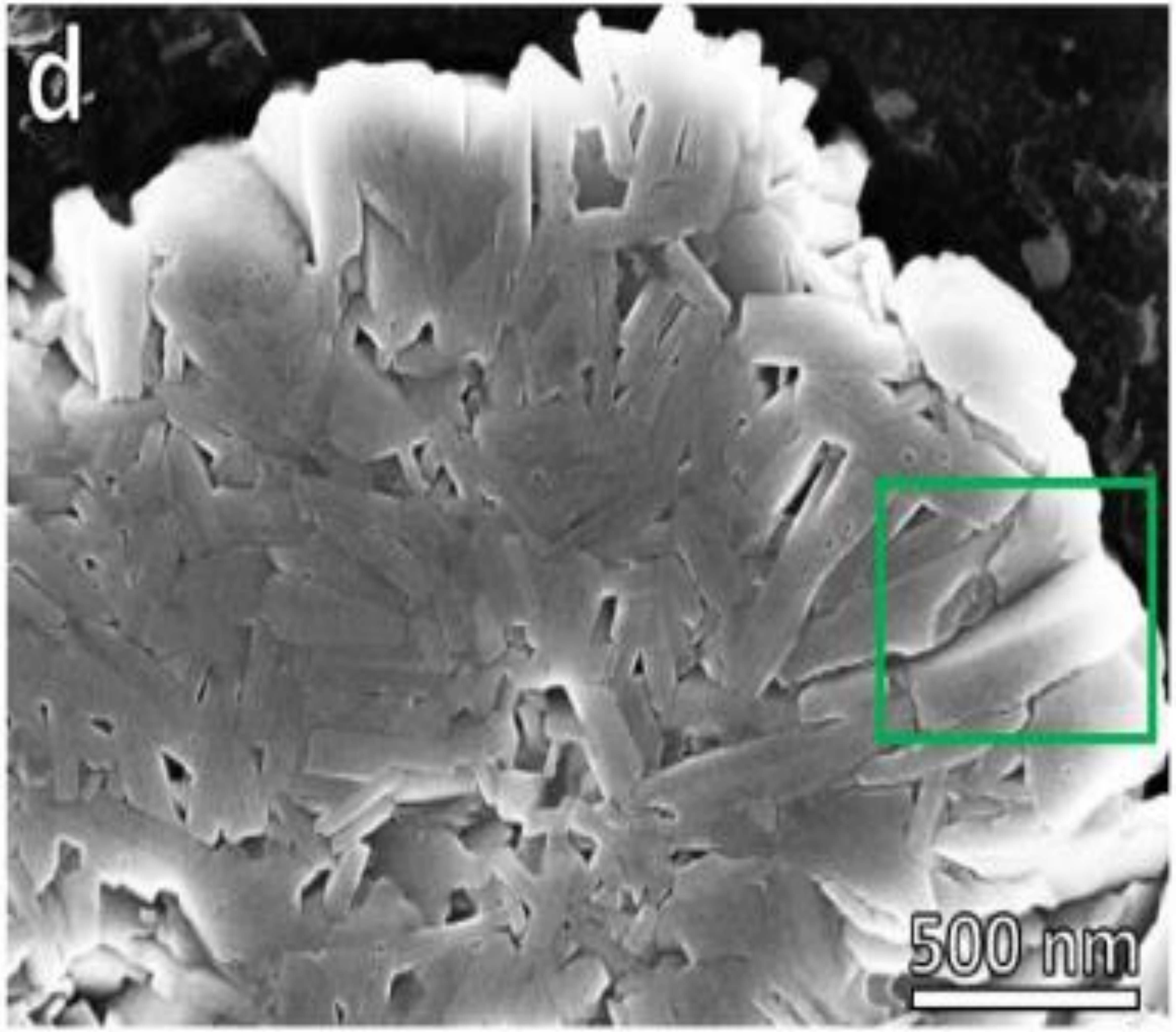

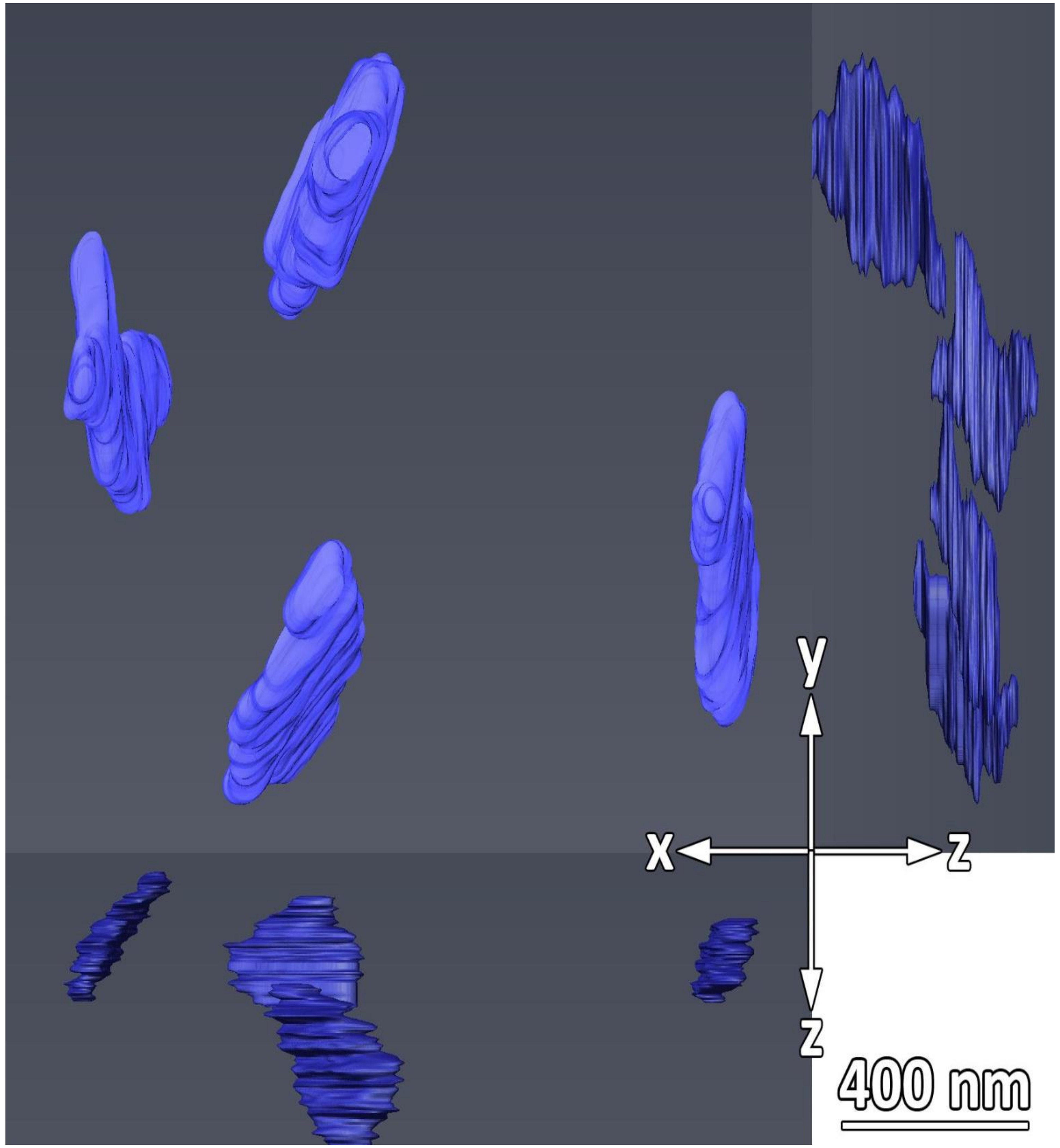

B-doping of NMC

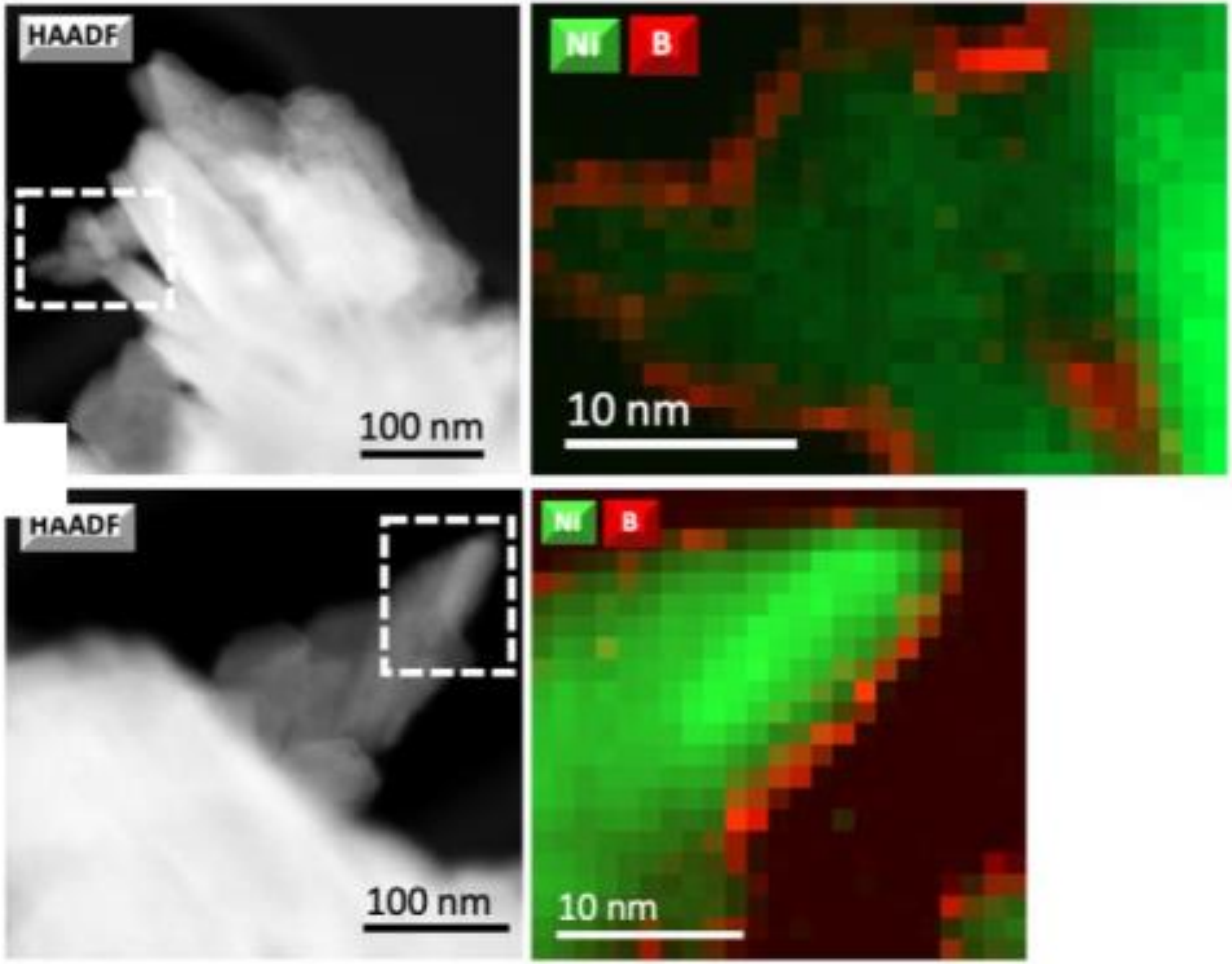

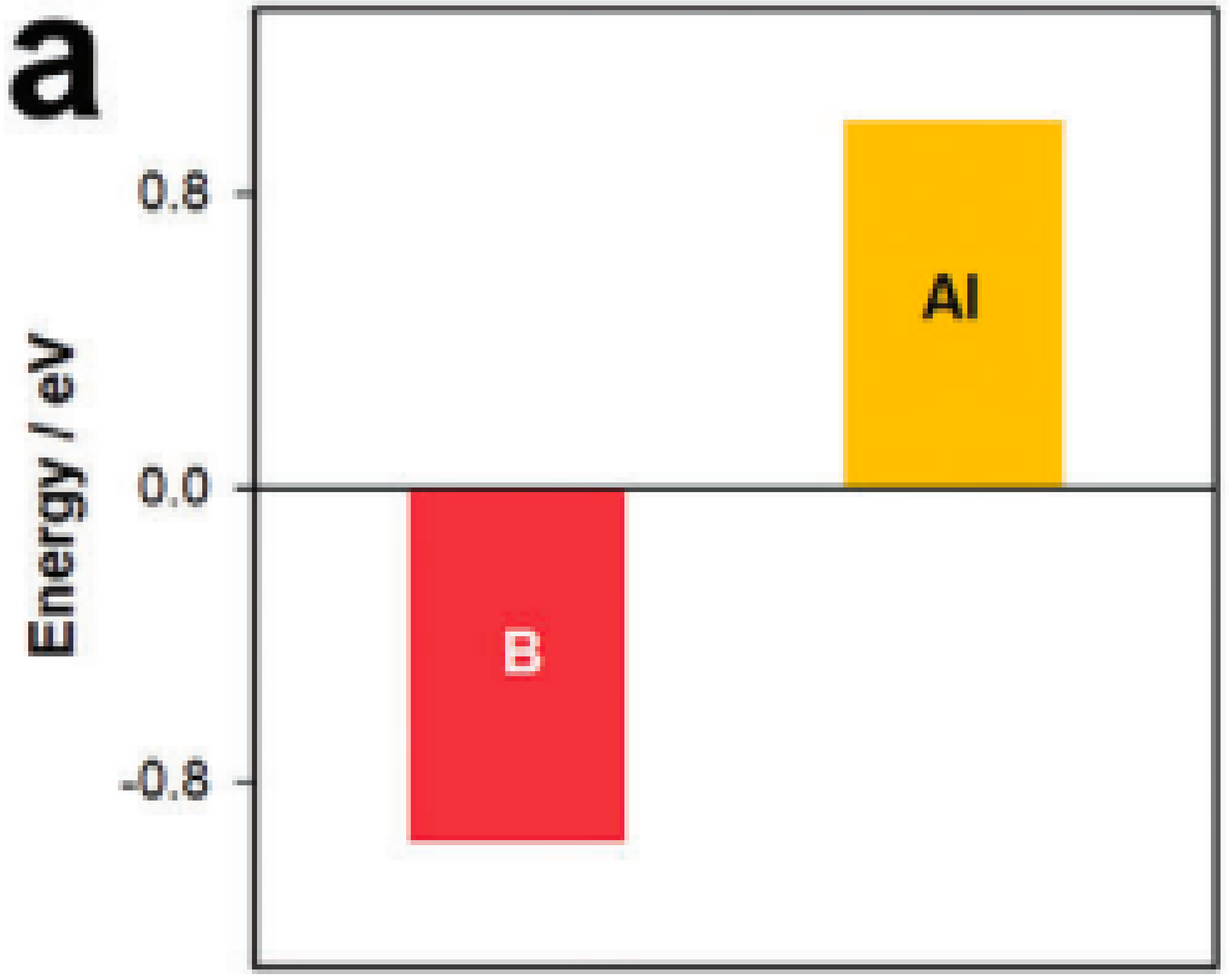

Insights into the Microstructural Engineering of Cobalt-Free, High-Nickel Cathodes Based on Surface Energy for Lithium-Ion Batteries

*Youngjin Kim, Hanseul Kim, Woochul Shin, Eunmi Jo, and Arumugam Manthiram**

erally prefers octahedral coordination.[17] Therefore, B^{3+} would tend to be on the surface as it can be coordinated to less number of neighbors on the surface, unlike Al^{3+}. This also supports that

a) total segregation energy of B and Al species in LNO;

Negative value means tendency to segregation here

Surface position

Bulk position

E_{seg} =

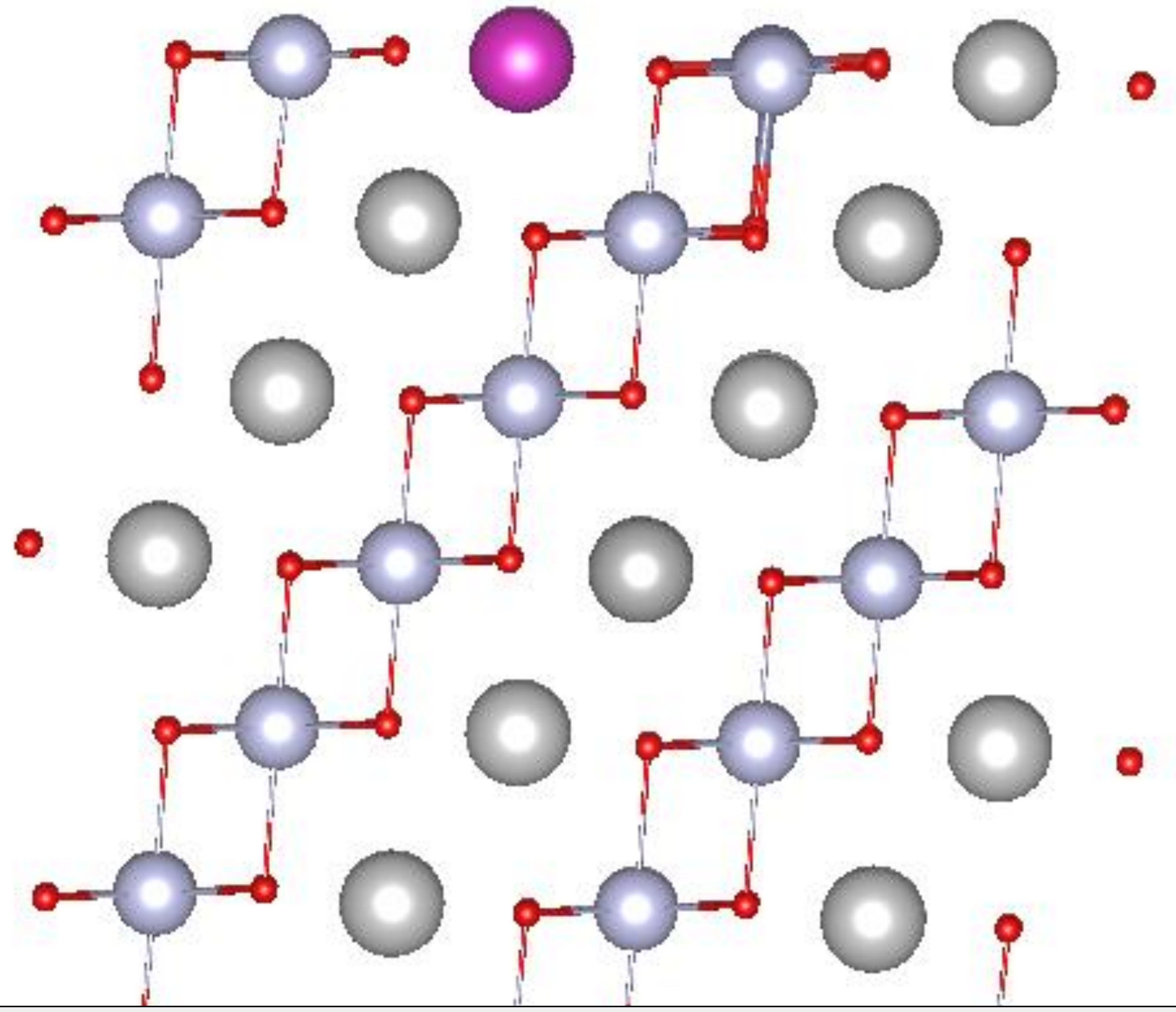

—

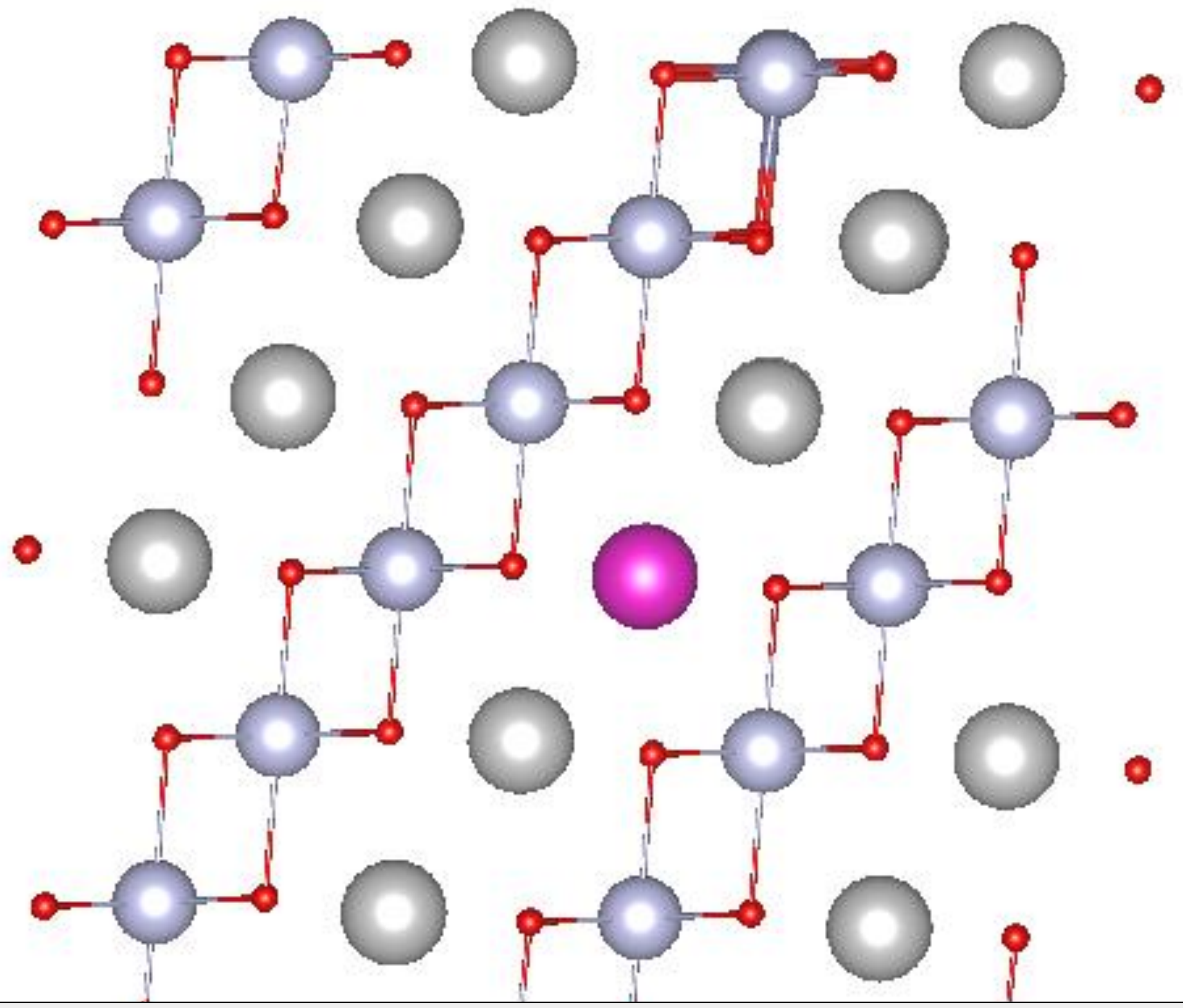

Using our values, we have: 2 eV − 3 eV = **−1 eV**,
that technically means tendency to segregation

However, **Boron is insoluble** both in bulk and at surface

B-doping of NMC

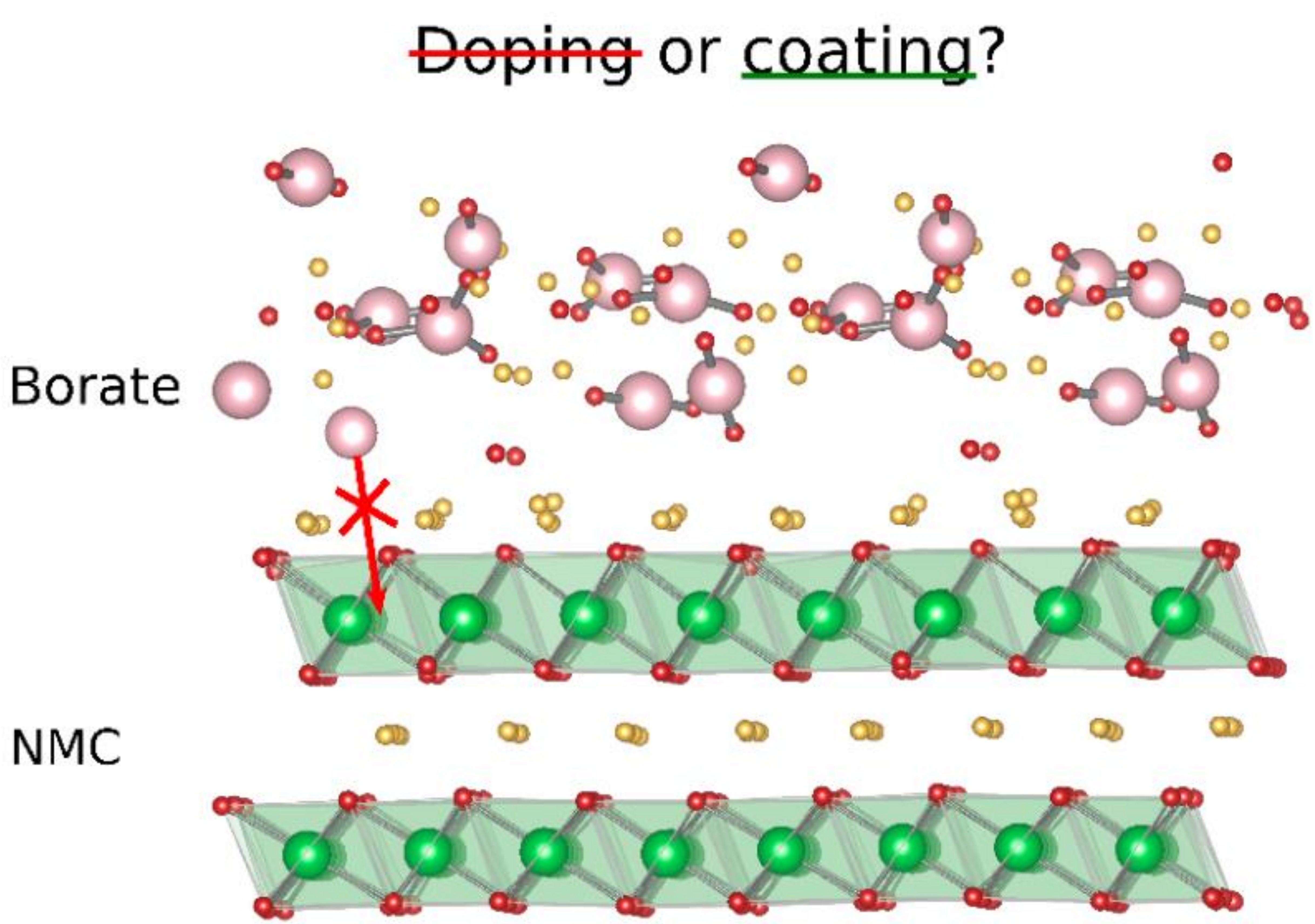

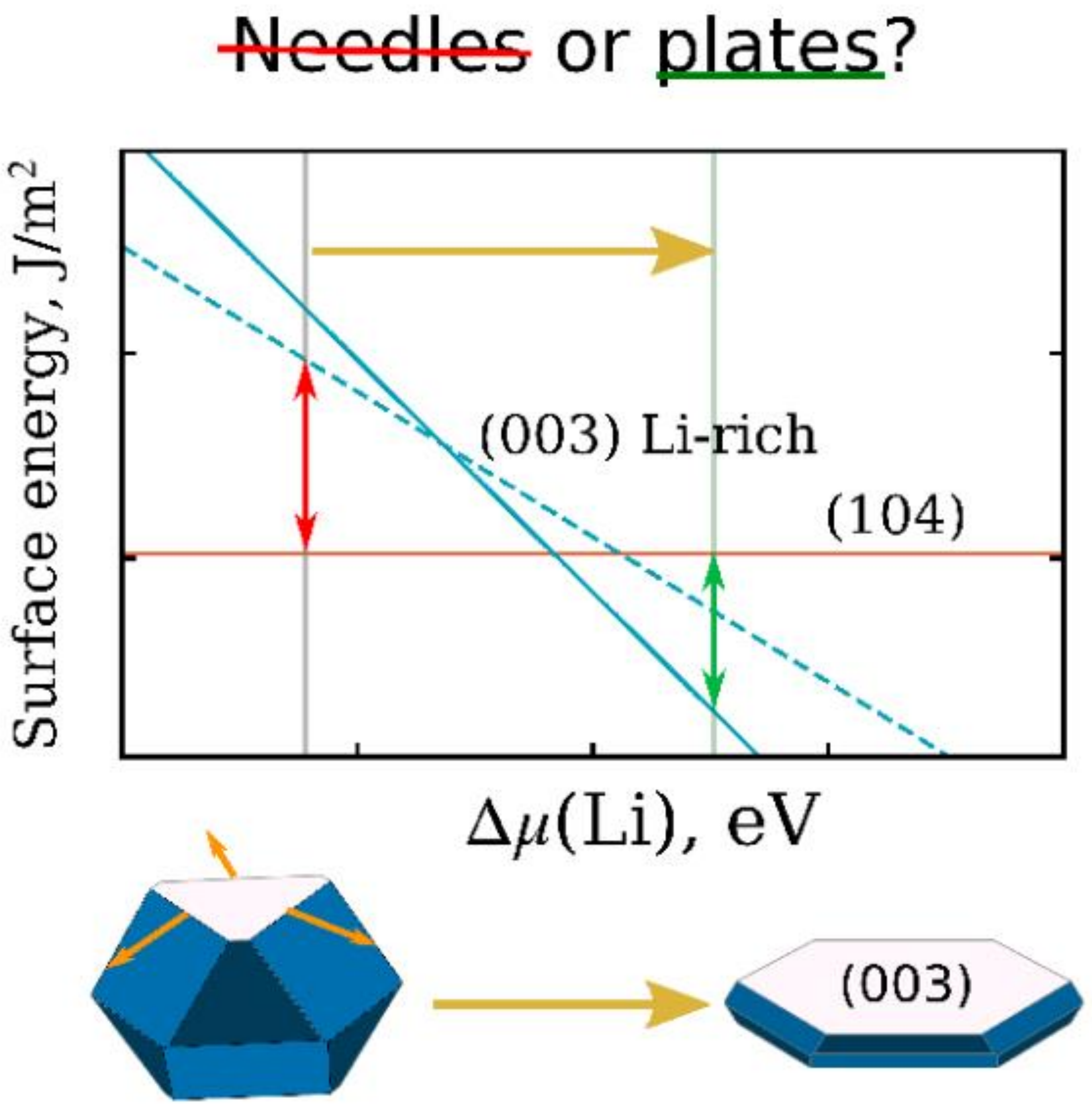

Example: Discovering of new phases

Discovering of new phases: Mo_2NiB_2- Ni cermet

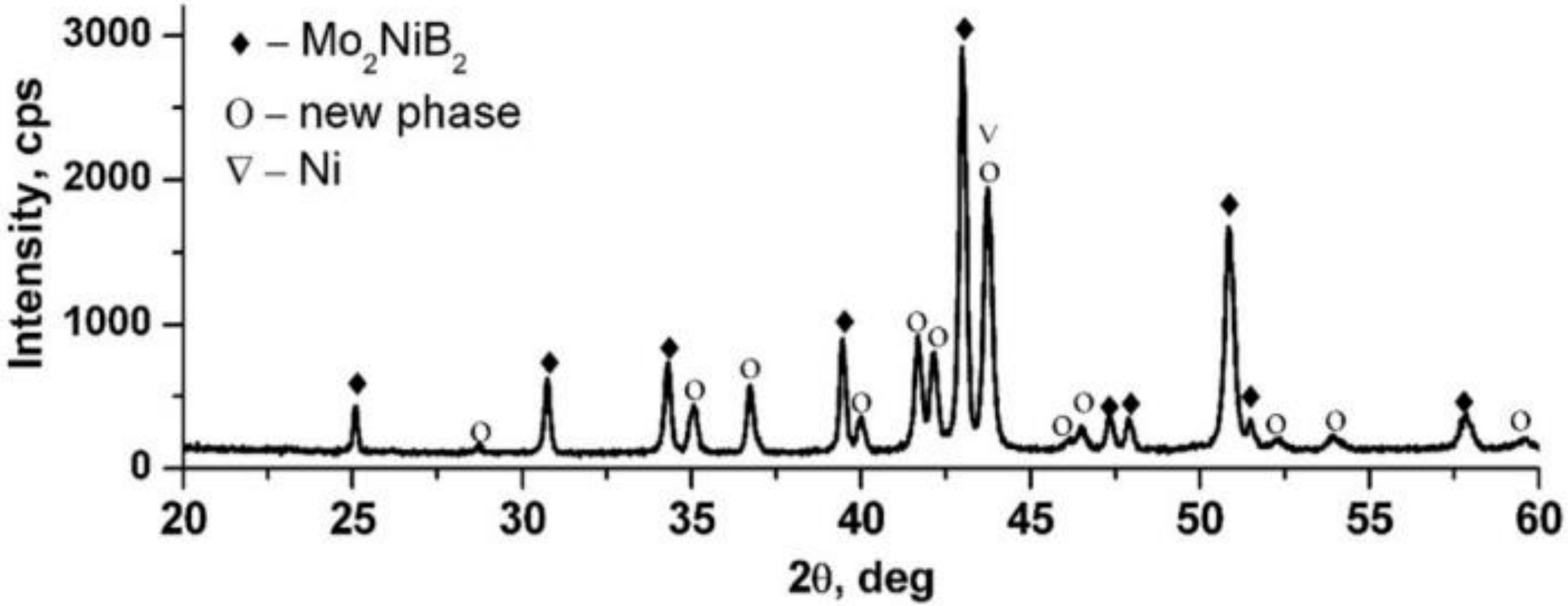

Fig. 2. XRD pattern of Mo_2NiB_2–Ni cermet doped with carbon.

Vershinina, T. N., **Boev, A. O.,** & Ivanov, M. B. (2020).. *Vacuum*, *172*, 109034.

Discovering of new phases: Mo_2NiB_2- Ni cermet

Table 1
DFT calculated formation energies (in eV) of supercells with different configurations of $Mo_9Ni_3C_3B$-type and $Mo_{10}Ni_3C_3B$-type phases.

$Mo_9Ni_3C_3B$-type			$Mo_{10}Ni_3C_3B$-type		
Composition	E_f, eV	V, Å^3	Composition	E_f, eV	V, Å^3
Stoichiometric					
$Mo_{18}Ni_6C_6B_2$ (1)	−0.46	405.34	$Mo_{20}Ni_6C_6B_2$ (1)	−5.88	420.79
$Mo_{18}Ni_6C_6B_2$ (2)	3.85	409.49	$Mo_{20}Ni_6C_6B_2$ (2)	2.93	433.25
$Mo_{18}Ni_6C_6B_2$ (3)	1.38	406.53	$Mo_{20}Ni_6C_6B_2$ (3)	−1.80	425.25
Boron partially substituted					
$Mo_{18}Ni_6C_2B_6$	2.55	420.68	$Mo_{20}Ni_6C_2B_6$	−3.94	430.71
Boron fully substituted					
$Mo_{18}Ni_6B_8$	0.89	419.52	$Mo_{20}Ni_6B_8$	−5.76	433.60
Carbon fully substituted					
$Mo_{18}Ni_6C_8$	1.55	404.72	$Mo_{20}Ni_6C_8$	−3.82	417.68
Mo-substituted					
$Mo_{19}Ni_5C_2B_6$	−0.50	409.85	$Mo_{21}Ni_5C_2B_6$	−4.78	426.28
$Mo_{20}Ni_4C_2B_6$	−0.65	414.05	$Mo_{22}Ni_4C_2B_6$	−4.33	432.21
$Mo_{21}Ni_3C_2B_6$	−0.25	419.05	$Mo_{23}Ni_3C_2B_6$	−3.57	437.27
Ni-substituted					
$Mo_{17}Ni_7C_2B_6$	0.63	401.33	$Mo_{19}Ni_7C_2B_6$	−4.46	416.86
$Mo_{16}Ni_8C_2B_6$	1.14	397.16	$Mo_{18}Ni_8C_2B_6$	−3.57	413.22
$Mo_{15}Ni_9C_2B_6$	1.98	392.66	$Mo_{17}Ni_9C_2B_6$	−2.57	409.54

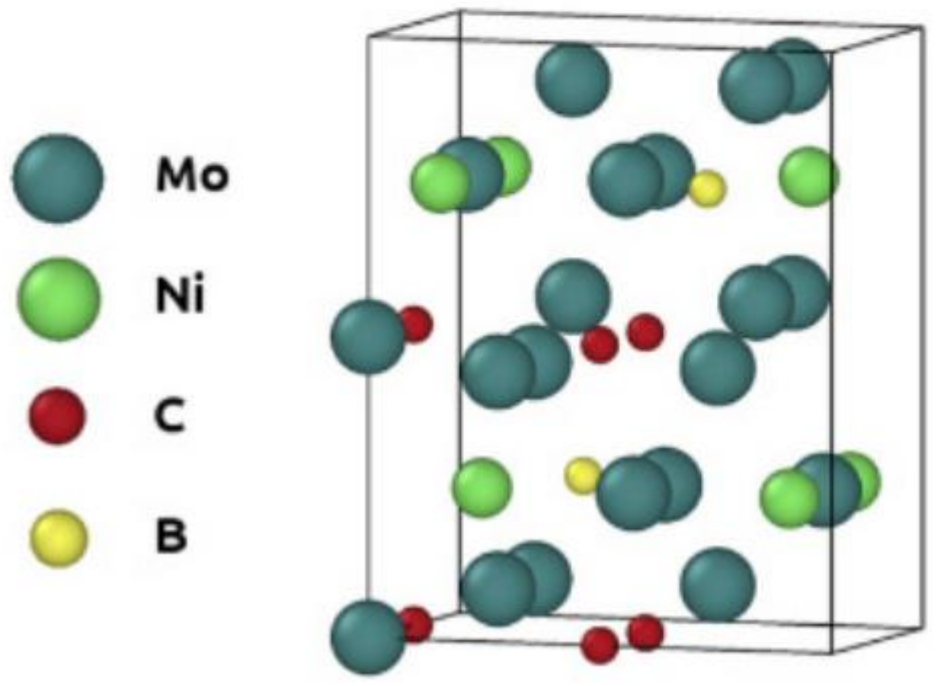

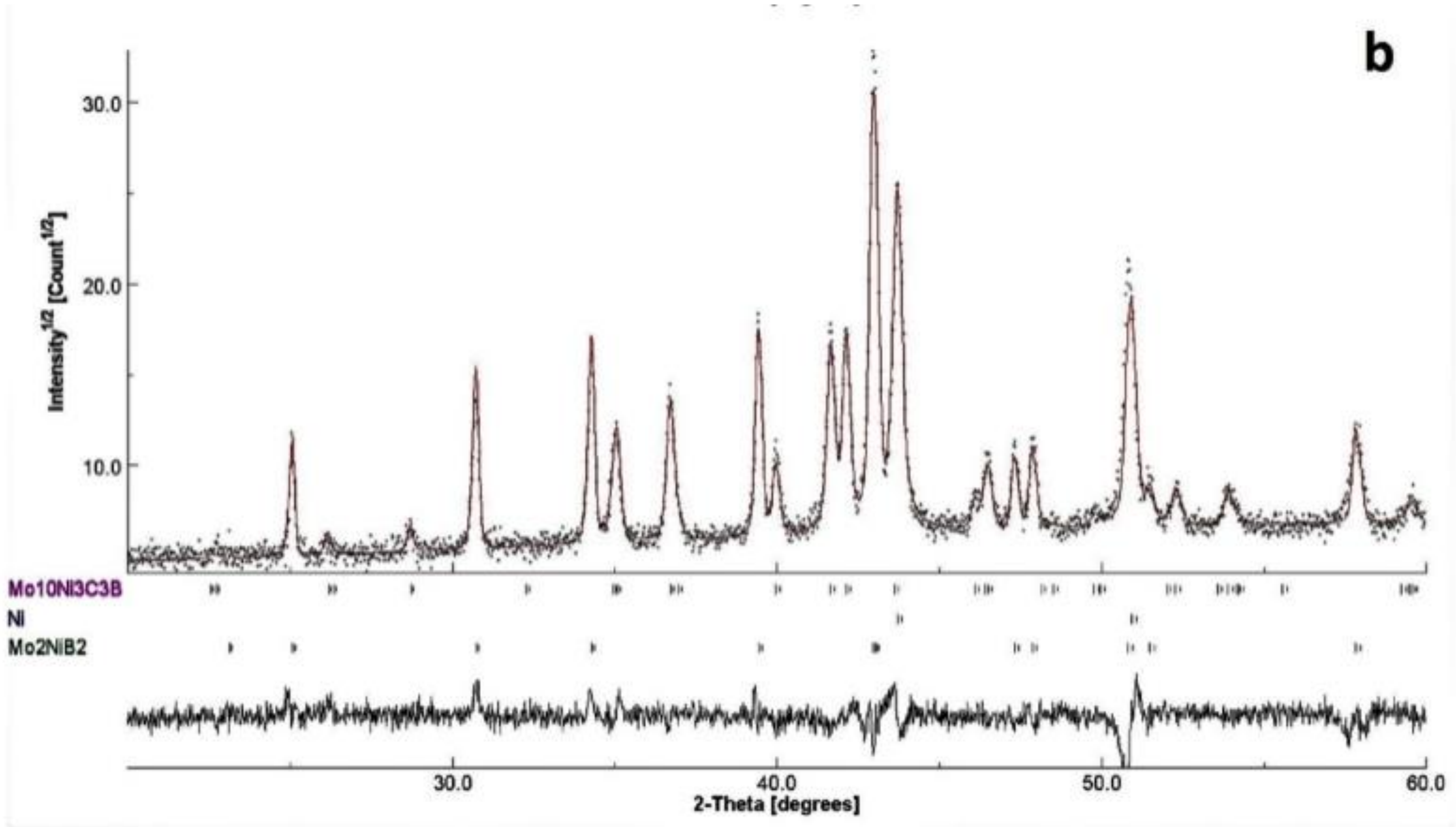

Vershinina, T. N., **Boev, A. O.**, & Ivanov, M. B. (2020).. *Vacuum*, *172*, 109034.

Material Project database

Materials explorer

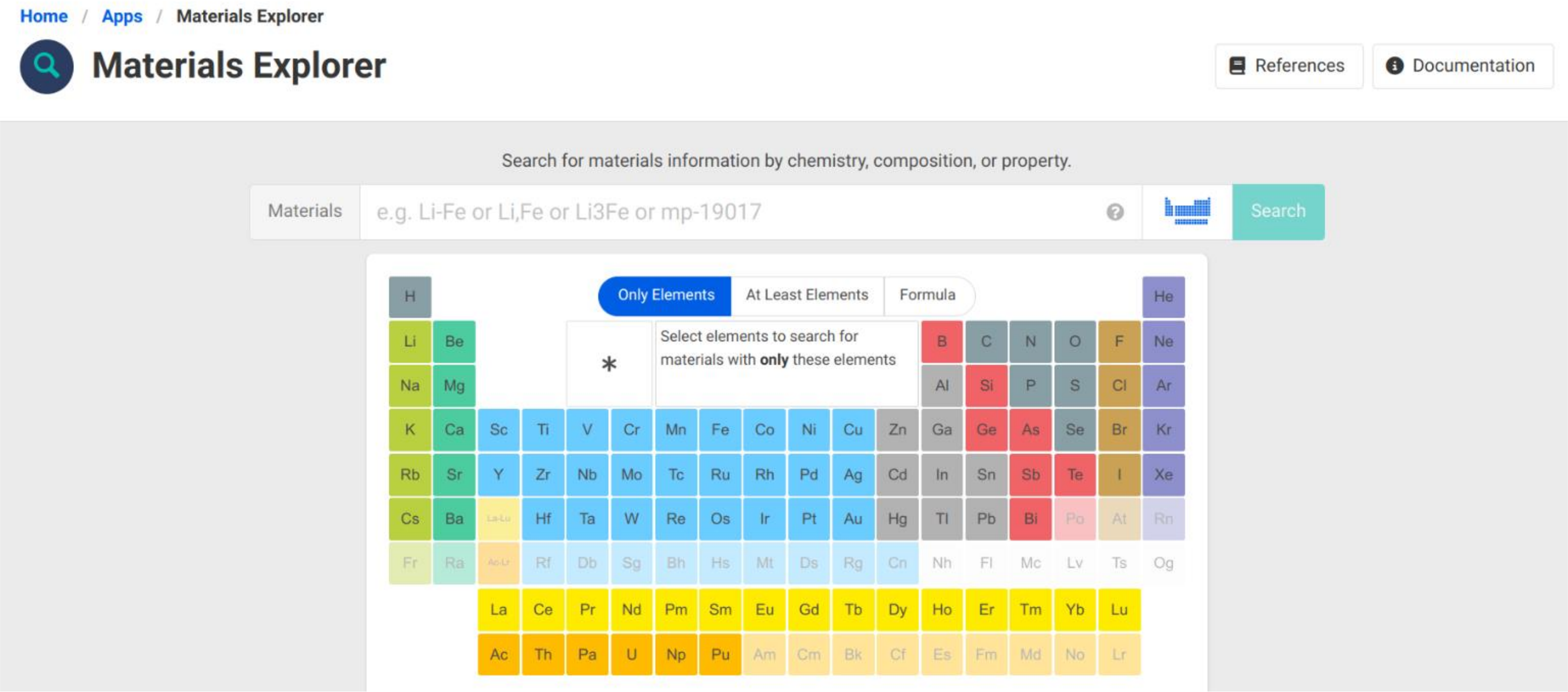

Materials explorer

Materials Explorer

References | Documentation

Search for materials information by chemistry, composition, or property.

Materials | Li-Co-O | Search

335 materials match your search

Showing 1-15

× Chemical System: Li-Co-O

Columns | Export Table

	Material ID	Formula	Crystal System	Space Group Symbol	Sites	Energy Above Hull (eV/atom)	Band Gap (eV)
	mp-774082	$Li(CoO_2)_2$	Monoclinic	P12_11̄	56	0	0.67
★	mp-18925	Li_6CoO_4	Tetragonal	$P4_2/nmc$	44	0	2.40
★	mp-22526	$LiCoO_2$	Trigonal	R3̄m	4	0	0.66
	mp-1173879	Li_2CoO_3	Monoclinic	C12/m1	24	0	0
	mp-849273	$LiCoO_2$	Cubic	Fd3̄m1	16	< 0.01	0
	mp-771155	$Li_7Co_5O_{12}$	Monoclinic	C12/m1	24	< 0.01	0
	mp-532301	$Li_{20}(CoO_2)_{21}$	Triclinic	P1̄	83	< 0.01	0
	mp-1175469	$Li_9Co_7O_{16}$	Triclinic	P1̄	32	< 0.01	0.71

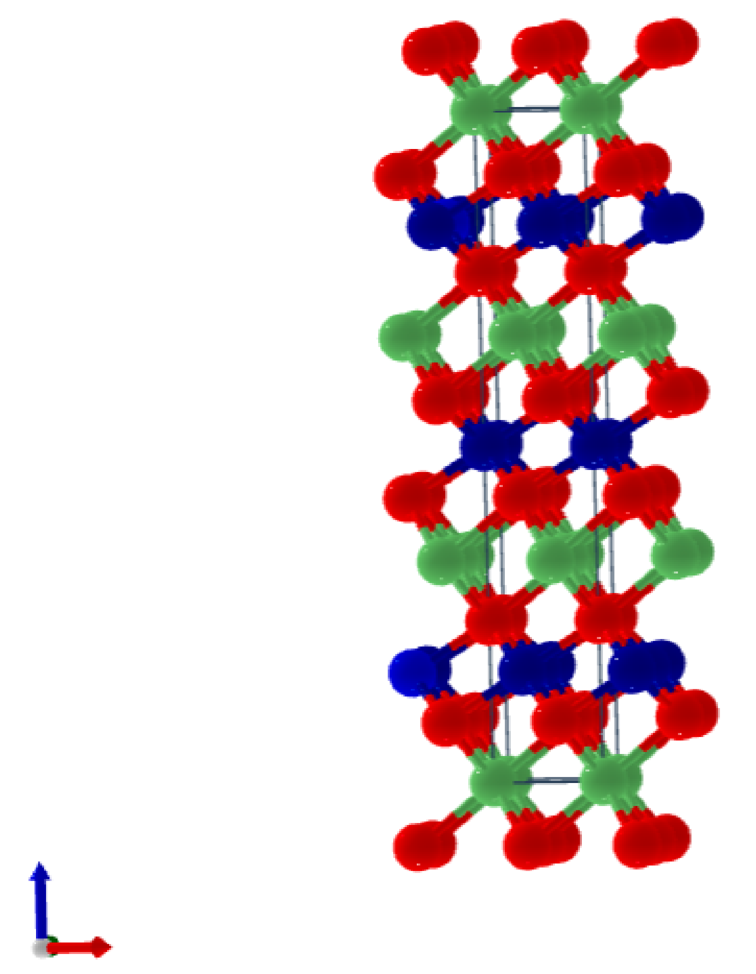

Energy Above Hull	0.000 eV/atom
Space Group	R3̄m
Band Gap	0.66 eV
Predicted Formation Energy	-1.744 eV/atom
Magnetic Ordering	Non-magnetic
Total Magnetization	0.00 μB/f.u.
Experimentally Observed	Yes

Description (Auto-generated)

$LiCoO_2$ is Caswellsilverite structured and crystallizes in the trigonal R3̄m space group. Li^{1+} is bonded to six equivalent O^{2-} atoms to form LiO_6 octahedra that share corners with six equivalent CoO_6 octahedra, edges with six equivalent LiO_6 octahedra, and edges with six

Synthesis explorer

Battery explorer

Home / Apps / Battery Explorer

Battery Explorer

References | Documentation

Explore candidate materials for lithium, magnesium and calcium batteries with predicted voltage profiles and oxygen evolution data.

Batteries | Li-Co-O | Search

mp-753251_Li	$Li_{2.5\text{-}3.5}CoO_3$	Li	$Li_5(CoO_3)_2$	$Li_7(CoO_3)_2$	0.059	2.311	204.241
mp-705847_Li	$Li_{0\text{-}0.67}CoO_2$	Li	CoO_2	$Li_2(CoO_2)_3$	0.057	4.301	186.980
mp-759339_Li	$Li_{4\text{-}5}CoO_4$	Li	Li_4CoO_4	Li_5CoO_4	0.030	2.678	170.022
mp-756488_Li	$Li_{0\text{-}0.5}CoO_2$	Li	CoO_2	$Li(CoO_2)_2$	0.032	4.531	141.953
mp-752662_Li	$Li_{2\text{-}3.5}CoO_3$	Li	Li_2CoO_3	$Li_7(CoO_3)_2$	0.094	2.307	306.361
mp-755386_Li	$Li_{0\text{-}0.5}CoO_2$	Li	CoO_2	$Li(CoO_2)_2$	0.036	3.956	141.953
mp-755508_Li	$Li_{0\text{-}1.25}CoO_2$	Li	CoO_2	$Li_5(CoO_2)_4$	0.183	3.199	336.336
mp-685270_Li	$Li_{0\text{-}2}Co_{21}O_{40}$	Li	$Co_{21}O_{40}$	$Li_{20}Co_{21}O_{40}$	0.053	3.632	265.836
mp-753473_Li	$Li_{0\text{-}1}CoO_2$	Li	CoO_2	$LiCoO_2$	0.106	3.410	273.839
mp-759702_Li	$Li_{4\text{-}5}CoO_4$	Li	Li_4CoO_4	Li_5CoO_4	0.034	2.792	170.022
mp-771191_Li	$Li_{4\text{-}5}Co_7O_{16}$	Li	$Li_4Co_7O_{16}$	$Li_5Co_7O_{16}$	0.015	4.558	38.112

Interface reactions

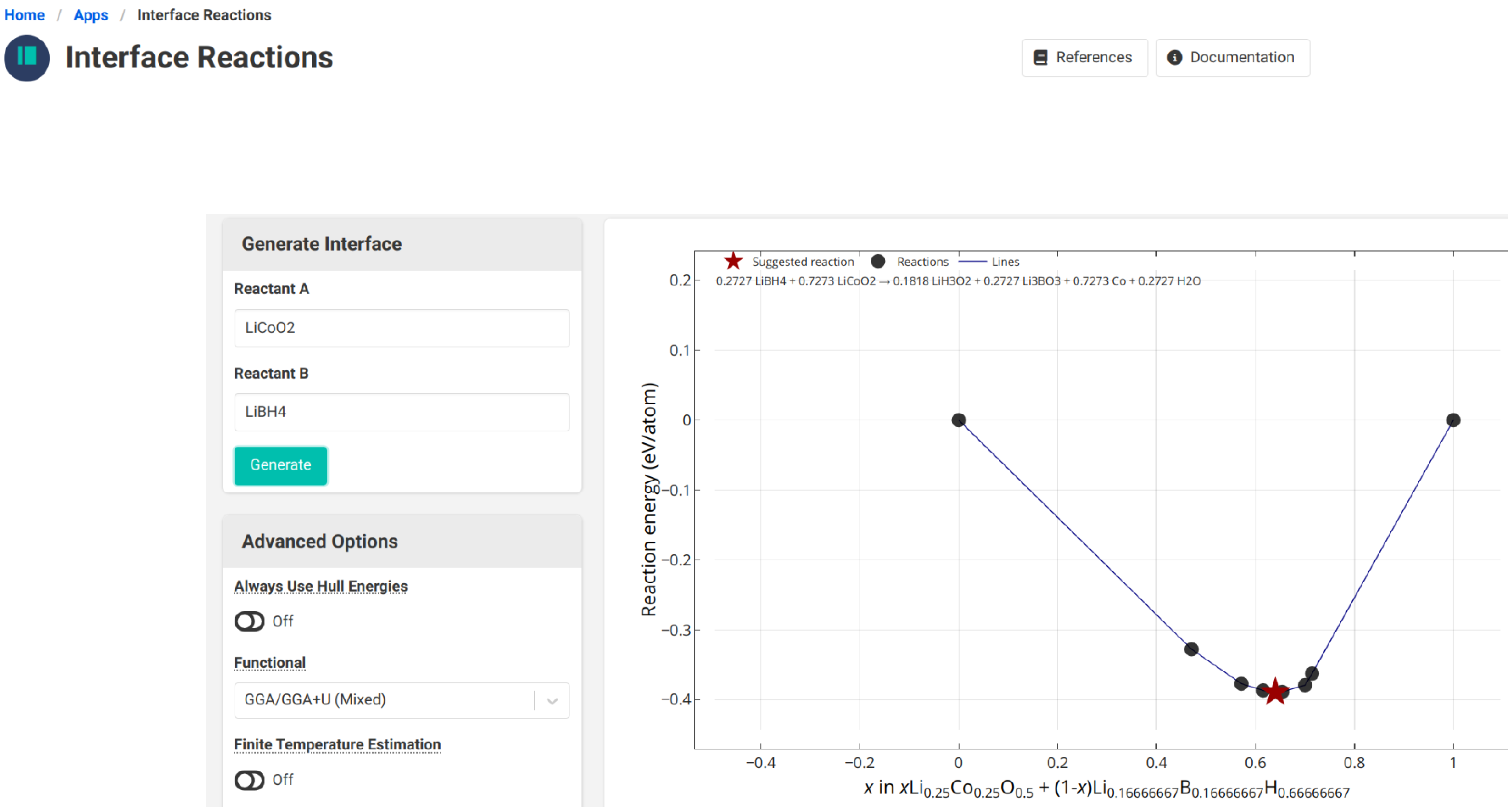

Pourbaix diagram

Home / Apps / Pourbaix Diagram

Pourbaix Diagram

References | Documentation

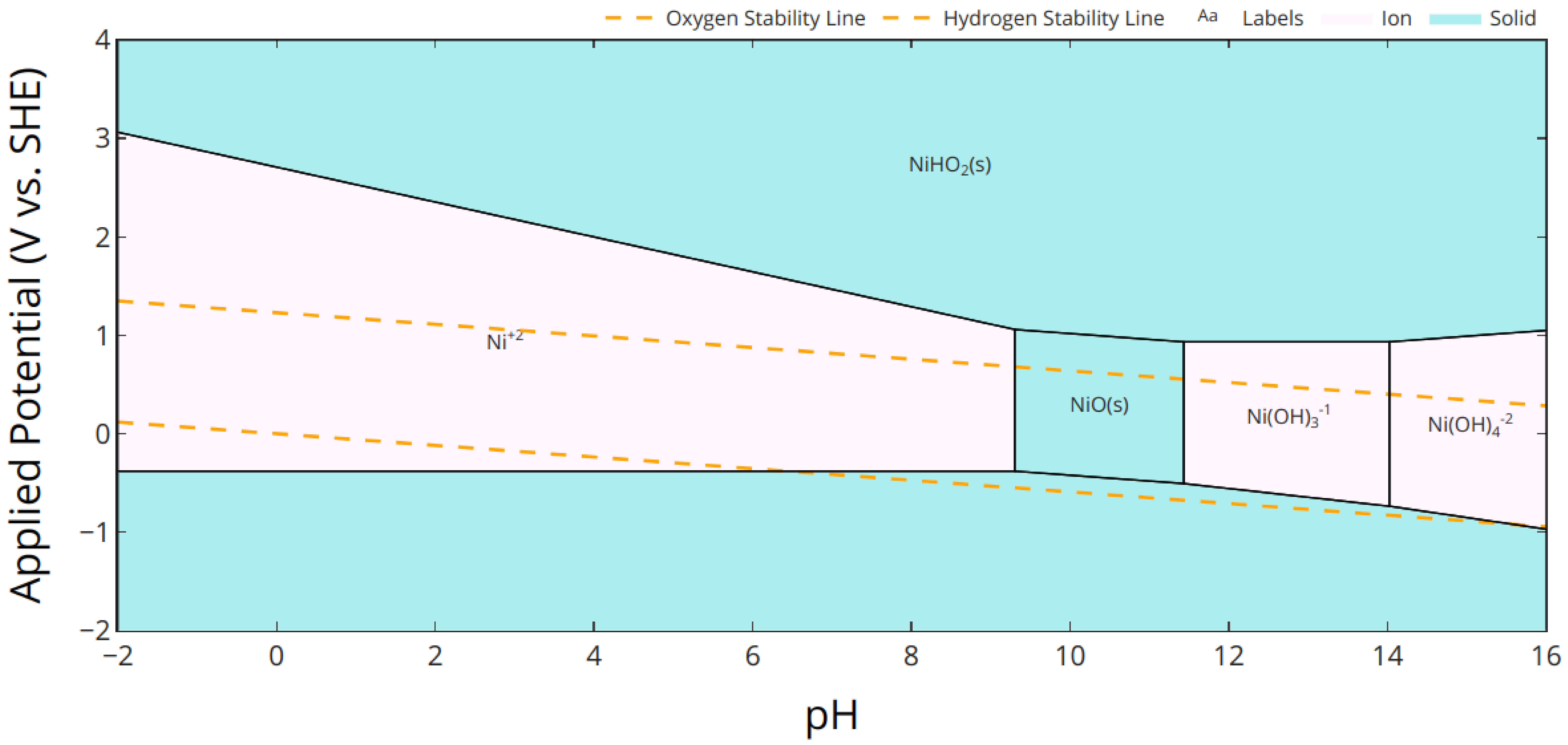

Our team


Sirius
University of Science and Technology
ART SCIENCE AND SPORT
I U P A C
2024
XXII
PHOSAGRO
SIBUR
GIREDMET
unesco

Acknowledgement

Skoltech
Energy

Center for
Energy Science
and Technology

COMPUTATIONAL
SCIENCE
Skoltech
MATERIALS

RSF
Russian Science
Foundation

Our group

Storion Research Lab

Center for Energy Science and Technology at Skoltech, Moscow

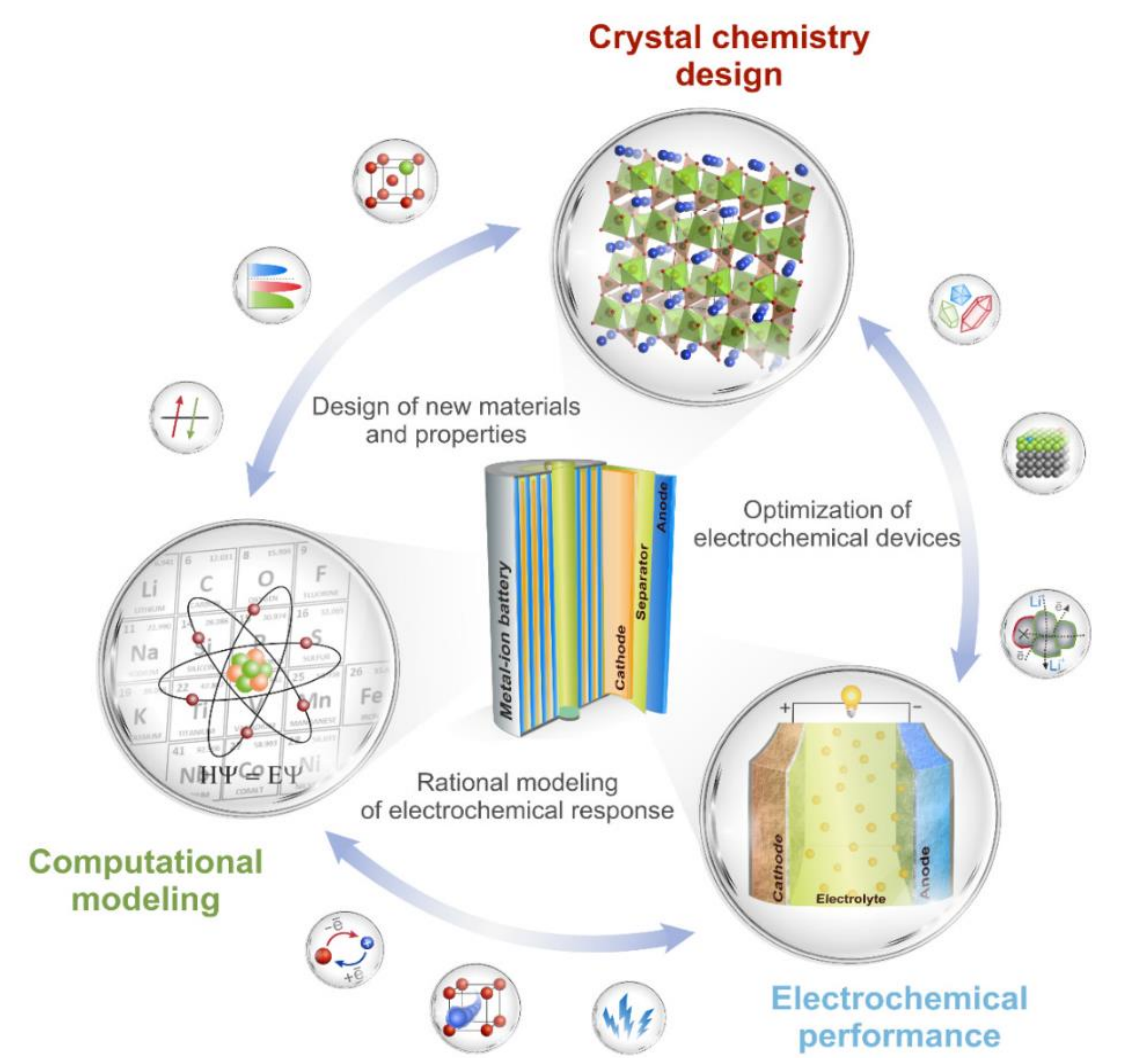

★ MatSolver - a web-service for predicting materials properties.

Thx!